Study of the Higgs-boson (H) properties in with the ATLAS detector at the LHC Run 2

Gaetano Αθανάσιος Barone

Brandeis University

Université de Genève,

April 2018

Overview

1. General introduction and motivation.
2. Experimental setup
3. Physics objects definition and selection criteria.

   Study of the Higgs boson properties:

   4. Measurement of its mass.
   5. Inclusive and differential fiducial cross sections
   6. Production mode measurements
7. Conclusions.

1. Introduction

Introduction

Matter

Fermions $s=1/2$

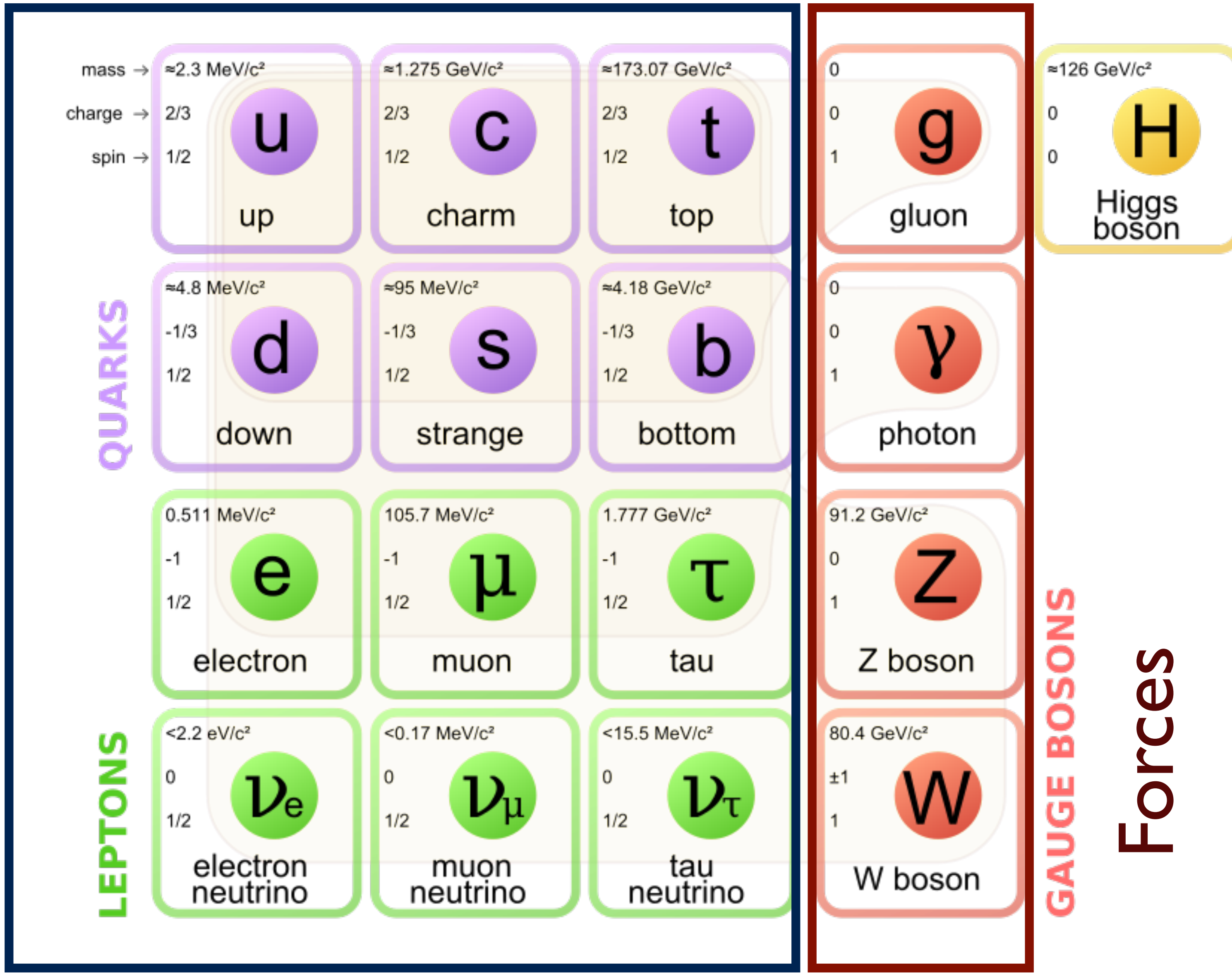

Forces

Fields

Introduction

- Higgs boson (*H*) production in proton-proton collisions:
  - Predominant production gluon-gluon fusion (87%) and VBF (6.8)
  - W,Z associated production (4%) and $t\bar{t}\ H/b\bar{b}\ H$ (<1%)

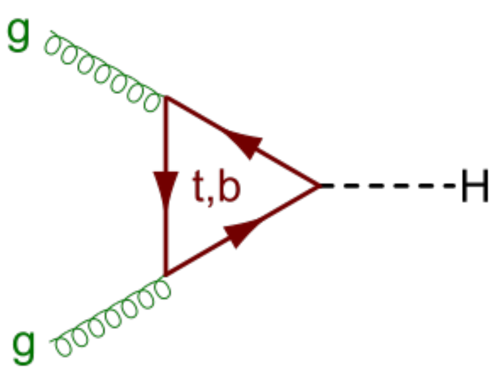

ggF

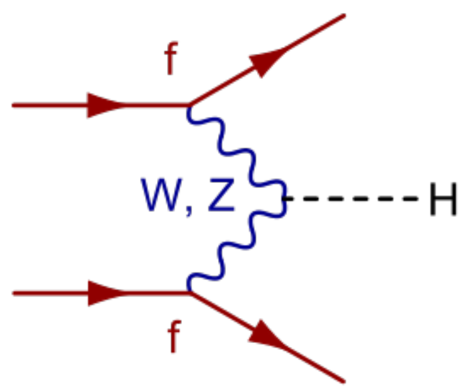

VBF

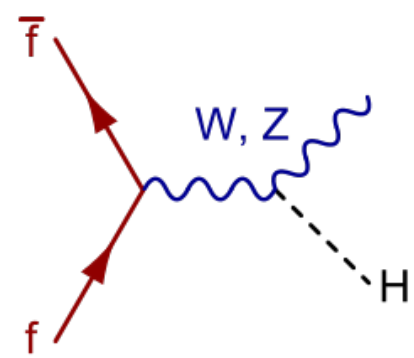

WH,ZH

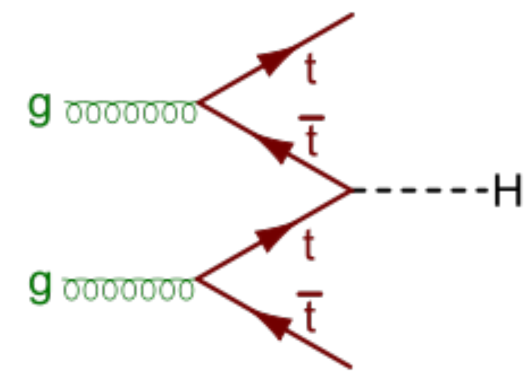

$t\bar{t}\ H$,
$b\bar{b}\ H$

- Experimentally challenging final states
  - In association with additional jets, same final state of many processes
  - forward jets with large rapidity gap, small rate

Introduction

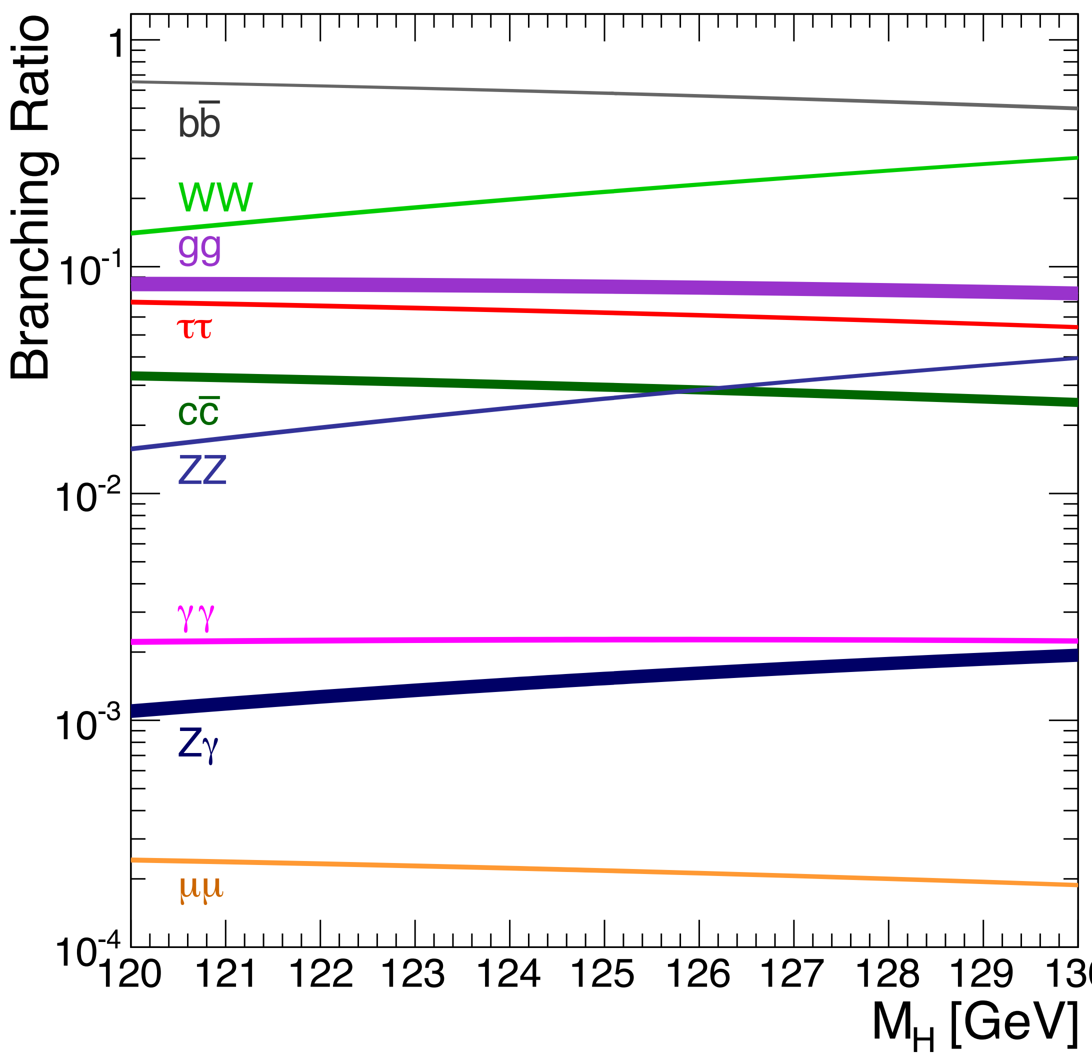

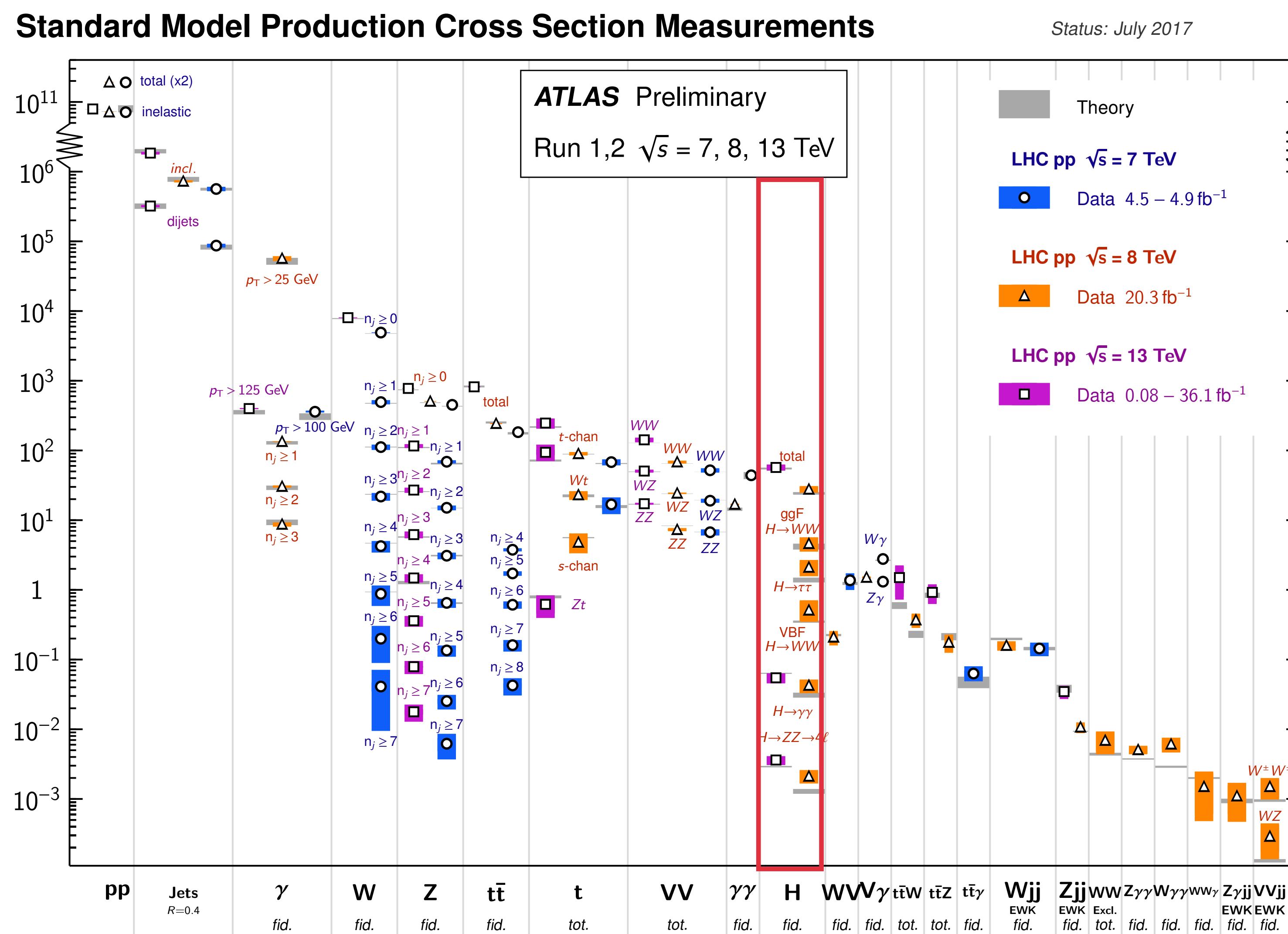

- Final states considered here:

  (i) $H \to \gamma\gamma$

  (ii) $H \to WW^* \to \ell\bar{\nu}\bar{\ell}\nu$

  (iii) $H \to ZZ^* \to 4\ell$

2. Experimental setup

Experimental Setup

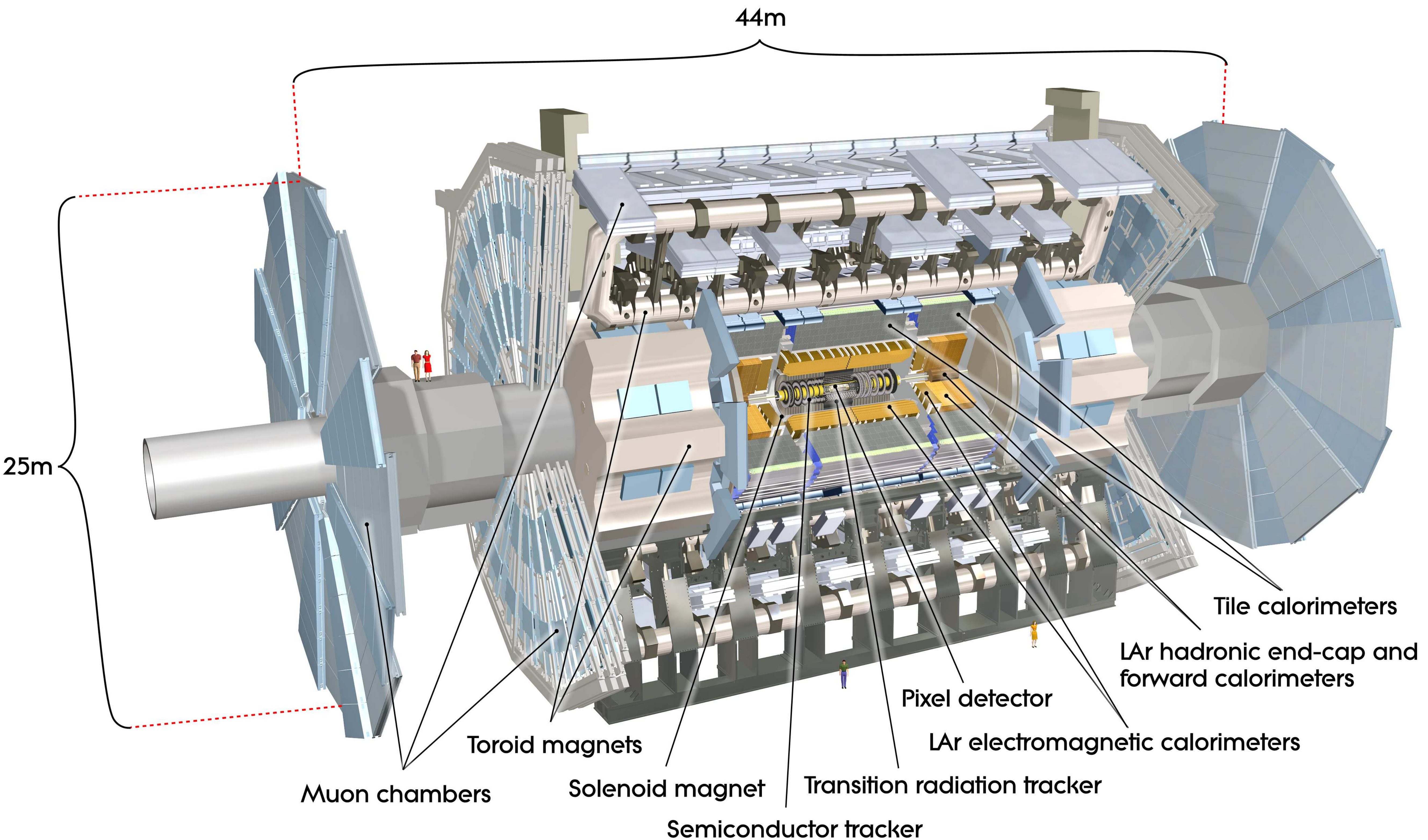

3. Physics objects definition and selection criteria.

- **Electrons** (e).
  - Clustering of calorimeter energy deposits with associated ID track.
  - E_T > 7 GeV, $|\eta|$ < 2.47 and $|z_0 \sin(\vartheta)|$ < 0.5 mm of "loose or tight quality" or

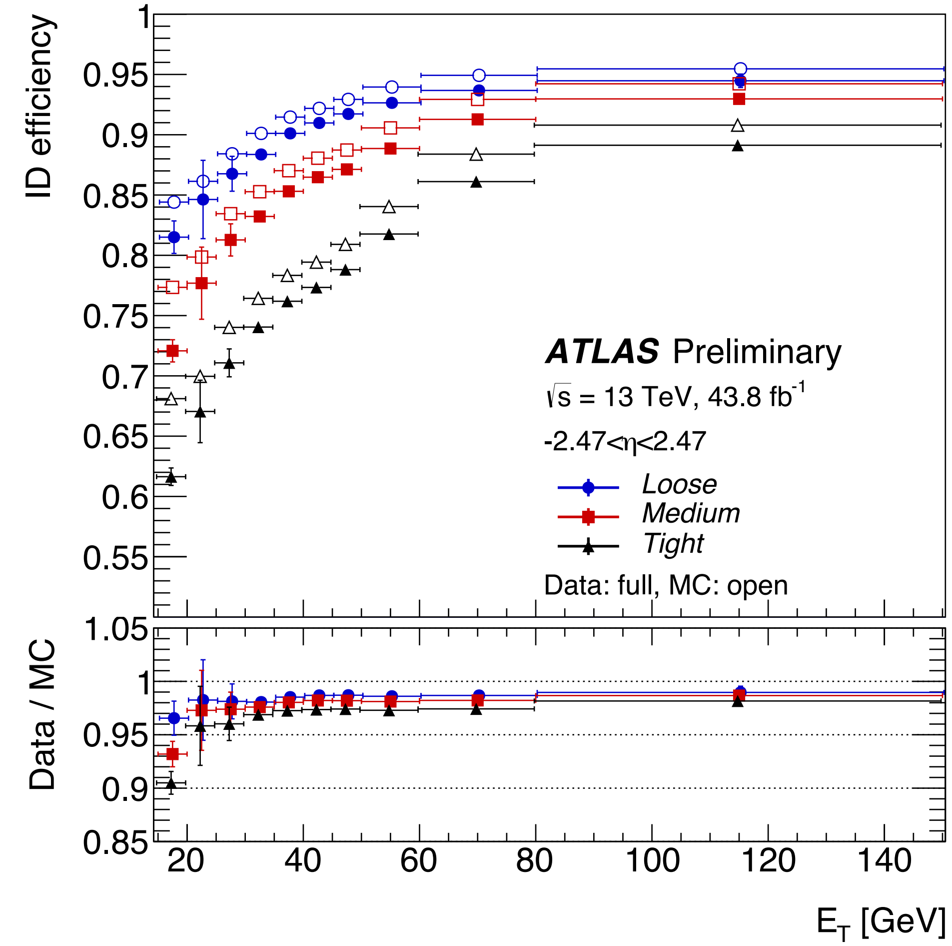

- **Muons** (μ).
  - Combined track fit of Inner Detector and Muon Spectrometer hits,
  - p_T > 5 GeV, $|\eta|$ < 2.7 $|z_0 \sin(\vartheta)|$ < 0.5 mm of "loose or medium quality"

- **Jets** (j).
  - Energy deposit grouping with *infra*-red safe algorithm:
  - p_T > 20 GeV and $|\eta|$ < 4.5
    - ✦ Clustering with anti-k_T, R=0.4

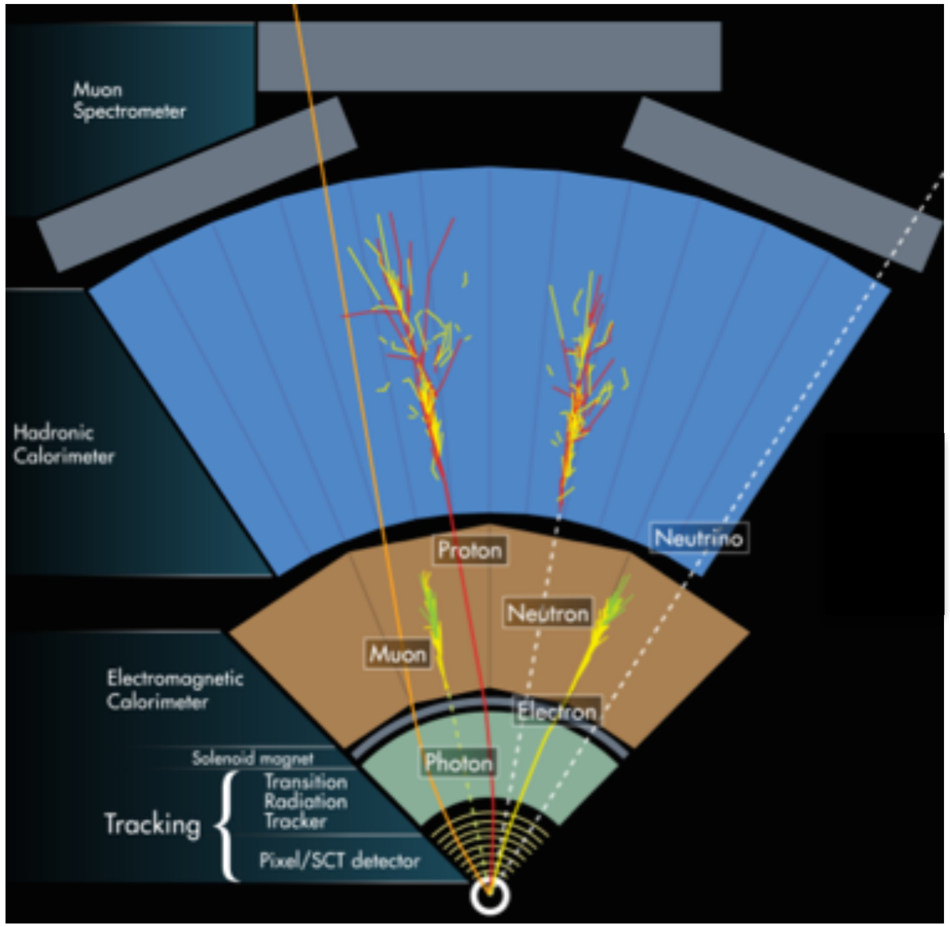

- Electrons (e).
  - Clustering of calorimeter energy deposits with associated ID track.
  - $E_T > 7$ GeV, $|\eta| < 2.47$ and $|z_0 \sin(\vartheta)| < 0.5$ mm of "loose or tight quality"

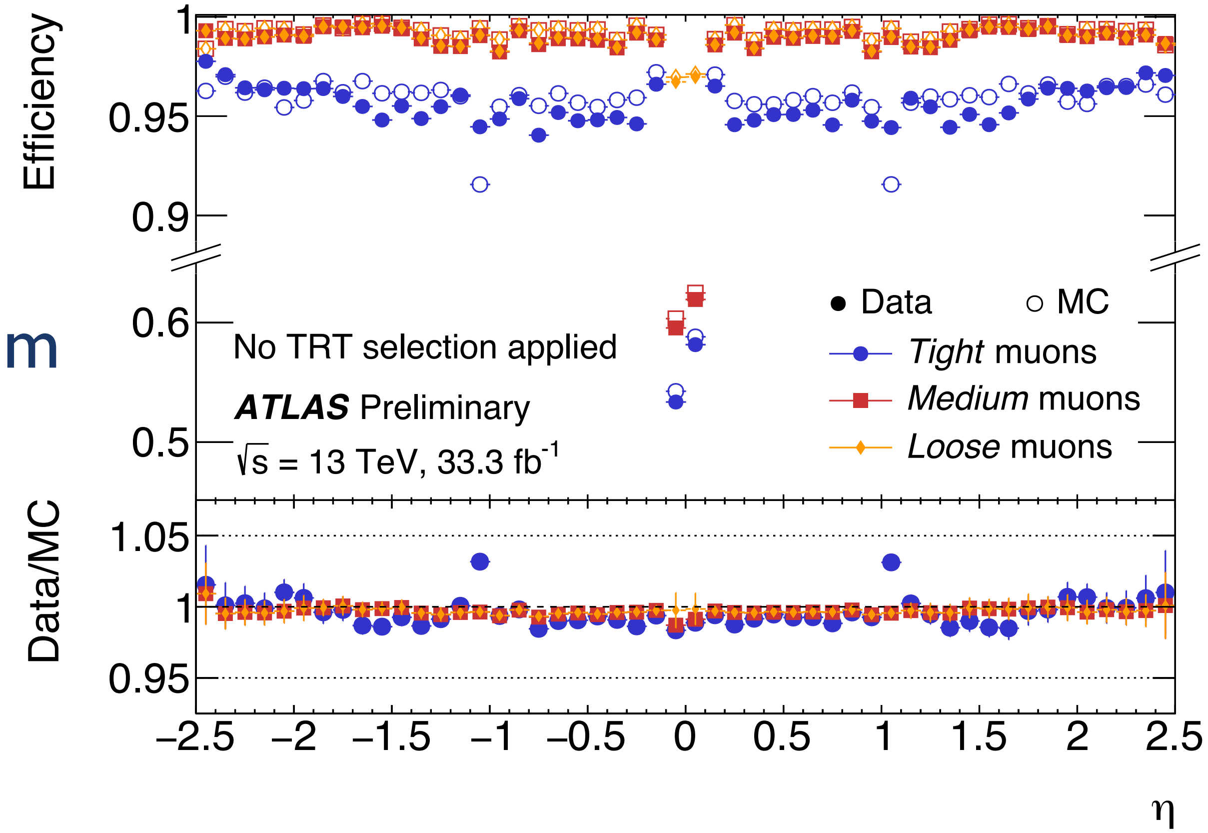

- Muons (μ).
  - Combined track fit of Inner Detector and Muon Spectrometer hits,
  - $p_T > 5$ GeV, $|\eta| < 2.7$ $|z_0 \sin(\vartheta)| < 0.5$ mm of "loose or medium quality"

- Jets (j).
  - Energy deposit grouping with *infra*-red safe algorithm:
  - $p_T > 30$ GeV and $|\eta| < 4.5$
    - Clustering with anti-k_T, $R=0.4$

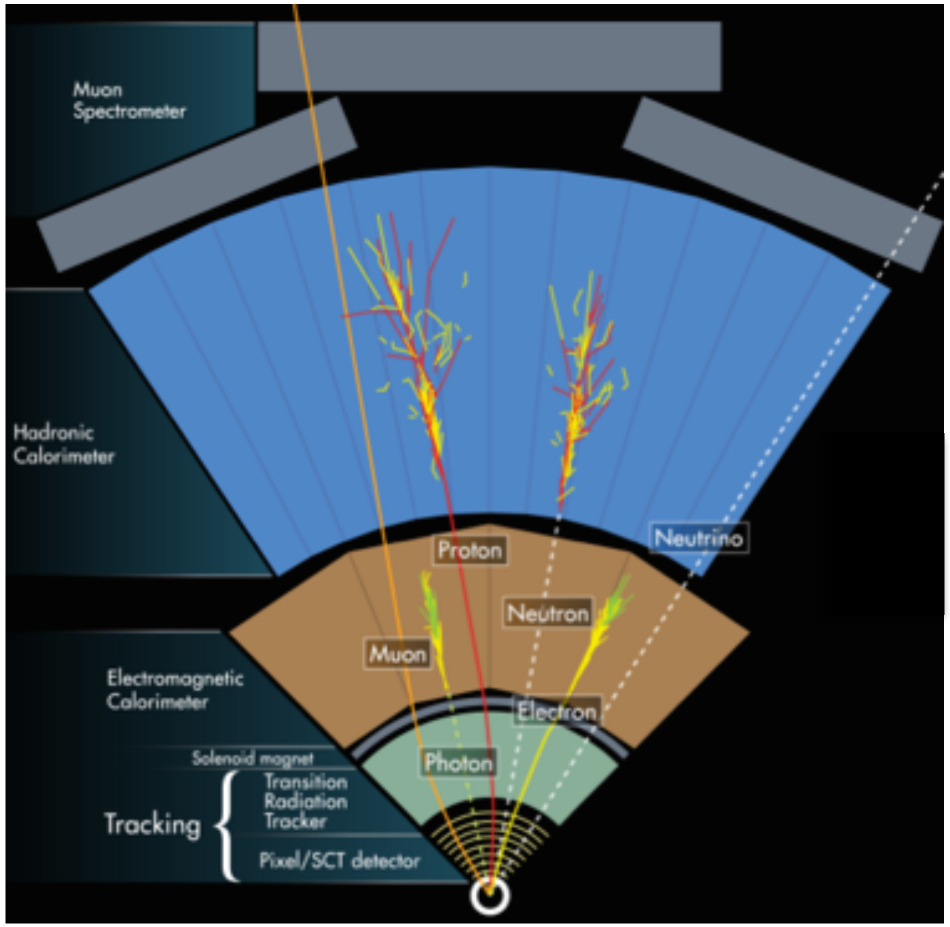

- **Electrons (e).**
  - Clustering of calorimeter energy deposits with associated ID track.
  - E_T > 7 GeV, $|\eta|$ < 2.47 and $|z_0 \sin(\vartheta)|$ < 0.5 mm of "loose or tight quality"

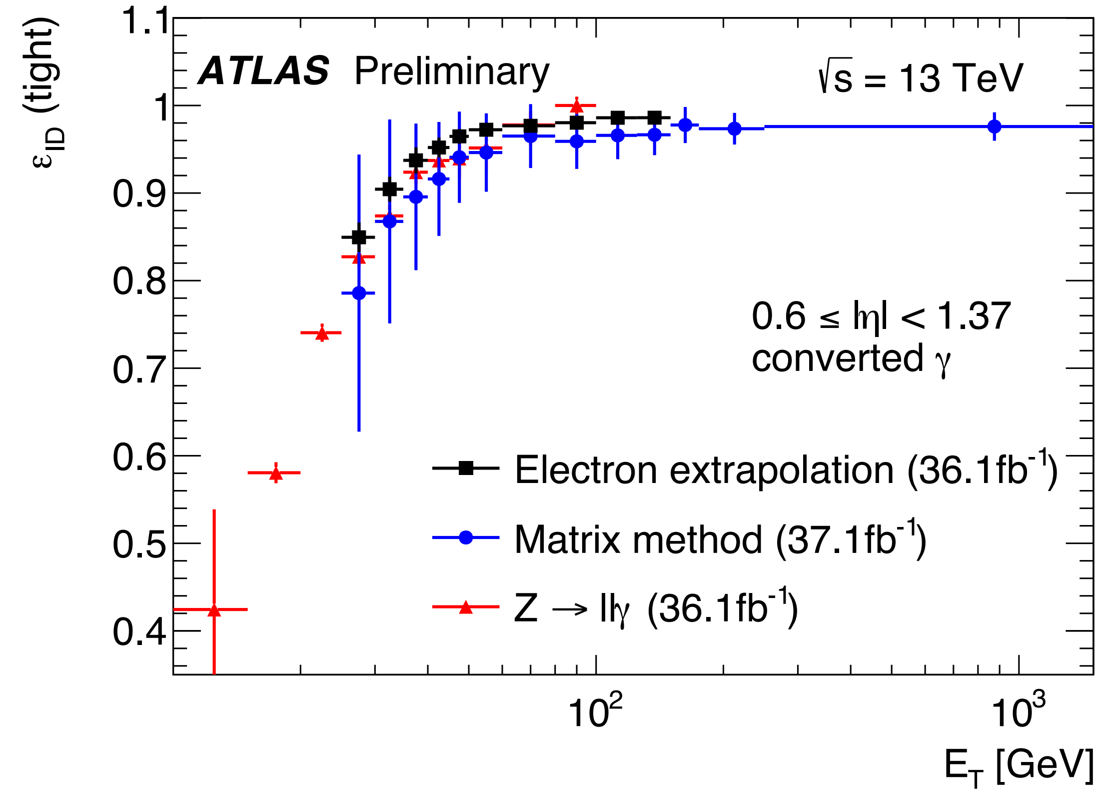

- **Muons (μ).**
  - Combined track fit of Inner Detector and Muon Spectrometer hits,
  - p_T > 5 GeV, $|\eta|$ < 2.7 $|z_0 \sin(\vartheta)|$ < 0.5 mm of "loose or medium quality"

- **Photons (γ).**
  - Clustering of calorimeter energy deposits.
  - Identified with rectangular cuts on shower shapes.

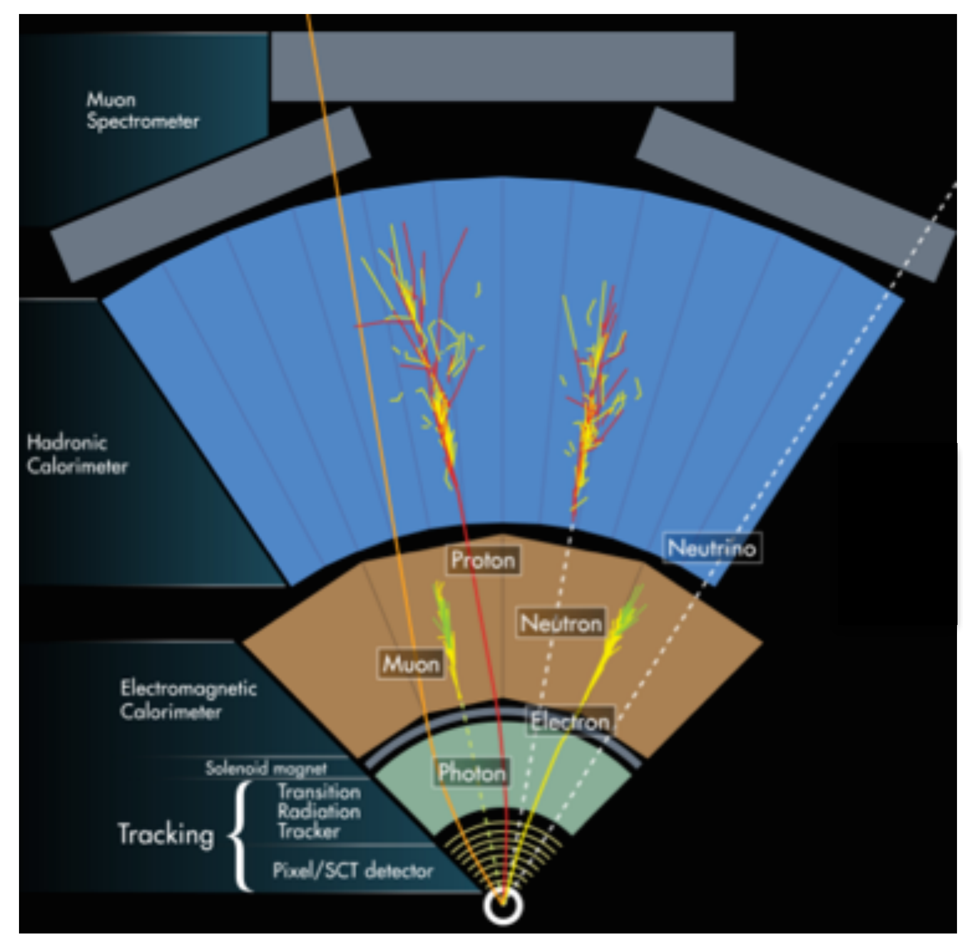

- **Electrons** (e).
  - Clustering of calorimeter energy deposits with associated ID track.
  - $E_T > 7$ GeV, $|\eta| < 2.47$ and $|z_0 \sin(\vartheta)| < 0.5$ mm of "loose or tight quality"

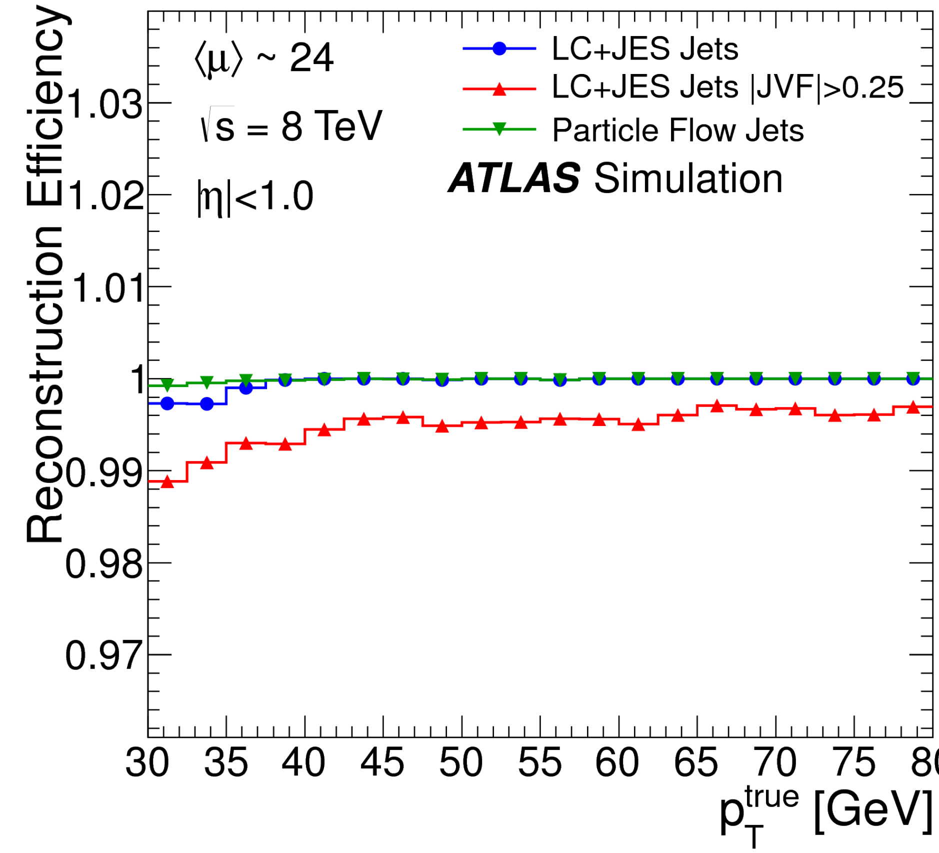

- **Muons** (μ).
  - Combined track fit of Inner Detector and Muon Spectrometer hits,
  - $p_T > 5$ GeV, $|\eta| < 2.7$ $|z_0 \sin(\vartheta)| < 0.5$ mm of "loose or medium quality"

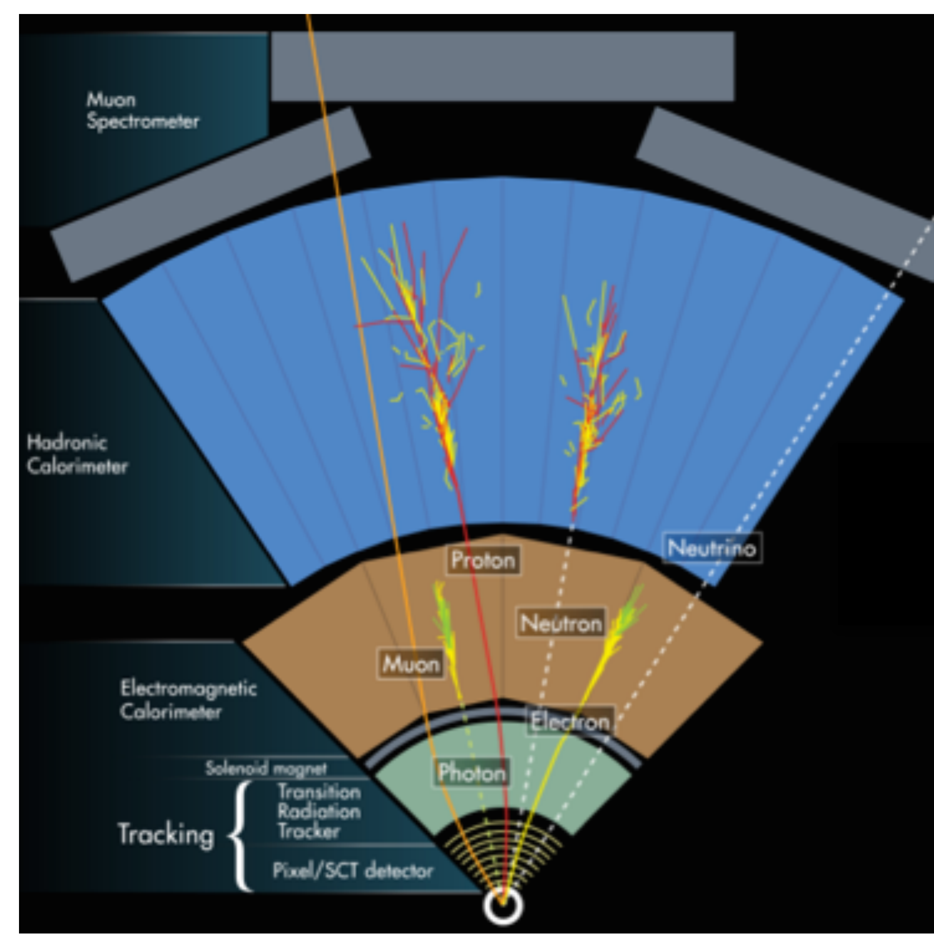

- **Jets** (j).
  - Energy deposit grouping with *infra*-red safe algorithm:
  - $p_T > 30$ GeV and $|\eta| < 4.5$
    - Clustering with anti-k_T, $R=0.4$

Object selection

- Electrons (e).
  - Clustering of calorimeter energy deposits with associated ID track.
  - $E_T > 7$ GeV, $|\eta| < 2.47$ and $|z_0 \sin(\vartheta)| < 0.5$ mm of "loose or tight quality"

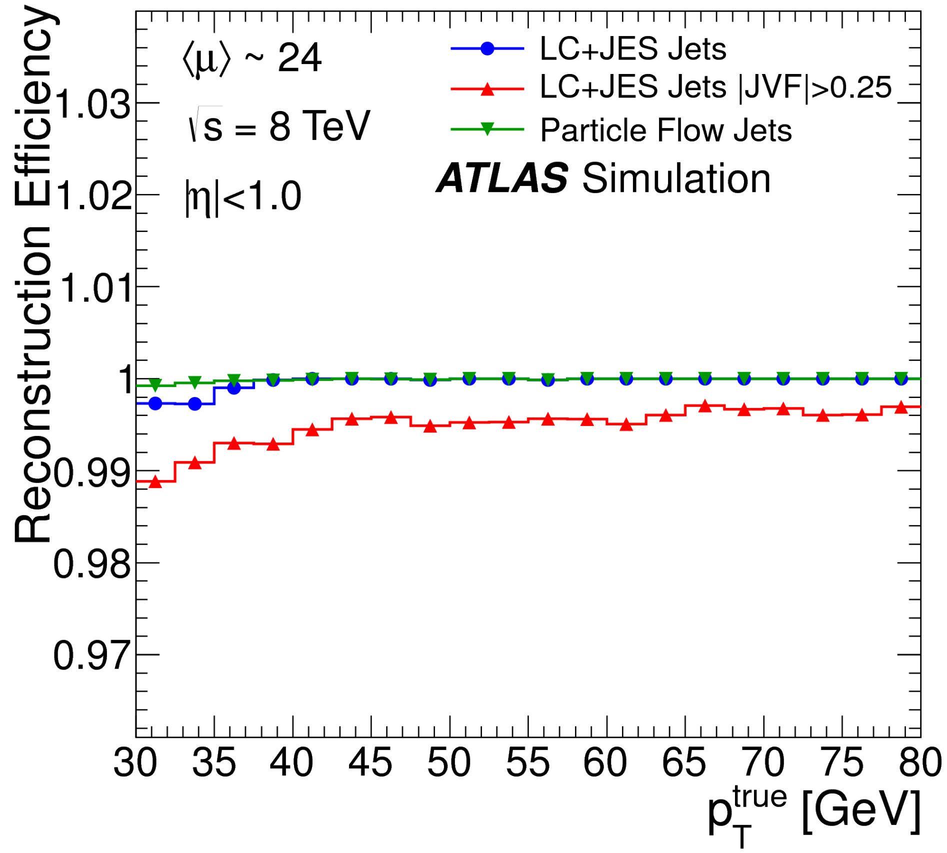

- Muons (μ).
  - Combined track fit of Inner Detector and Muon Spectrometer hits,
  - $p_T > 5$ GeV, $|\eta| < 2.7$ $|z_0 \sin(\vartheta)| < 0.5$ mm of "loose or medium quality"

- Missing transverse energy (E_T^{miss}).
  - Inferred from momentum imbalance

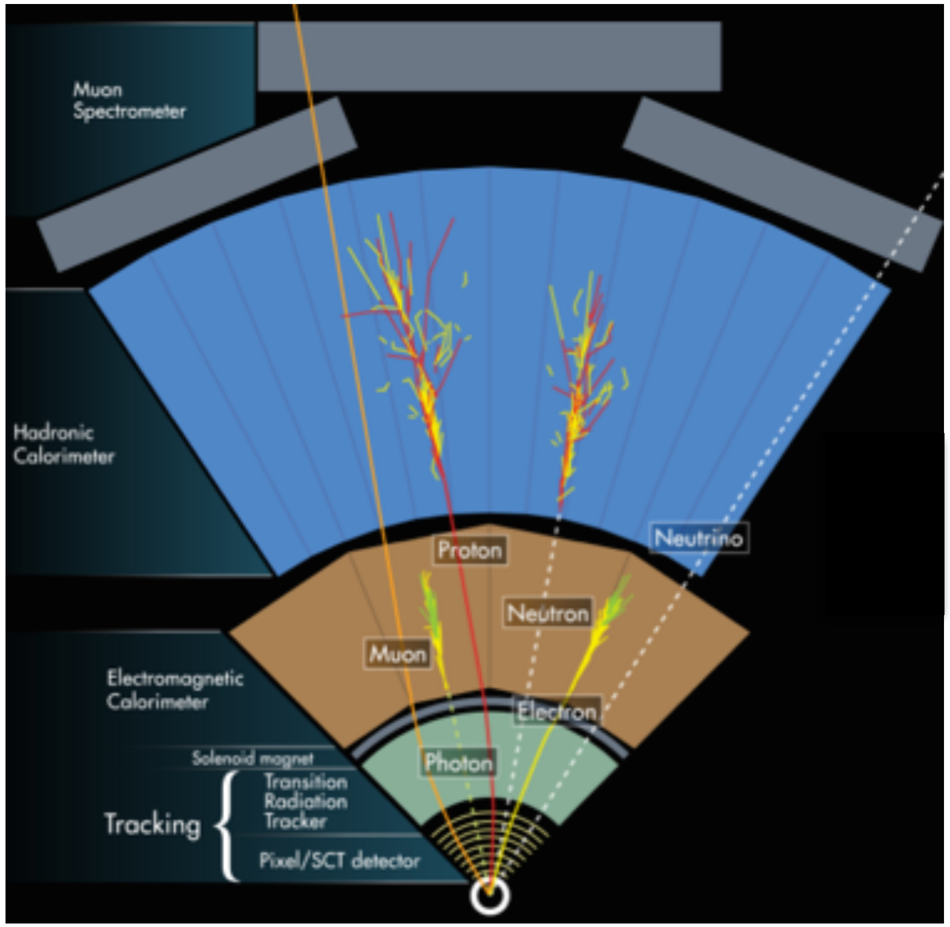

- $ZZ^*\rightarrow 4\ell$ (ℓ= μ,e) selection:
  - Isolated leptons with: $p_T(\ell)$ > 20 GeV , 15 GeV 10 GeV and 5 (7) GeV
  - Leading pair: pair closest to m_Z,
  - Vertex refit: χ^2 cut at 99.5% signal efficiency
  - Final state photon emission recovered

Final state	Signal (125 GeV)	Expected	Observed
4μ	20.6 ± 1.7	38.5 ± 2.1	38
$2e2\mu$	14.6 ± 1.1	27.5 ± 1.4	34
$2\mu 2e$	11.2 ± 1.0	20.8 ± 1.3	26
$4e$	11.1 ± 1.1	20.3 ± 1.3	24
Total	57 ± 5	107 ± 6	122

$$110\ \text{GeV} < m_{4\ell} < 130\ \text{GeV}$$

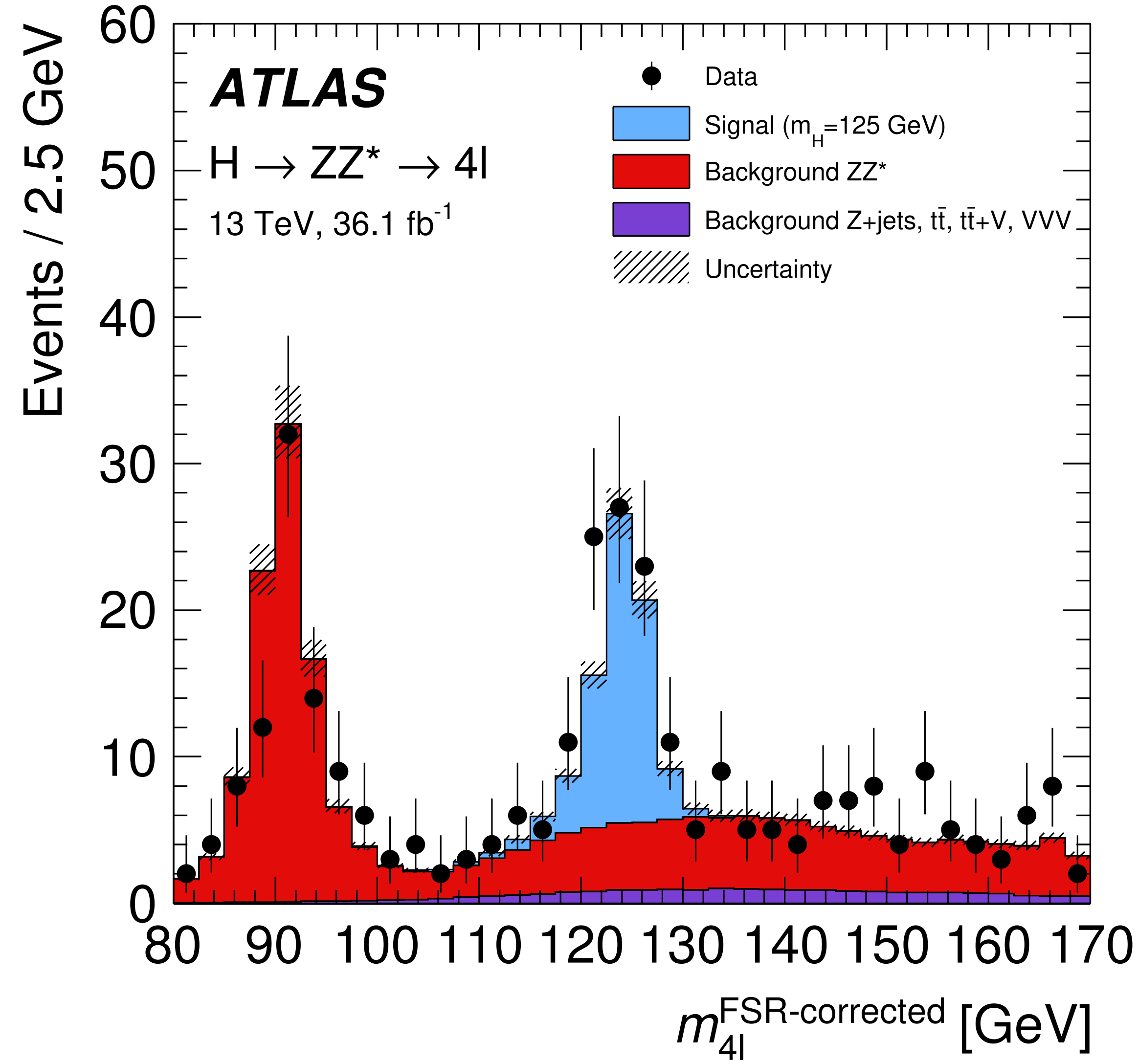

- Background estimation

1. ZZ^* production in 4ℓ (dominant)
   - From $q\bar{q}$ annihilation and gg fusion (subdominant)
2. ZZZ, WZZ and WWZ (small).

Based on simulation

3. Hadrons misidentified as leptons:
   - Z+jets $t\bar{t}$ and WZ production
   - Extrapolation to signal region making use of simulation

Based on data

Reconstruction and selection

- Diphoton event selection
  - At least two photon with E_T> 25 GeV
  - Highest E_T pair forms candidate.
  - Vertex identification with Neural Network
    - ✦ Vertex within 0.3 mm for 79% of ggH events.

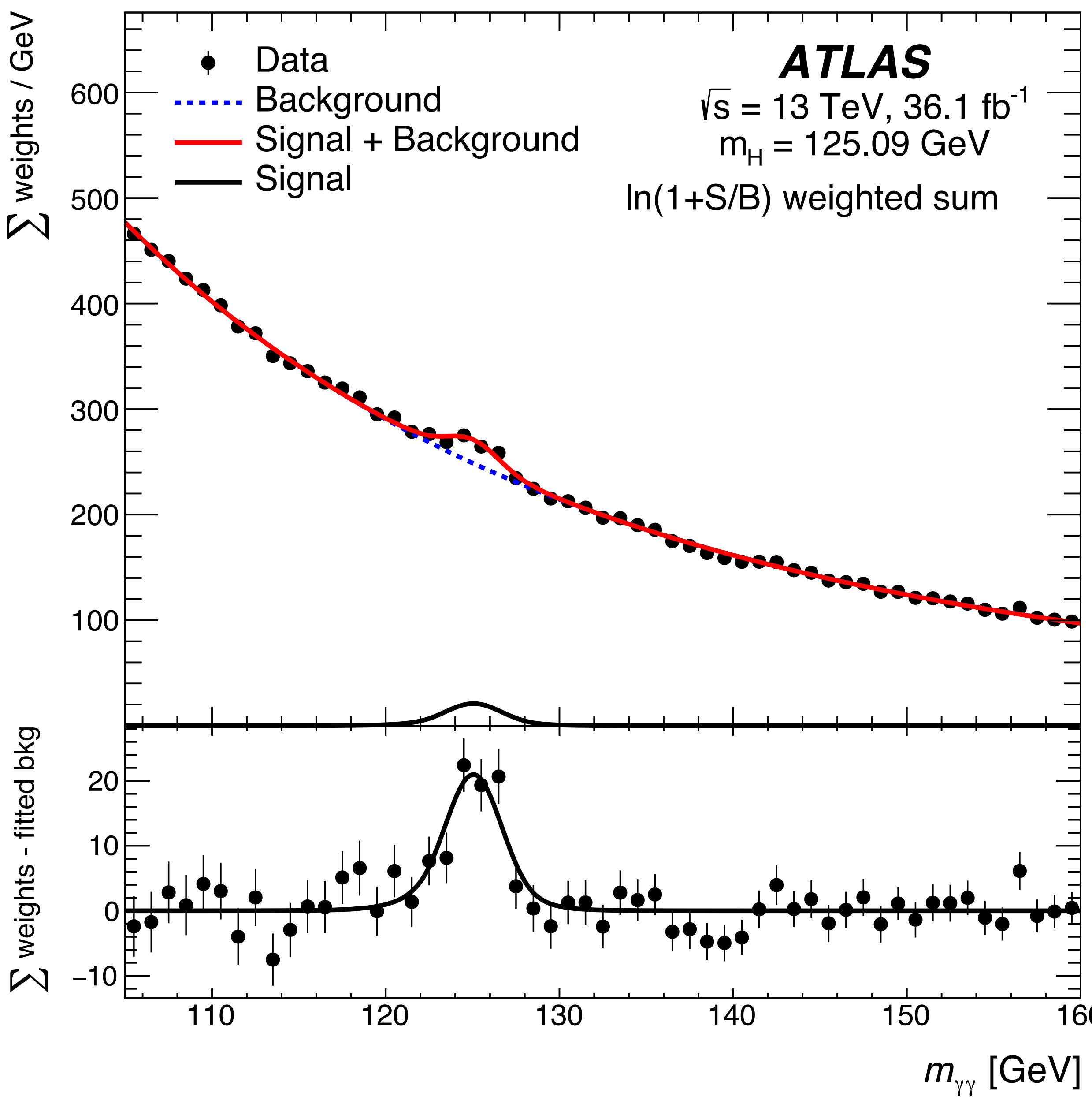

- Background estimation
  - Entirely estimated from data
  - Prompt photons: maximum likelihood fit to $m_{\gamma\gamma}$ spectrum
  - Jets misidentified as photons: from control sample

- $WW^*\to e\nu\mu\nu$ selection
  - Two isolated leptons $p_T(\ell)$ > 22 GeV and $p_T(\ell)$ > 15 GeV
  - E_T^{miss} > 20 GeV
- Signal-to-background discriminants
  - Trasnverse mass (m_T) for ggF production and Boosted Decision Tree (BDT) for VBF production
- Background estimation

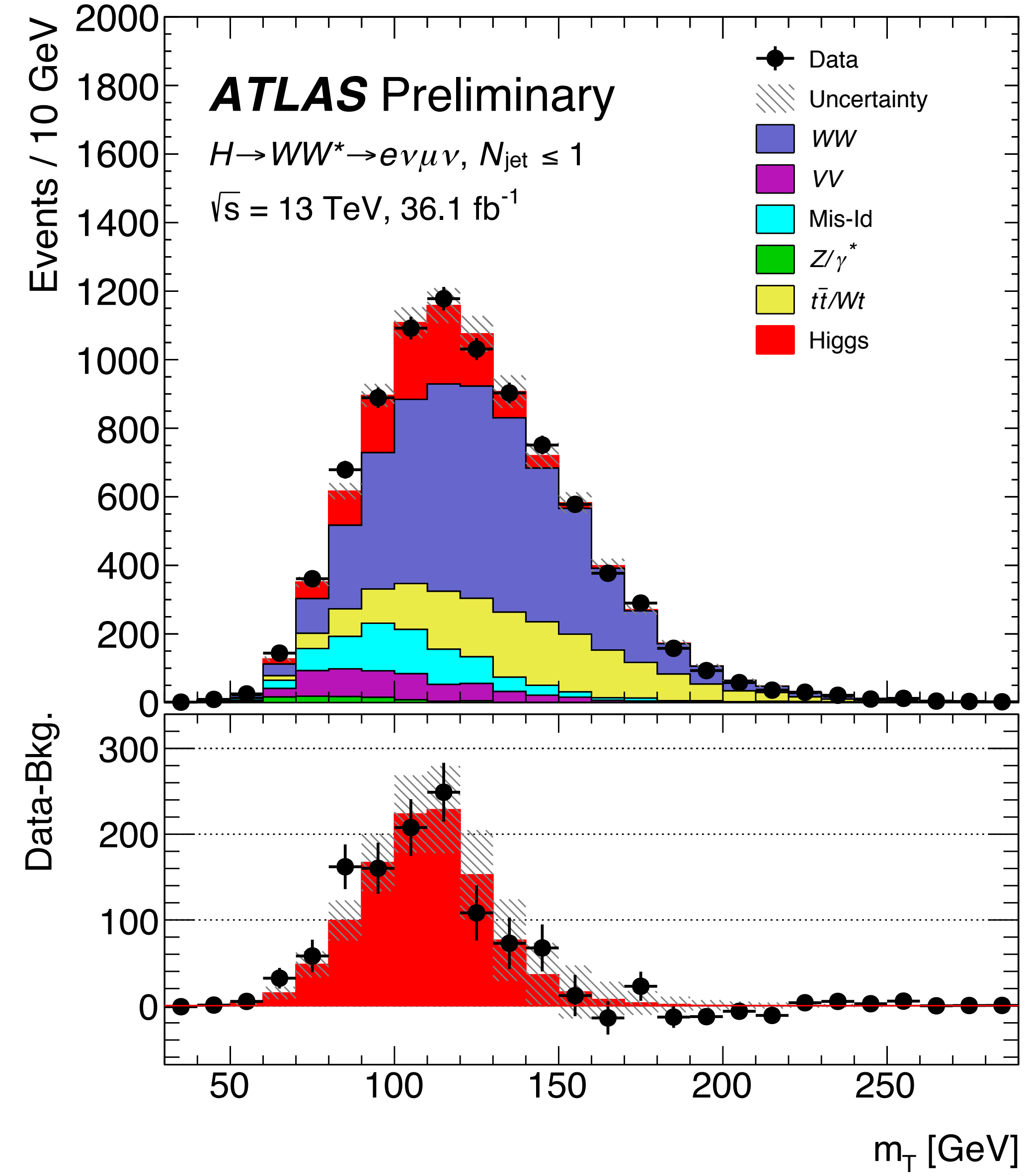

1. Non resonant *WW* production
2. $t\bar{t}$ production
3. Drell-Yan: $Z\to\tau^+\tau^-$
4. Hadrons misidentified as leptons:
   - W+jets $t\bar{t}$ and WZ production

Based on data

5. $ZZ^*,\ WZ,\ W\gamma(^*)$ production in
6. Single-top-quark (Wt) production

Based on simulation

4. Mass Measurement

- ATLAS run I precision on m_H of 0.33%
  - combined measurement from $H\to\gamma\gamma$ and $H\to ZZ^*\to 4\ell$.

Channel	Mass measurement [GeV]
$H\to\gamma\gamma$	$125.98 \pm 0.42\,(\text{stat}) \pm 0.28\,(\text{syst}) = 125.98 \pm 0.50$
$H\to ZZ^*\to 4\ell$	$124.51 \pm 0.52\,(\text{stat}) \pm 0.06\,(\text{syst}) = 124.51 \pm 0.52$
Combined	$125.36 \pm 0.37\,(\text{stat}) \pm 0.18\,(\text{syst}) = 125.36 \pm 0.41$

  - For both channels dominated by statistical uncertainty
- Compatibility within 2.0 σ
  - *p*-value of about 0.05.
- Aim in improving significantly on δm_H
  - Expect 1.7 times more candidates, with 36 fb^{-1} at $\sqrt{s}$=13 TeV

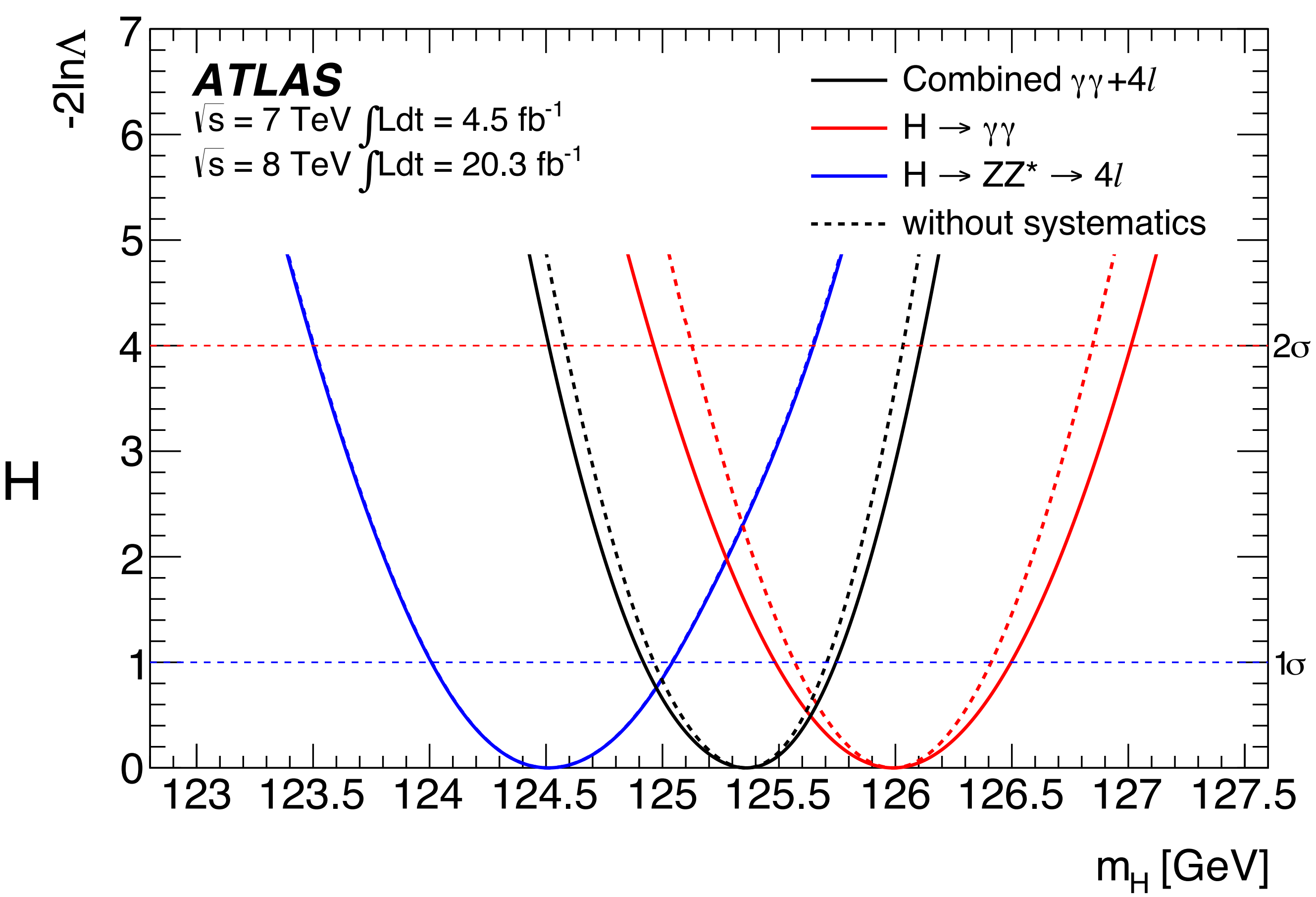

- For γγ and 4ℓ, signal is narrow resonant peak above a background continuum
  - Allows for precise Higgs boson mass measurement
  - Minimise the model dependency.
- Ingredients for optimal measurement of Higgs boson mass:
  - Detector performance driven measurement

$$\delta m_H \simeq \frac{\sigma(m_{4\ell,\gamma\gamma})}{\sqrt{N - N_{\mathrm{b}}}}$$

(I) Statistical precision precision depends upon:

- resolution of the reconstructed final state,
- number of signal events.

(II) Systematic uncertainty from understanding of detector performance:

- energy and momentum scale,
- resolution uncertainty.

Muon p_T resolution

- Local misalignments and second order effects:
  - Charge dependent sagitta bias, with net effect of worsening resolution
  - In-situ correction based on $Z \rightarrow \mu\mu$ data, recovers up to 5% in resolution.

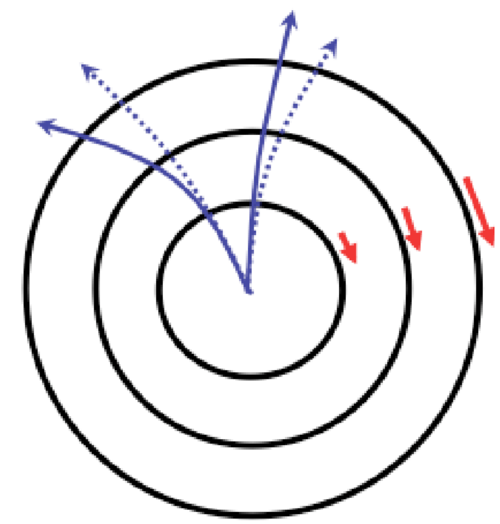

- Momentum scale understood down to the per mille level
  - Precision down to 0.5 per mille for $|\eta|<1.0$

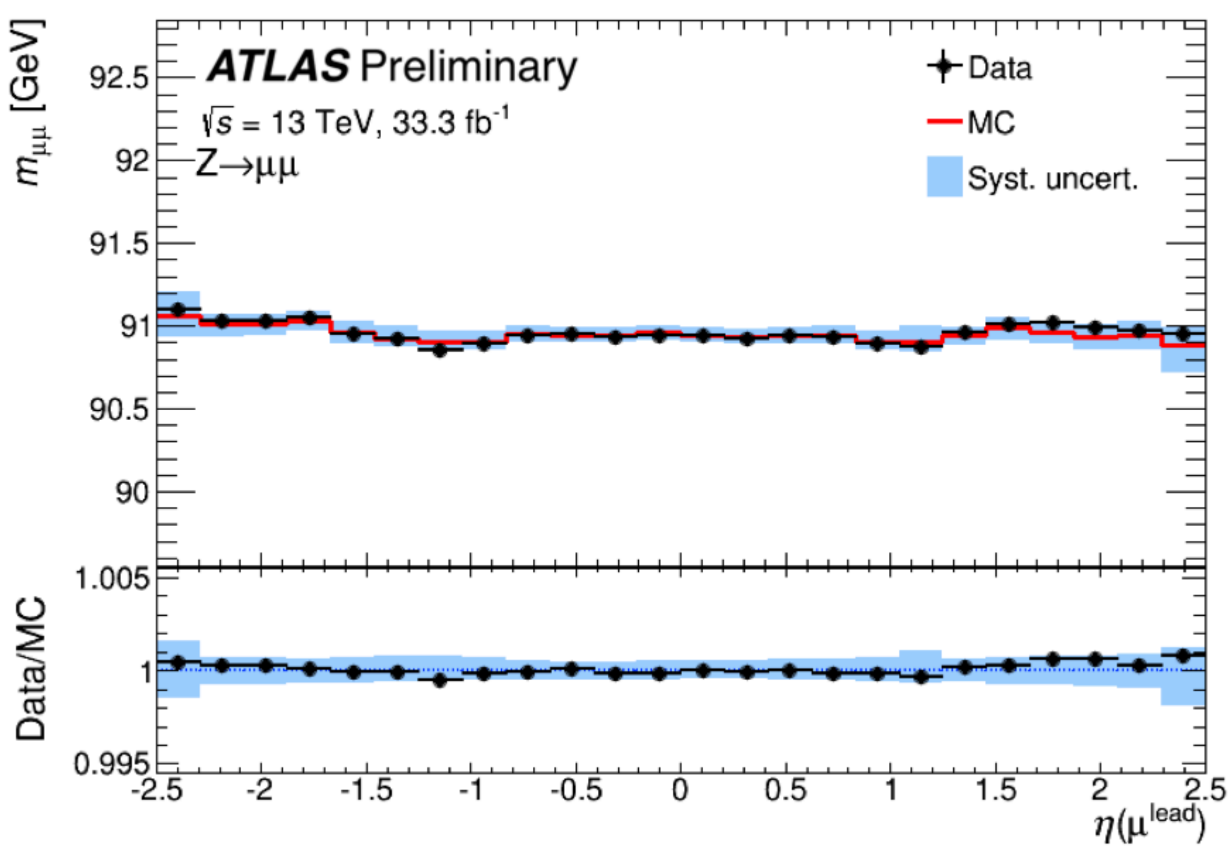

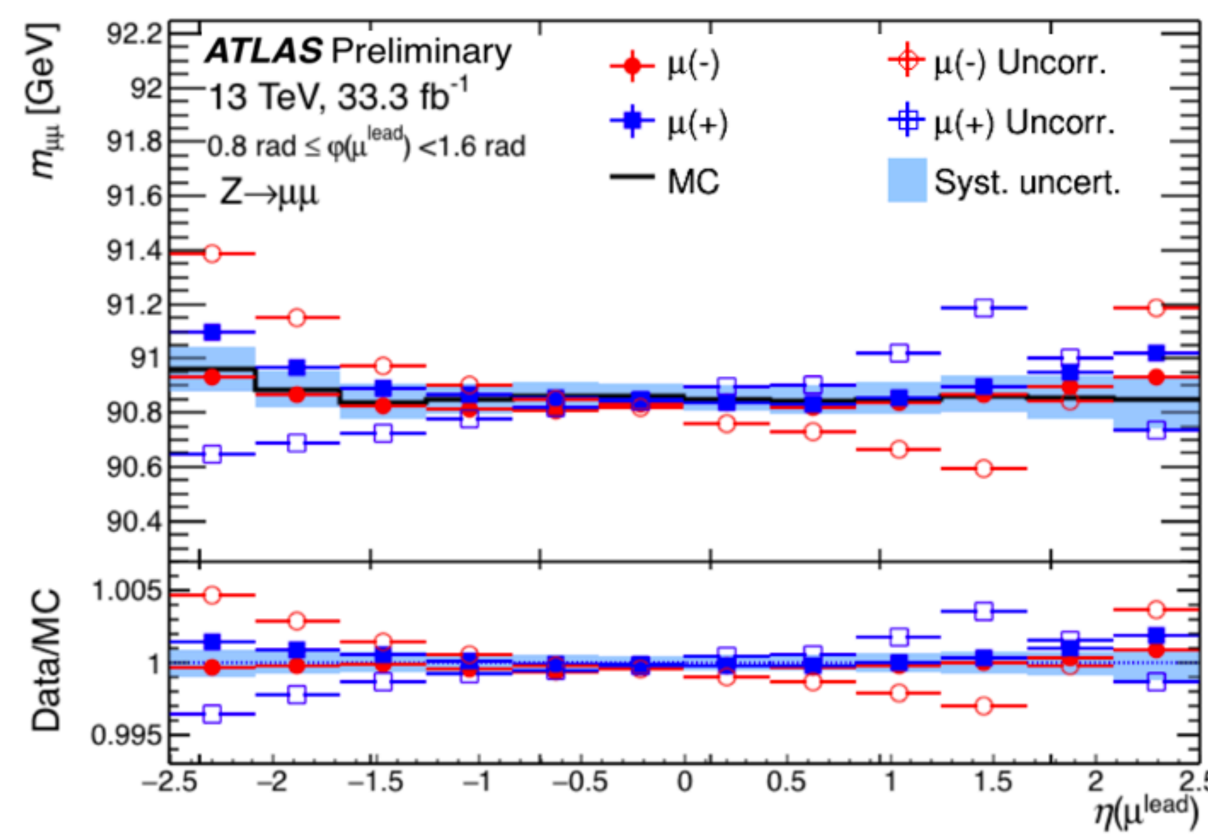

- Resolution muon channels (4μ, 2e2μ and 4μ) crucial for m_H uncertainty:
  - bigger signal yield because of larger acceptance.
  - Excellent momentum resolution of about 1% *Z* scale.
- Simulated momenta calibrated to J/ψ and Z samples in data
  - for residual mis modelling of E^{loss} in calorimeters, alignment precision etc.
  - Uncertainty of about 10%

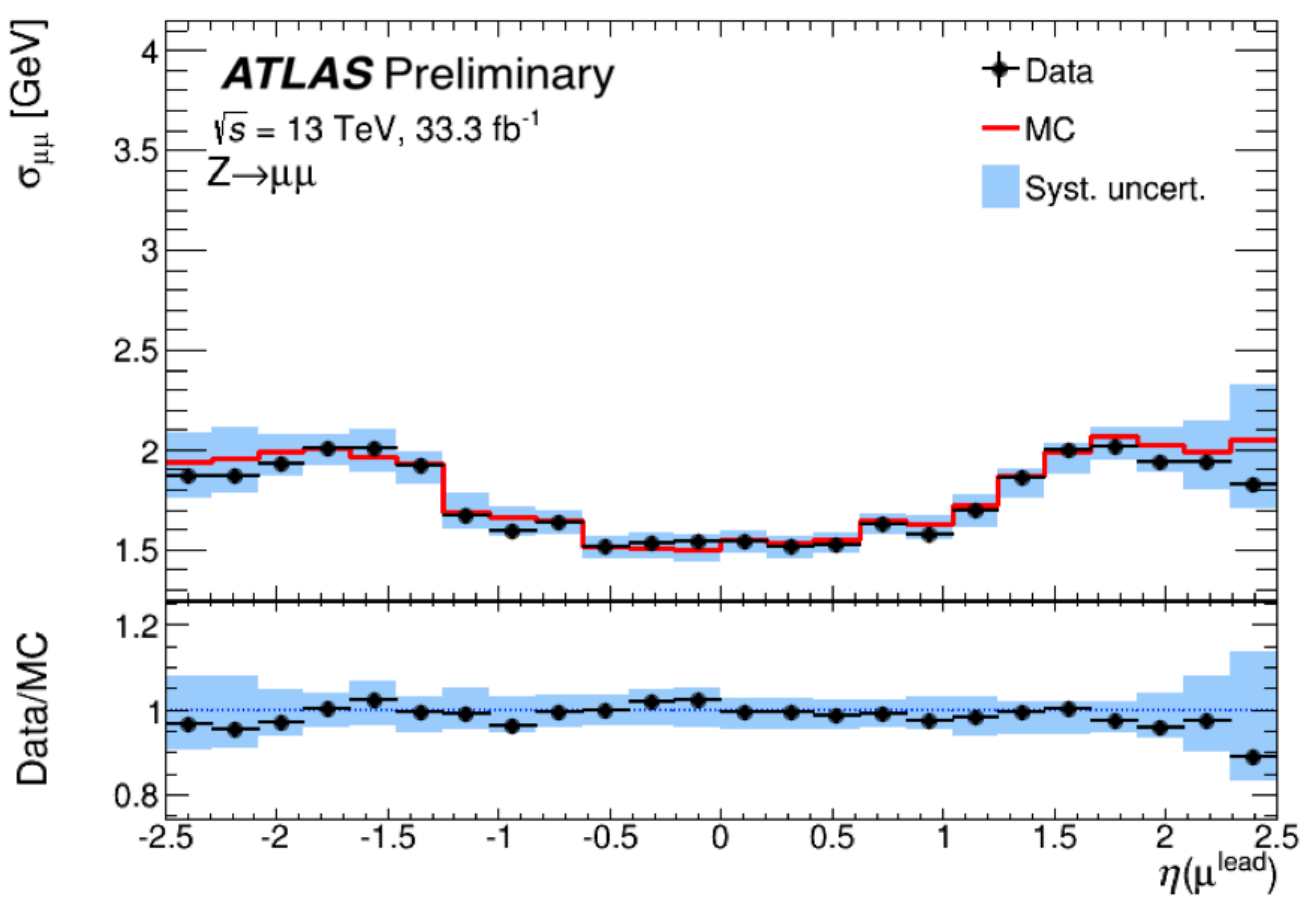

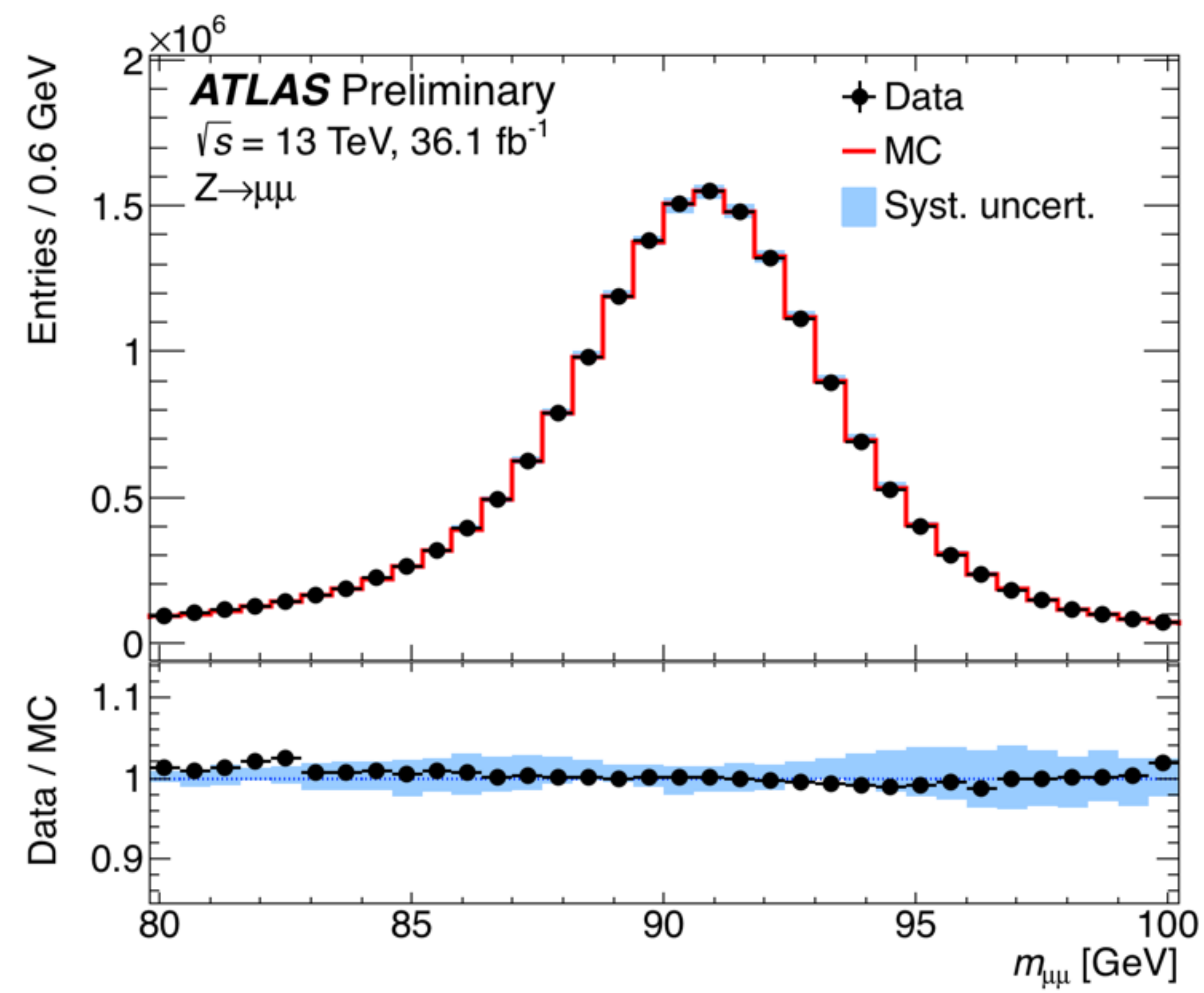

$E_T(e/\gamma)$ resolution

- Good energy calibration necessary for increased precision on m_H
  - Two step approach: i) material energy loss and ii) global calorimetric scale from data
- Total scale uncertainty of at 40 GeV at the per-mille level.
  - 2 per mille central and 10 per mille forward.

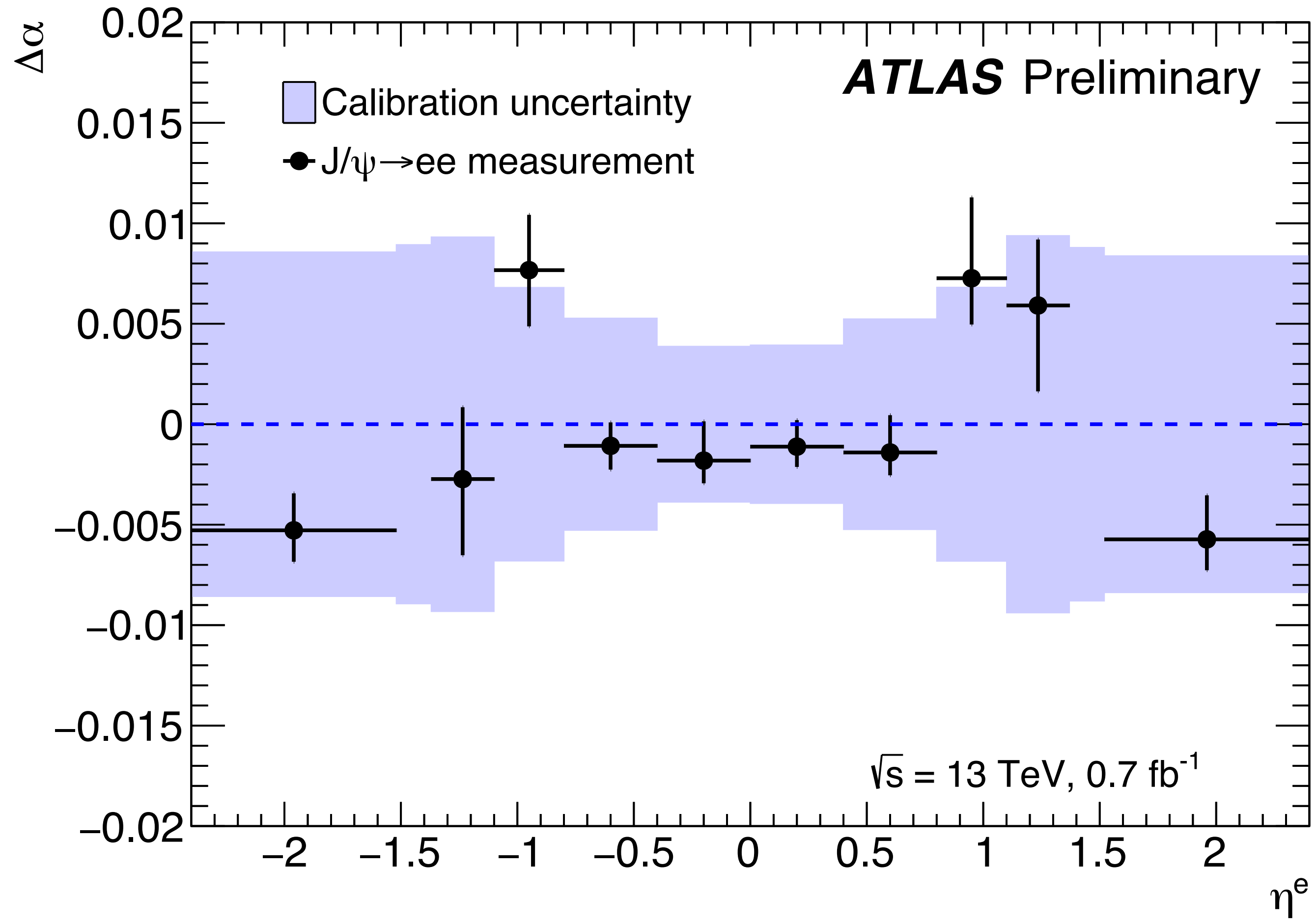

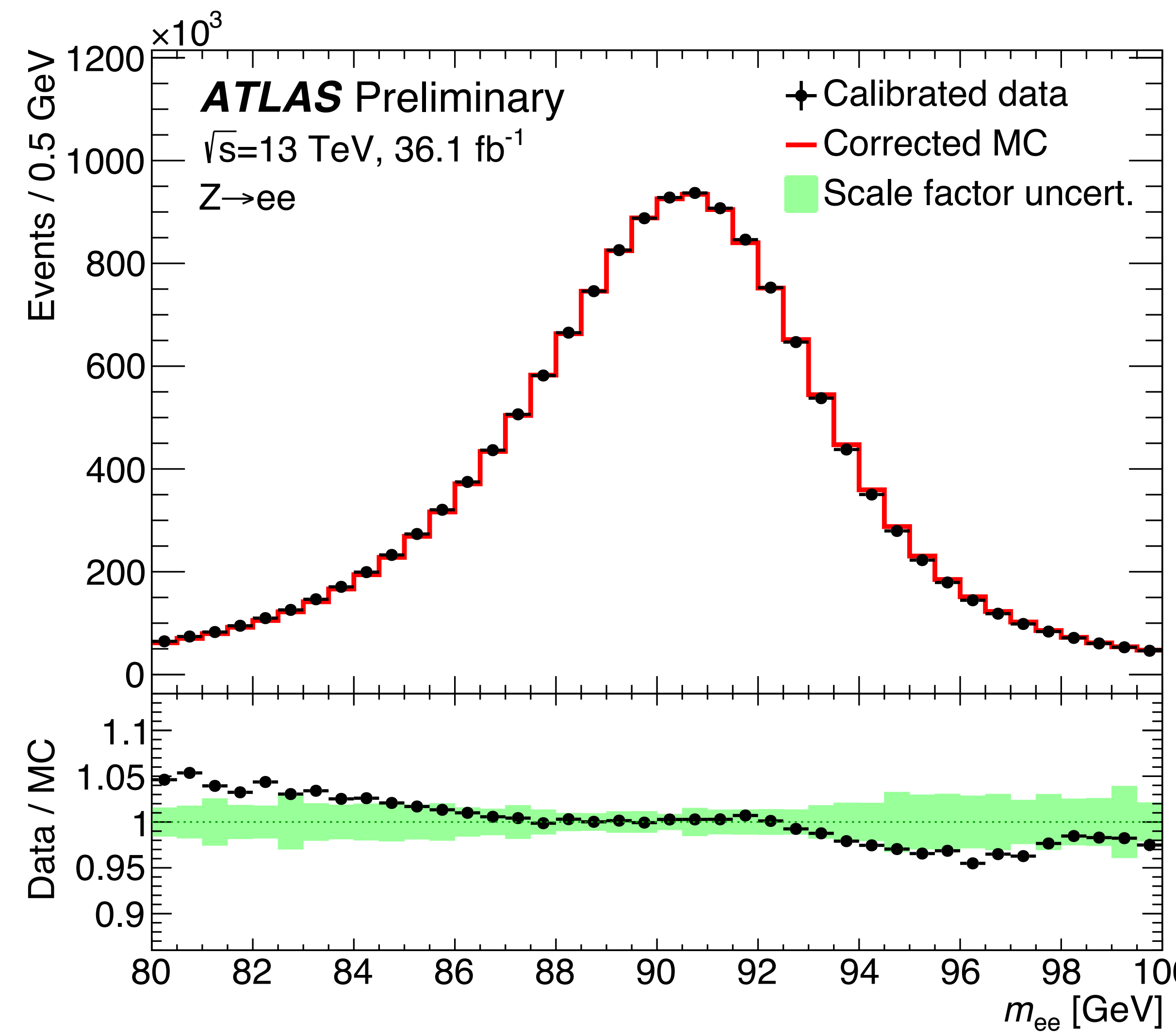

- Three-prong approach to reduce uncertainty at analysis level:

(i) 14% from m_{12} constraint to m_Z with kinematic fit.

(i) 2.4% from per-event likelihood.

- Per lepton energy response as a function of kinematics of event

(ii) 6.3 % from kinematic discriminant selecting signal and background events

- Boosted Decision Tree on $p_T(4\ell)$, $y(4\ell)$ and $\log(|\mathcal{M}_H|^2/|\mathcal{M}_{ZZ^*}|^2)$

- Expected statistical uncertainty of 340 MeV.
  - Validation on $Z \to 4\ell$ decays
  - Template fit as cross check method

Category	m_Z in simulation [GeV]	m_Z in data [GeV]
4μ	$91.19^{+0.41}_{-0.41}$	$91.46^{+0.42}_{-0.41}$
$4e$	$91.19^{+1.02}_{-1.03}$	$91.75^{+1.08}_{-1.06}$
$2\mu 2e$	$91.18^{+1.11}_{-1.11}$	$91.31^{+1.62}_{-1.33}$
$2e2\mu$	$91.19^{+0.90}_{-0.90}$	$92.49^{+0.91}_{-0.94}$
Combined	$91.19^{+0.34}_{-0.34}$	$91.62^{+0.35}_{-0.35}$

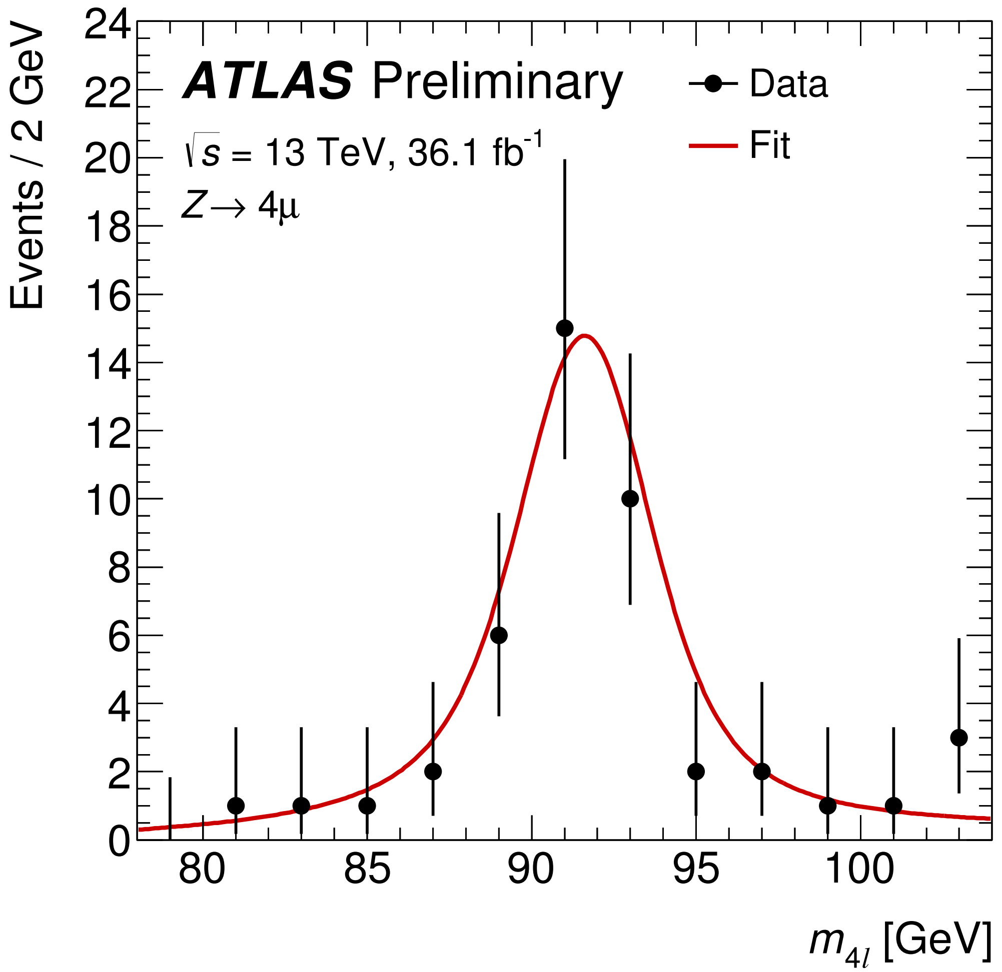

- Final estimate from 4x4 simultaneous un-binned fit
  - Four kinematic categories and four final states
- Systematic uncertainty of 50 MeV

Systematic effect	Uncertainty on $m_H^{ZZ^*}$ [MeV]
Muon momentum scale	40
Electron energy scale	20
Background modelling	10
Simulation statistics	8

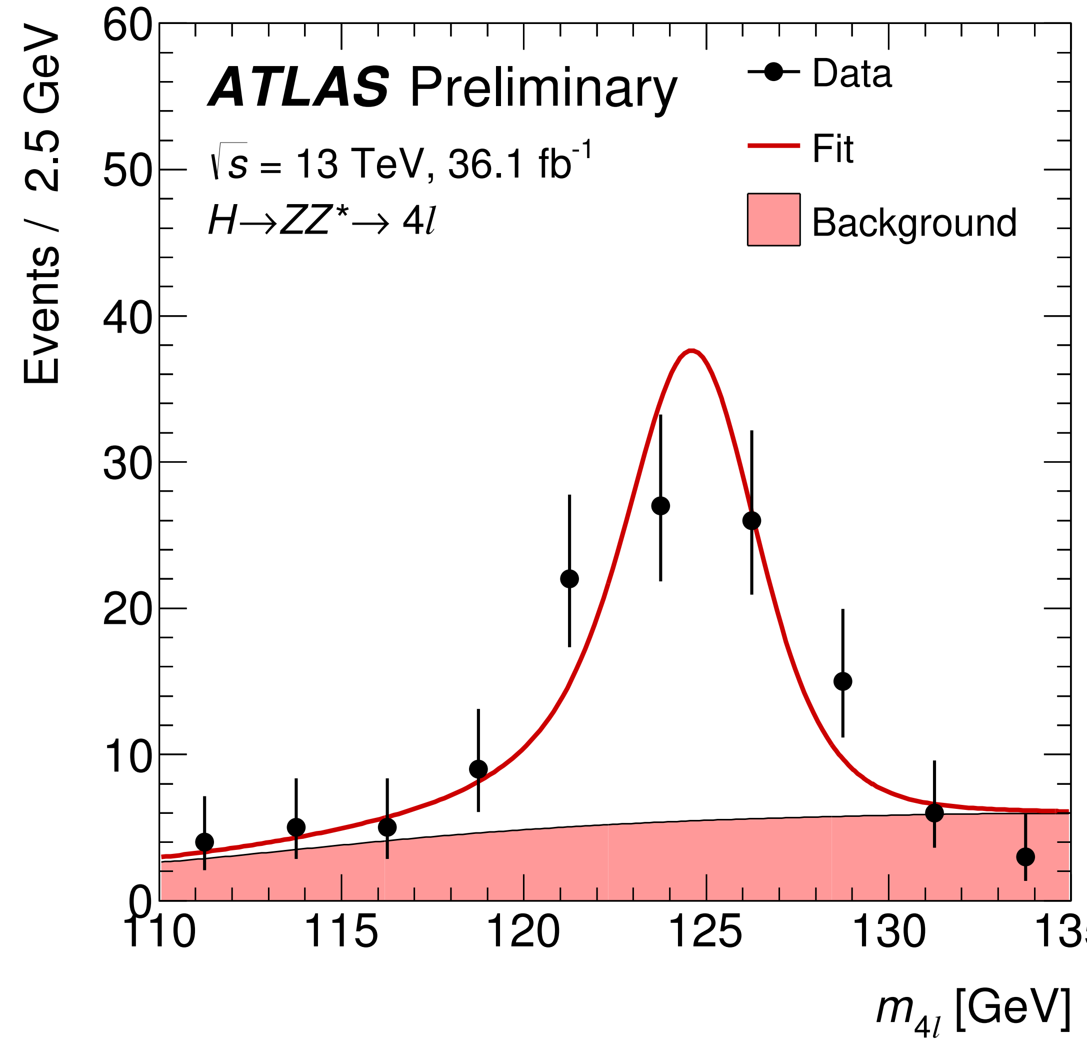

  - Energy (20 MeV) and momentum (40 MeV) scale dominate
- Result:

$$m_H^{ZZ^*} = 124.88 \pm 0.37\ (\text{stat}) \pm 0.05\ (\text{syst})\ \text{GeV}$$

  - 25% improved precision with respect to Run I ATLAS Combination.

- $H\to\gamma\gamma$ updated result at Run II.
  - Analytical function in kinematic and detector categories.
  - Reduction of uncertainty through categorisation of events as a function of resolution and signal significance.
- Expected statistical uncertainty of 0.25 GeV and 0.33 GeV systematic uncertainty

$$m_H^{\gamma\gamma} = 125.11 \pm 0.21\ (\text{stat}) \pm 0.36\ (\text{syst})\ \text{GeV}$$

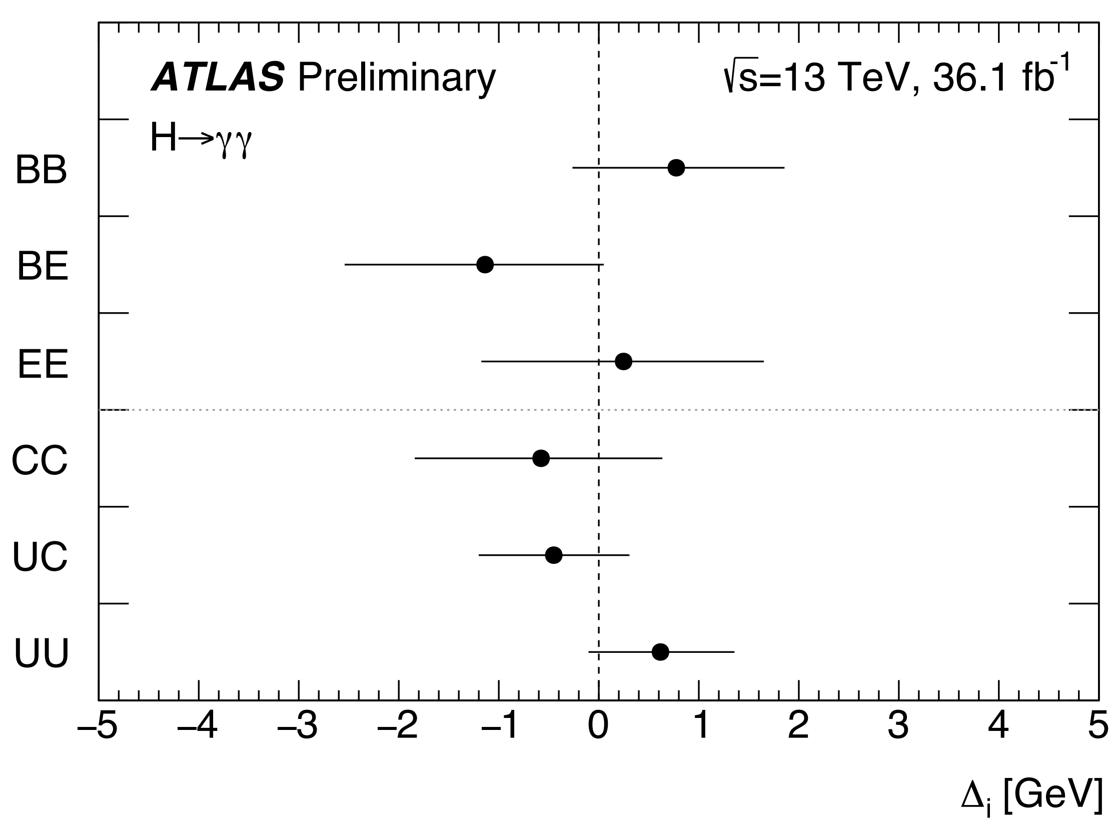

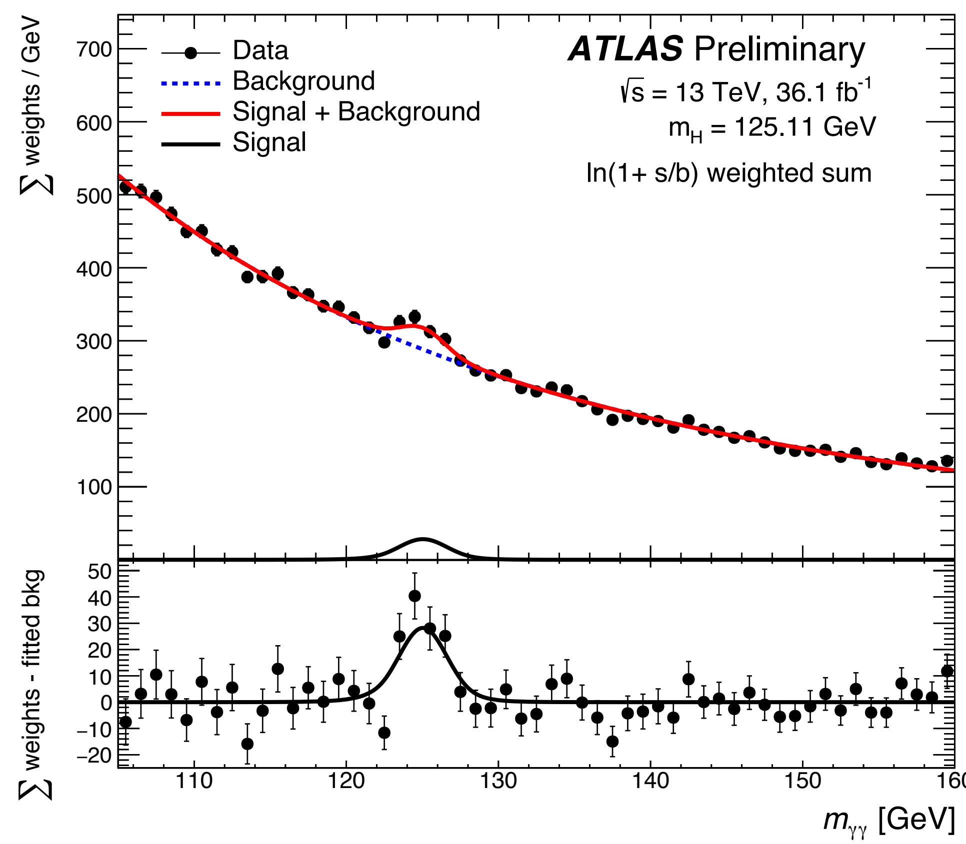

- $H\rightarrow\gamma\gamma$ updated result at Run II.
  - Analytical function in kinematic and detector categories.
  - Reduction of uncertainty through categorisation of events as a function of resolution and signal significance.

- Expected statistical uncertainty of 0.25 GeV and 0.33 GeV systematic uncertainty

$$m_H^{\gamma\gamma} = 125.11 \pm 0.21\ (\text{stat}) \pm 0.36\ (\text{syst})\ \text{GeV}$$

Source	Systematic uncertainty on $m_H^{\gamma\gamma}$ [MeV]
LAr cell non-linearity	± 200
LAr layer calibration	± 190
Non-ID material	± 120
Lateral shower shape	± 110
ID material	± 110
Conversion reconstruction	± 50
$Z \rightarrow ee$ calibration	± 50
Background model	± 50
Primary vertex effect on mass scale	± 40
Resolution	$^{+20}_{-30}$
Signal model	± 20

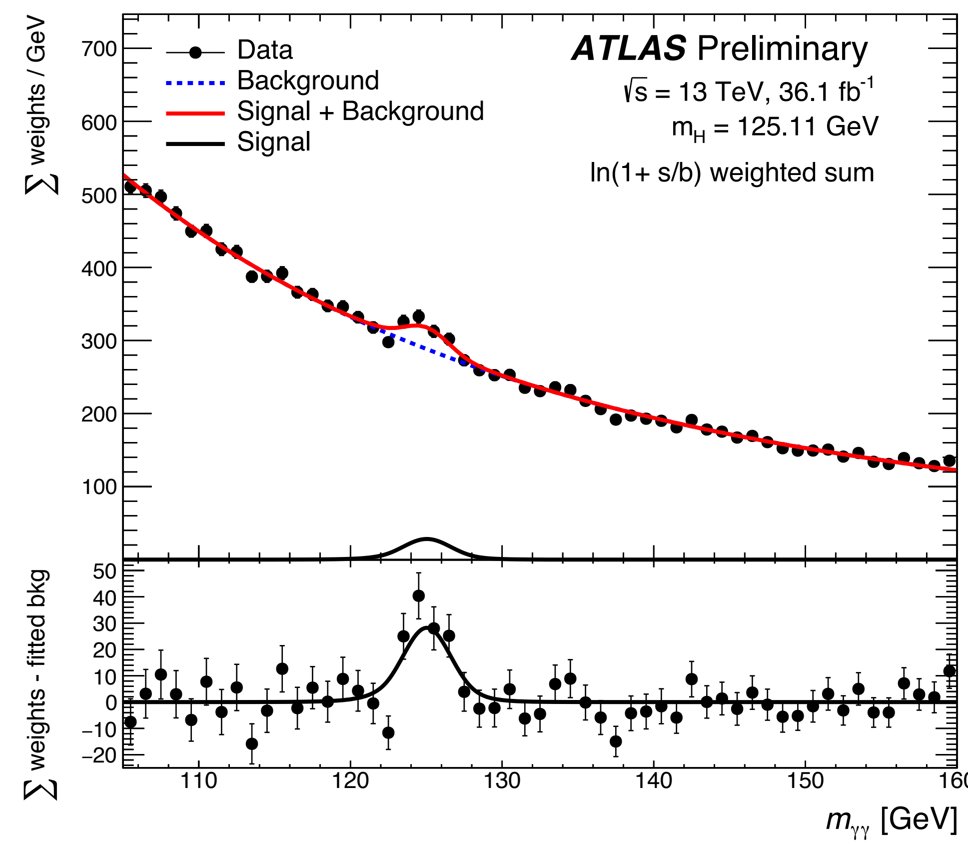

- Combination with m_H^{ZZ*}
  - Precision comparable to ATLAS + CMS LHC Run 1 combination
  - Measurement precision of 2 per mille.

$$m_H = 124.98 \pm 0.19\ (\text{stat}) \pm 0.21\ (\text{syst})\ \text{GeV}$$

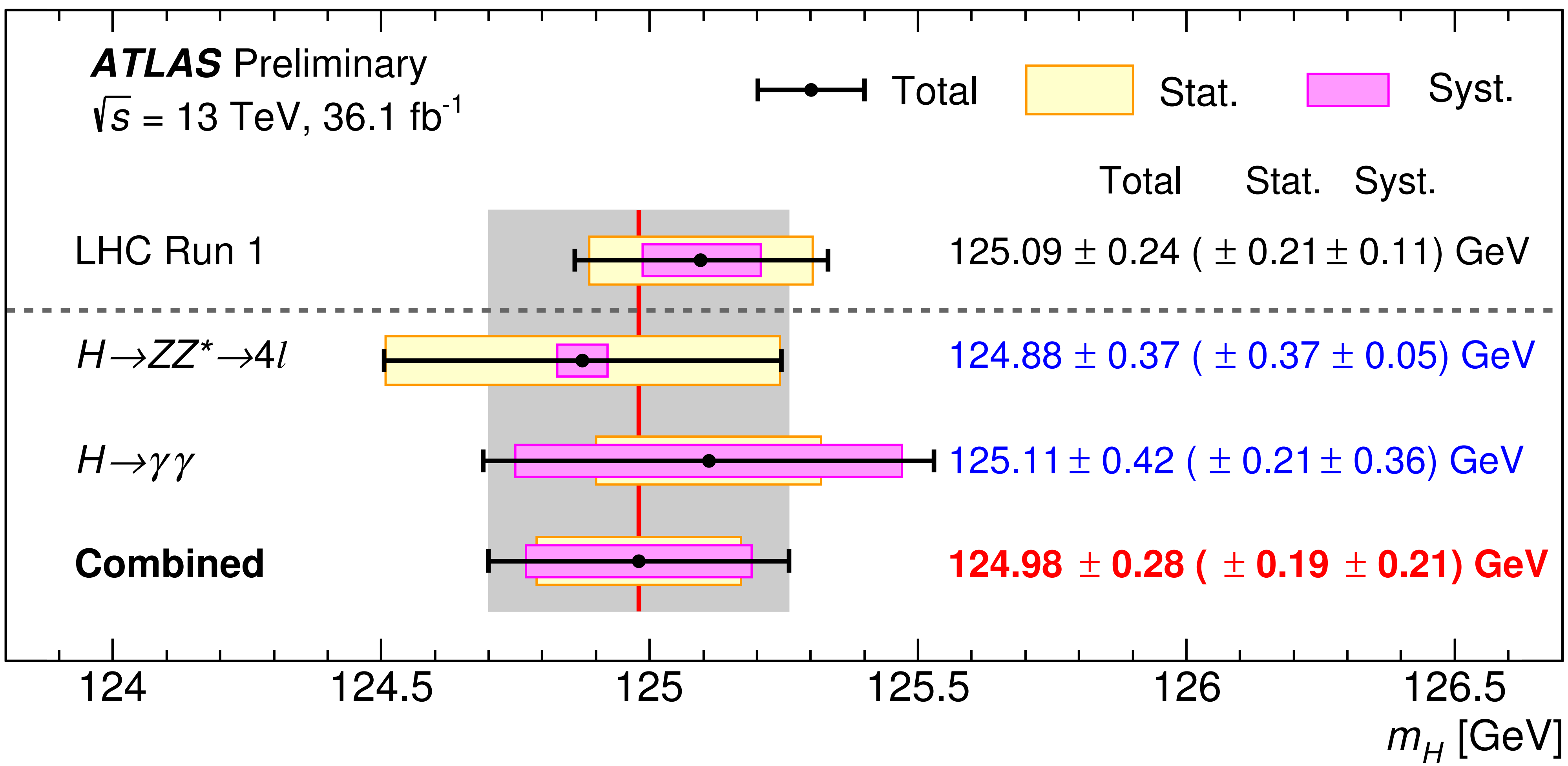

- Updated m_H measurement with Run-2 data.
  - With 4ℓ channel alone.
- Strategy of "3D" fit:
  - Leading lepton pair constrained to m_Z (-8%);
  - Matrix element discriminant for background rejection (-3.2%)
  - Propagation of per-lepton tracking and ECAL uncertainties to $m_{4\ell}$ (8%)

Similar to ATLAS

Per-event resolution prediction in ATLAS

- Result
  - Expectation of ± 0.23 (stat) ± 0.08 (sys) GeV.
    - ✦ p-value of uncertainty of 0.03

$$m_H = 125.26 \pm 0.20\ (\text{stat.}) \pm 0.08 (\text{sys.})\ \text{GeV}$$

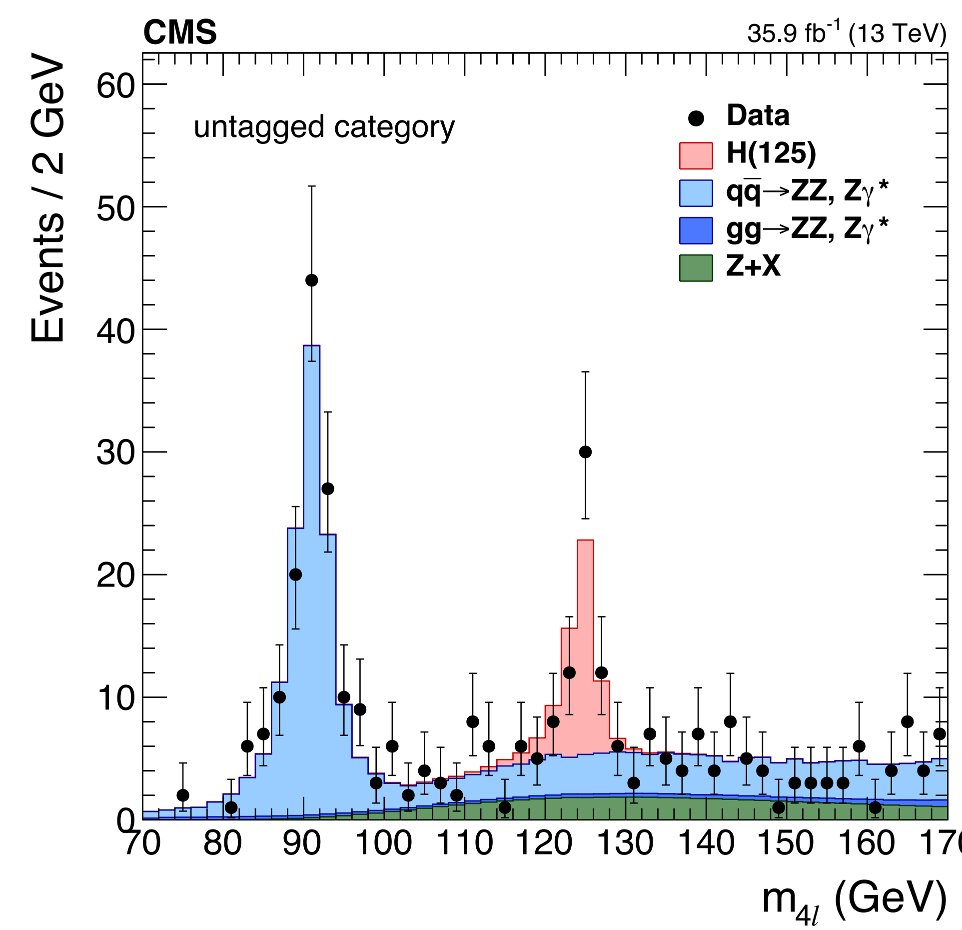

- Resolution is better than for ATLAS
  - ✦ expected from solenoidal magnetic field.
- Muon momentum scale uncertainty on lepton modelling ~1.6 times higher than ATLAS

Comparison with CMS

- Updated m_H measurement with Run-2 data.
  - With 4ℓ channel alone.
- Strategy of "3D" fit:
  - Leading lepton pair constrained to m_Z (-8%);
  - Matrix element discriminant for background rejection (-3.2%)
  - Propagation of per-lepton tracking and ECAL uncertainties to $m_{4\ell}$ (8%)

Similar to ATLAS (first two items)

Per-event resolution prediction in ATLAS (third item)

- Result
  - Expectation of ± 0.23 (stat) ± 0.08 (sys) GeV.
    - p-value of uncertainty of 0.03

$$m_H = 125.26 \pm 0.20\ (\text{stat.}) \pm 0.08 (\text{sys.})\ \text{GeV}$$

  - Resolution is better than for ATLAS
    - expected from solenoidal magnetic field.
  - Muon momentum scale uncertainty on lepton modelling ~1.6 times higher than ATLAS

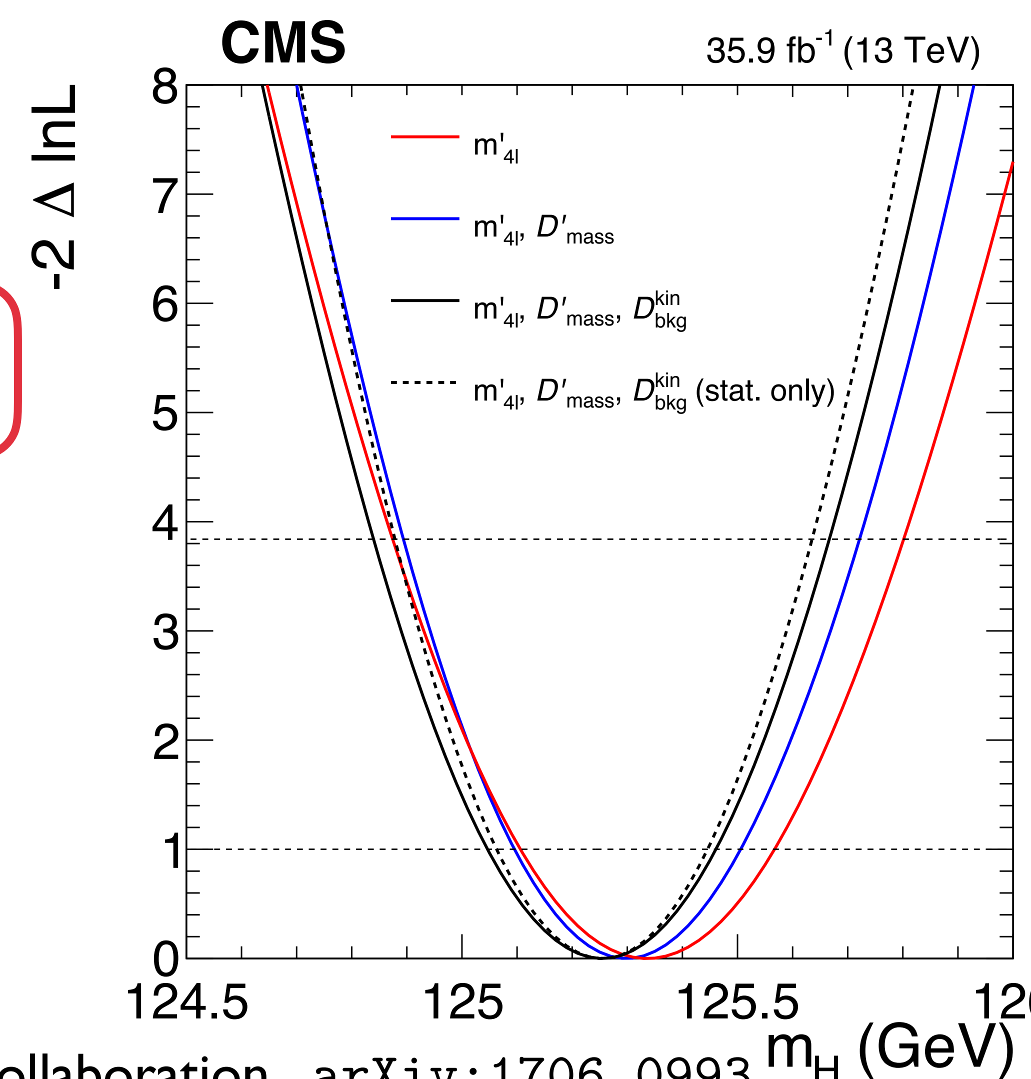

CMS Collaboration, arXiv:1706.0993

5. Differential cross section measurements

Inclusive cross section → Differential cross section

- At Run II sufficient statistics for constraining differential measurements
- Inclusive (fiducial) cross sections from all diboson channels
- Measurements dominated by statistical uncertainty

Channel	Statistical	Systematic
$H \to ZZ^*$	15%	7%
$H \to \gamma\gamma$	16%	7%
$H \to WW^*$	10%	15%

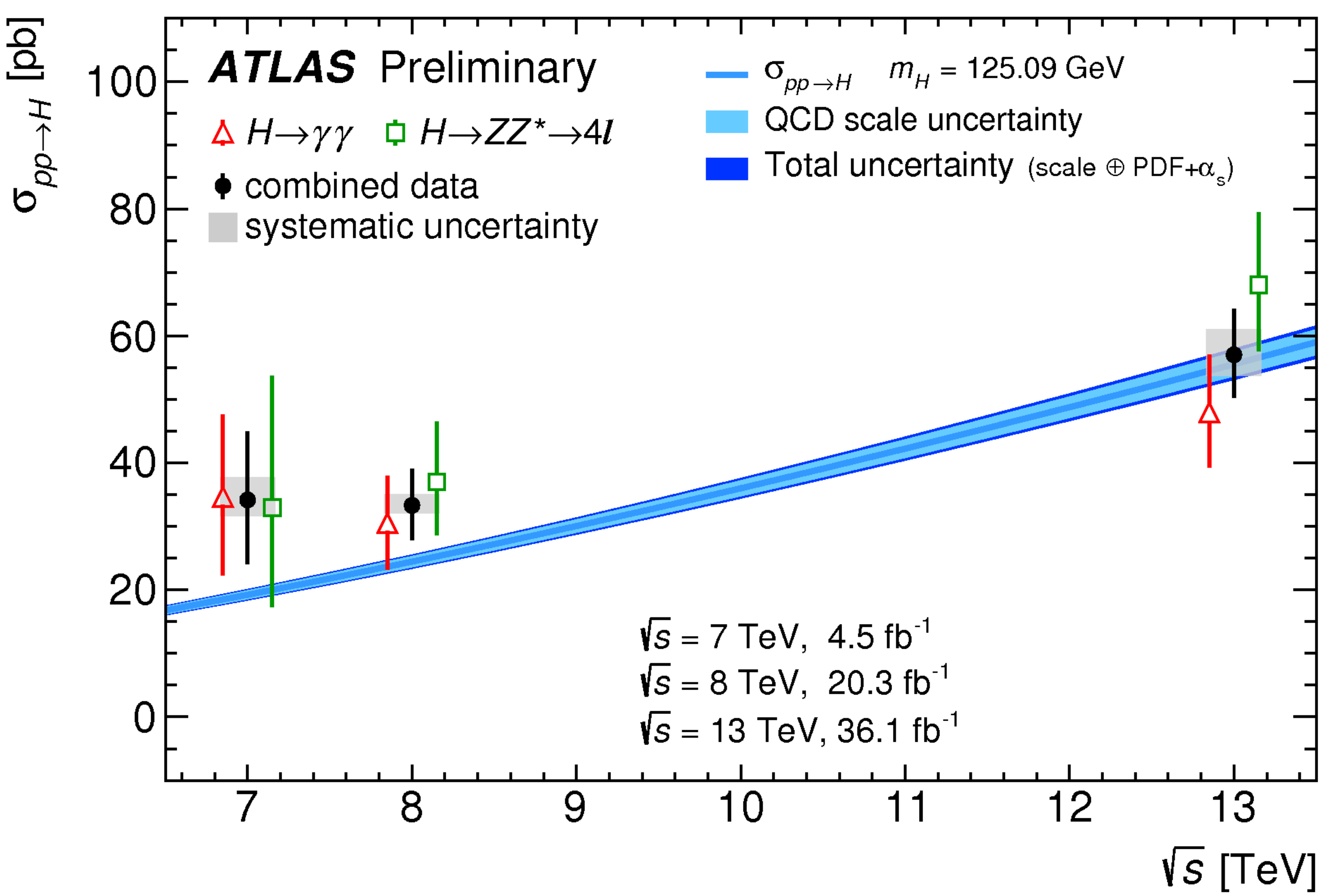

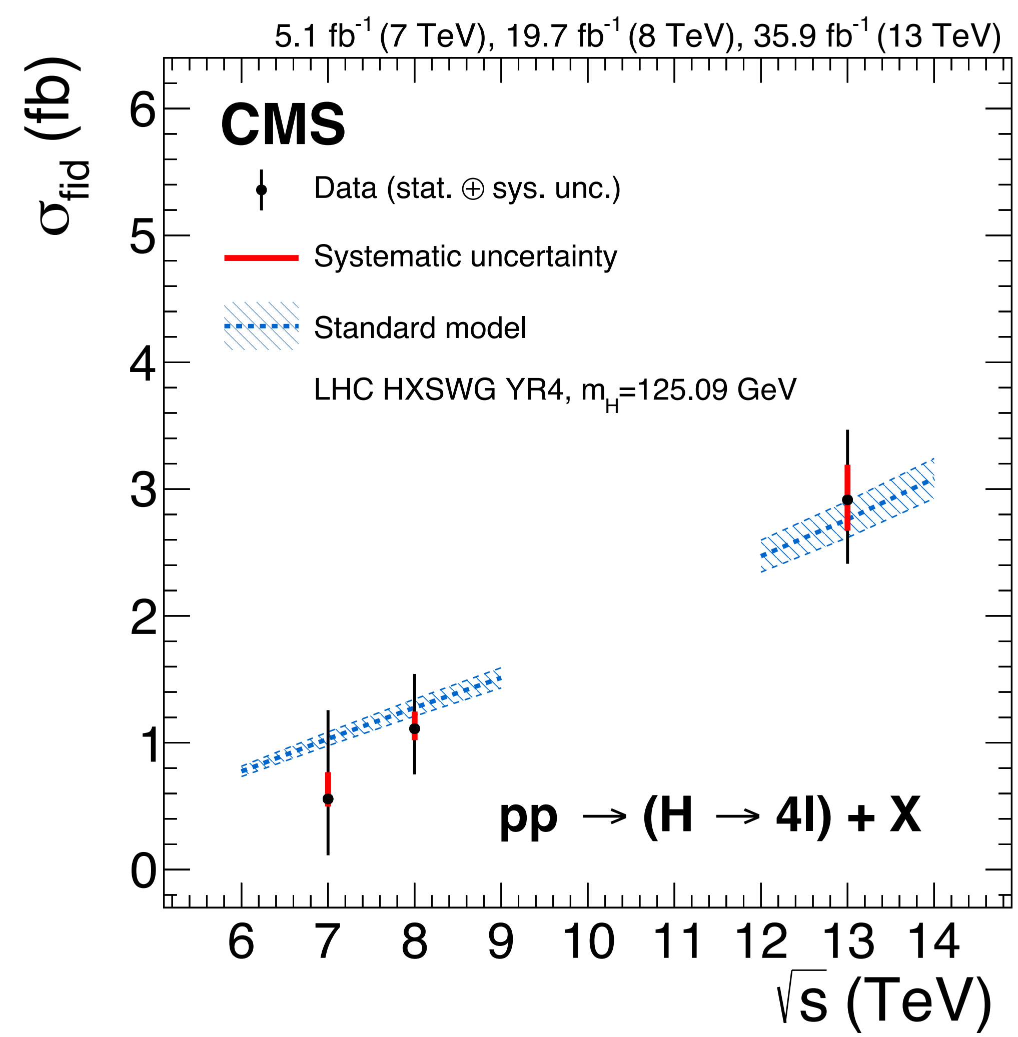

- Inclusive fiducial cross sections:

$$H\to ZZ \quad 3.62 \pm 0.50\,(\text{stat})\,^{+0.25}_{-0.20}\,(\text{sys})\ \text{fb},$$
$$H\to\gamma\gamma \quad 55 \pm 9\,(\text{stat.}) \pm 4(\text{sys.}) \pm 0.1(\text{theo.})\ \text{fb}$$

- For ZZ also cross section per final state
  - Eventually sensitivity to final state interference (10%) in same flavour quadruplets

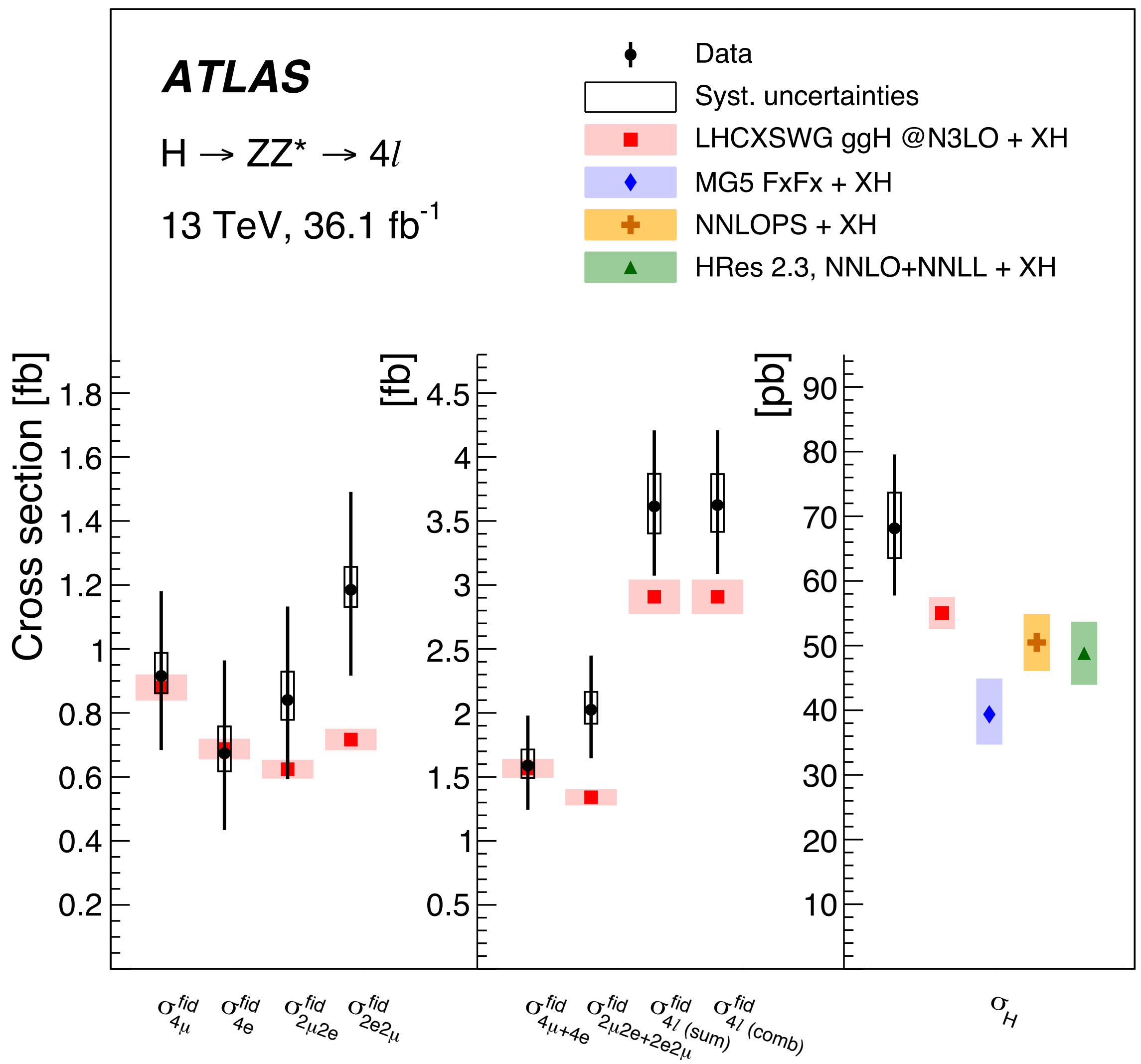

- γγ also targeting inclusive fiducial regions sensitive to VBF production:
  - m_{jj}> 400 GeV and $|\Delta y_{jj}|$ > 2.8

Fiducial region	Measured cross section
Diphoton fiducial	55 ± 9 (stat.) ± 4 (exp.) ± 0.1 (theo.) fb
VBF-enhanced	3.7 ± 0.8 (stat.) ± 0.5 (exp.) ± 0.2 (theo.) fb

Fiducial region	SM prediction	
Diphoton fiducial	64 ± 2 fb	[N^{3}LO + XH]
VBF-enhanced	2.3 ± 0.1 fb	[default MC + XH]

Higgs boson kinematics — Differential cross section

- Higgs boson $p_{T,4\ell}$ and rapidity ($y_{4\ell}$) probe:
  - $p_{T,4\ell}$: Lagrangian structure of H interactions.
  - $y_{4\ell}$: Sensitivity to proton's parton density functions.
- Agreement from different computations:
  - models normalised to N3LO prediction: p-values > 20%
  - good agreement with the pdf set

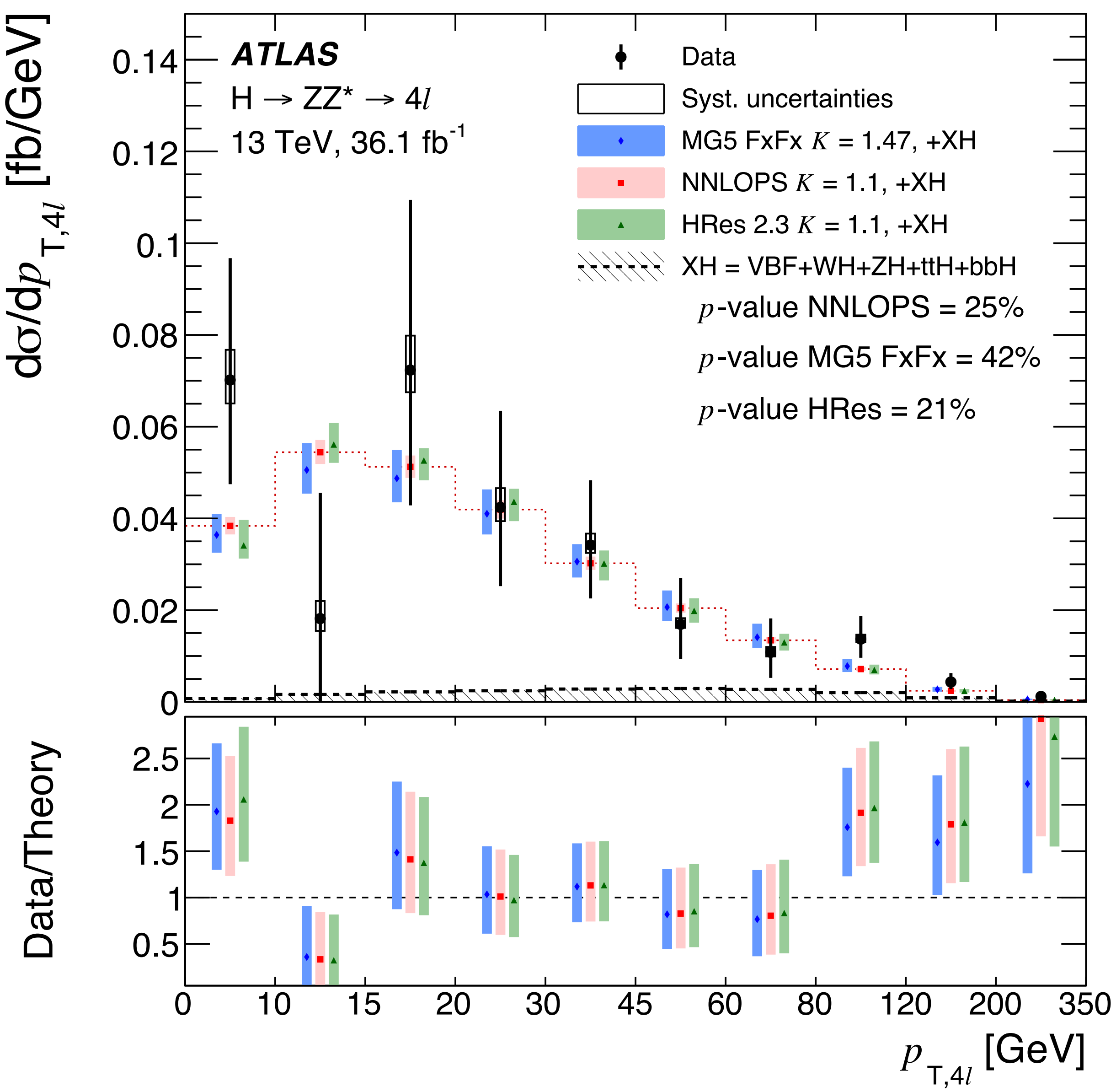

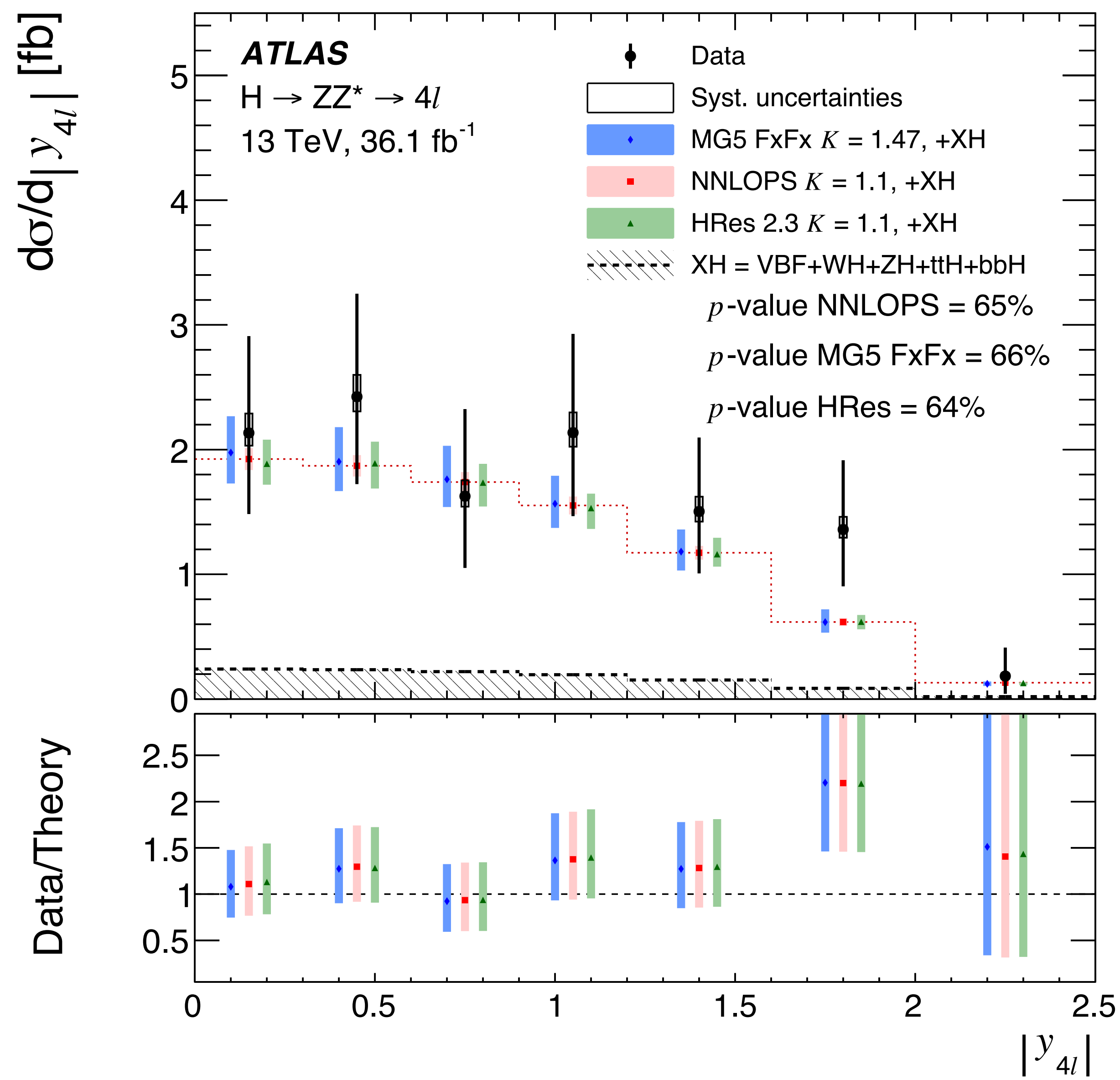

- Higgs boson $p_{T,4\ell}$ and rapidity ($y_{4\ell}$) probe:
  - $p_{T,4\ell}$: Lagrangian structure of H interactions.
  - $y_{4\ell}$: Sensitivity to proton's parton density functions.
- Agreement from different computations:
  - models normalised to N3LO prediction: p-values > 20%
  - good agreement with the pdf set

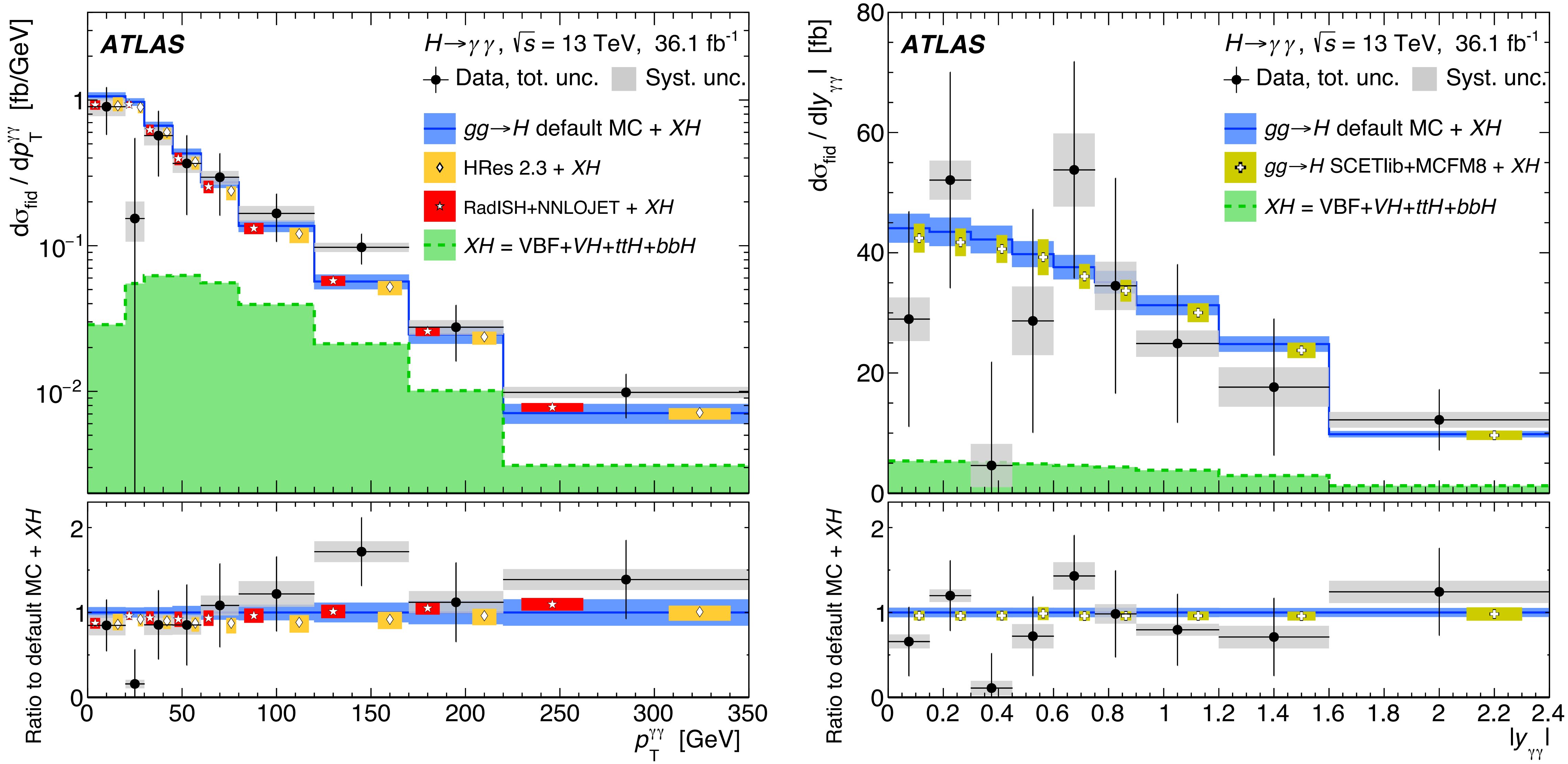

- Jet multiplicity (N_j) with jet p_T
  - modelling of high-p_T quark kinematics

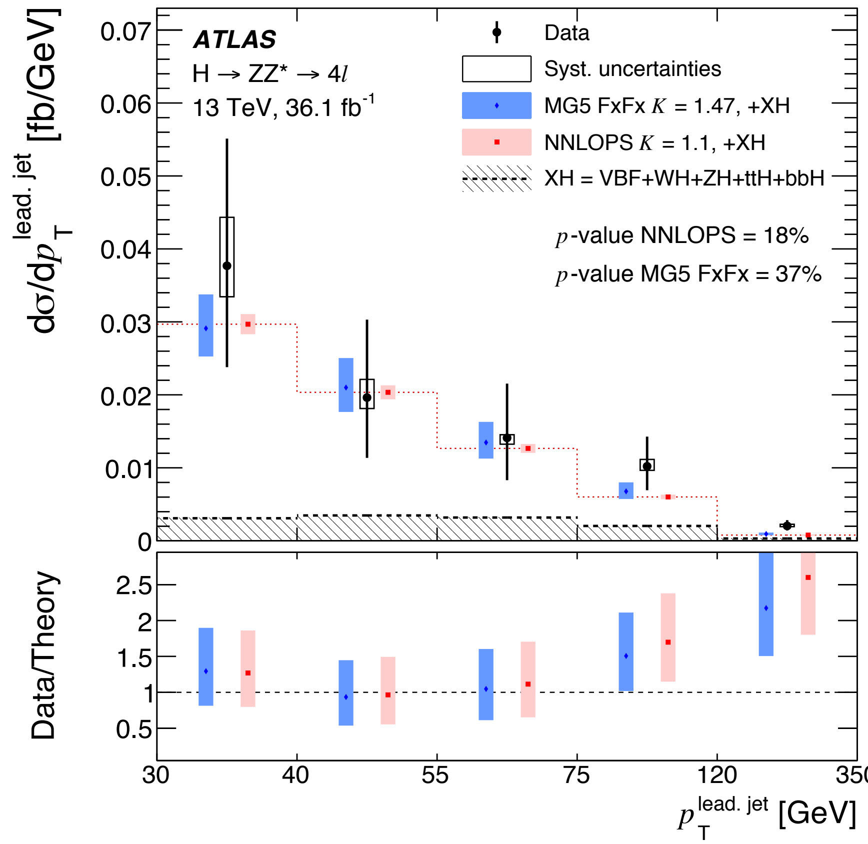

- Double differential $\mathrm{d}^2\sigma/\mathrm{d}p_\mathrm{T}\mathrm{d}N_\mathrm{J}$:
  - Probe the Higgs production mode
  - Nj = 0 dominated buy ggF production
  - Nj > 1 VBF enriched production

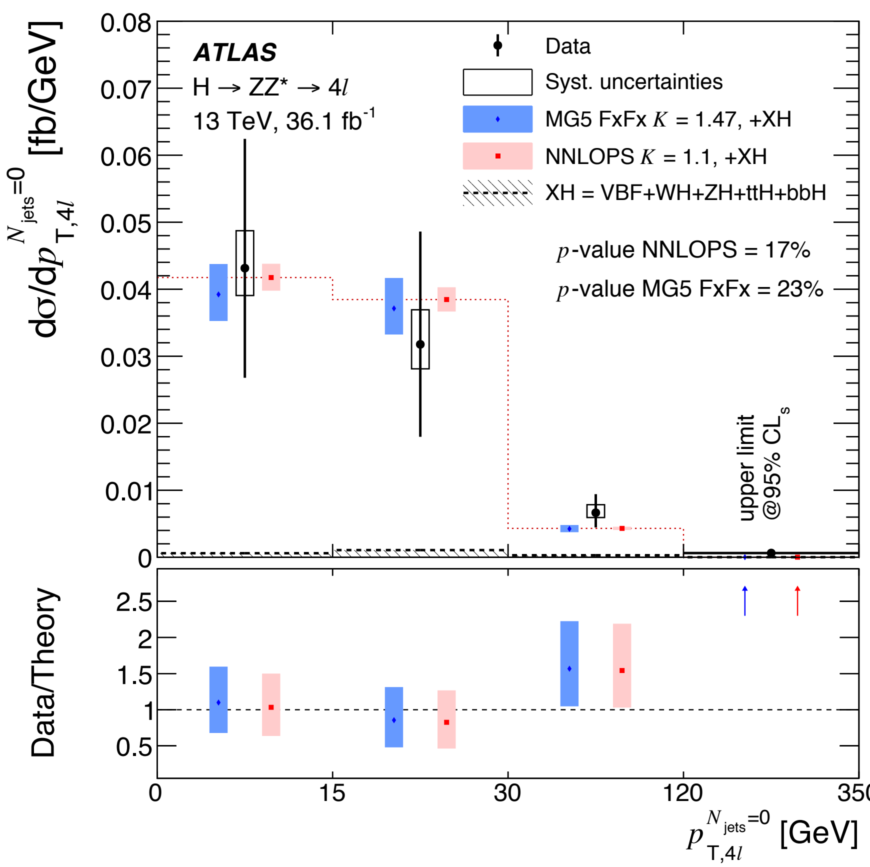

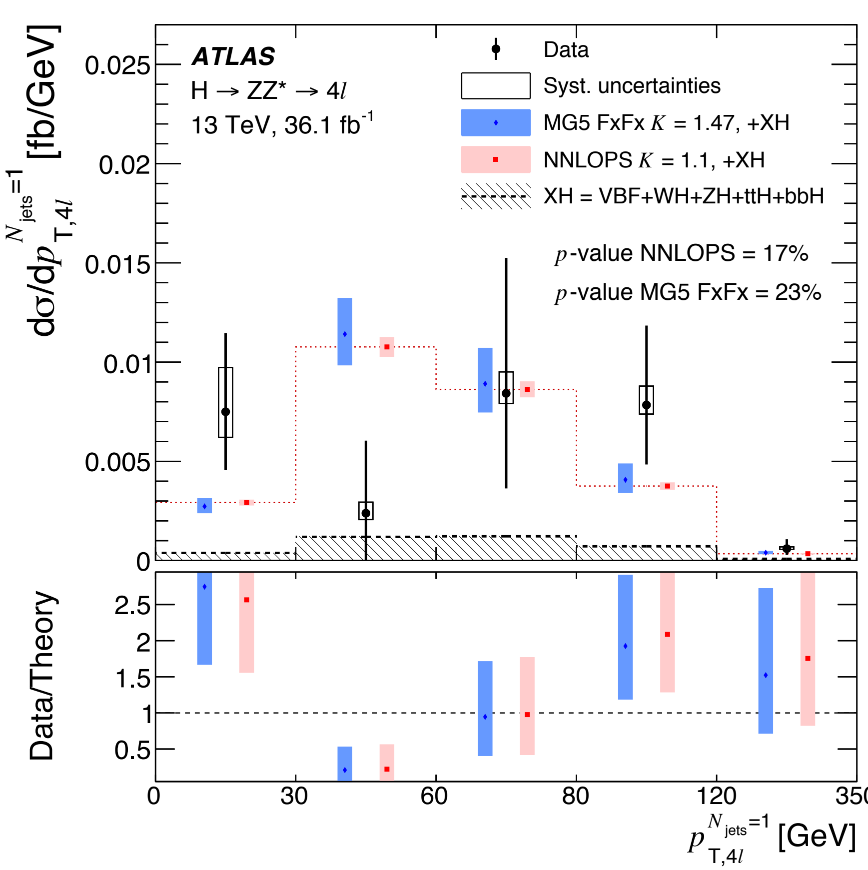

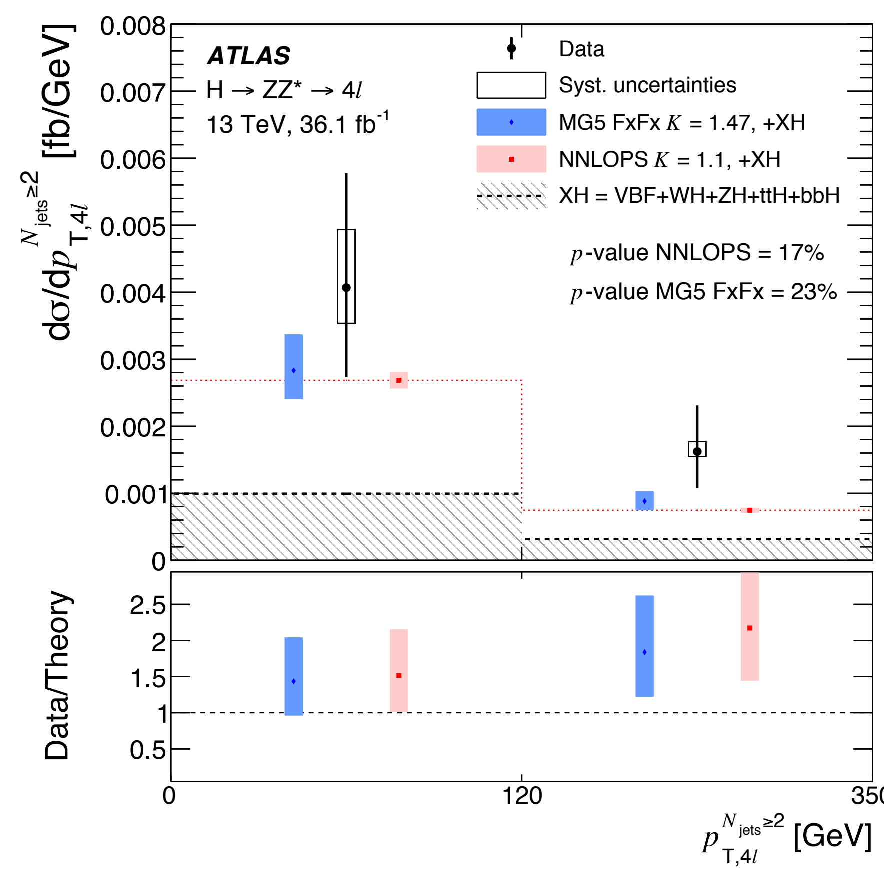

- Jet multiplicity (N_j) with jet p_T
  - modelling of high-p_T quark kinematics

- Double differential $d^2\sigma/dp_T dN_J$:
  - Probe the Higgs production mode
  - Nj = 0 dominated buy ggF production
  - Nj > 1 VBF enriched production

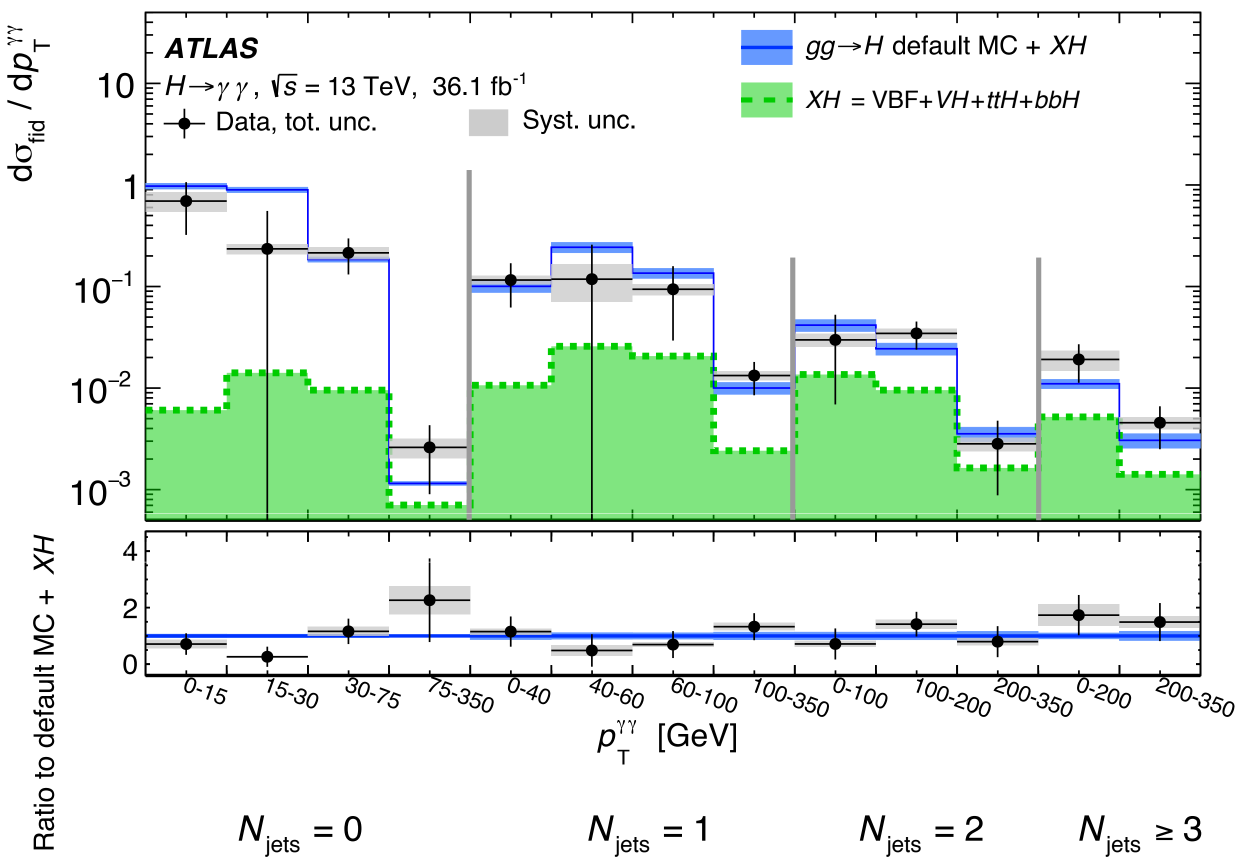

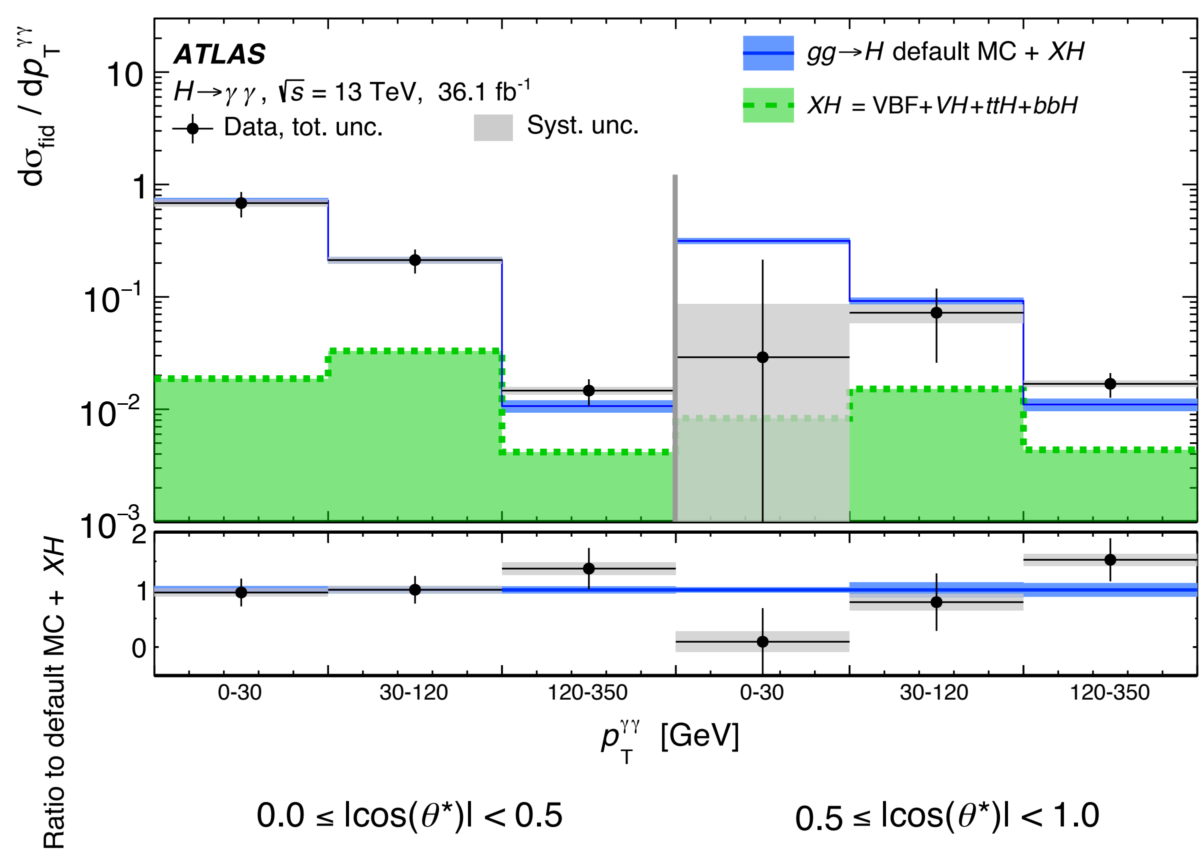

6. Production mode measurements

- Measurement of cross sections sensitive to:
  - (i) production modes and
  - (ii) probes of BSM contributions in tensor couplings.
- Strategy is classification into exclusive event categories (truth level)

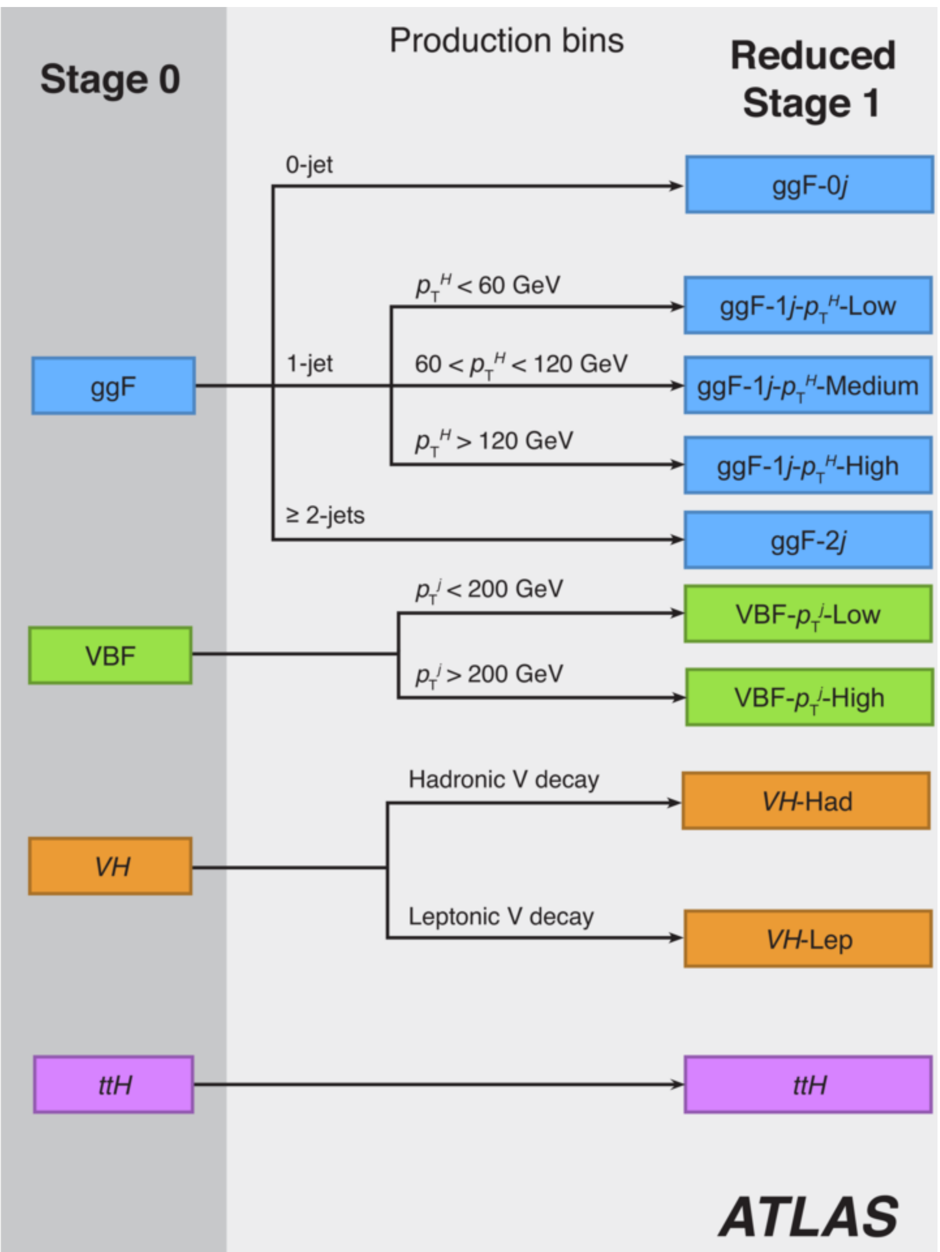

coupling modifiers

EFT coefficients

BSM

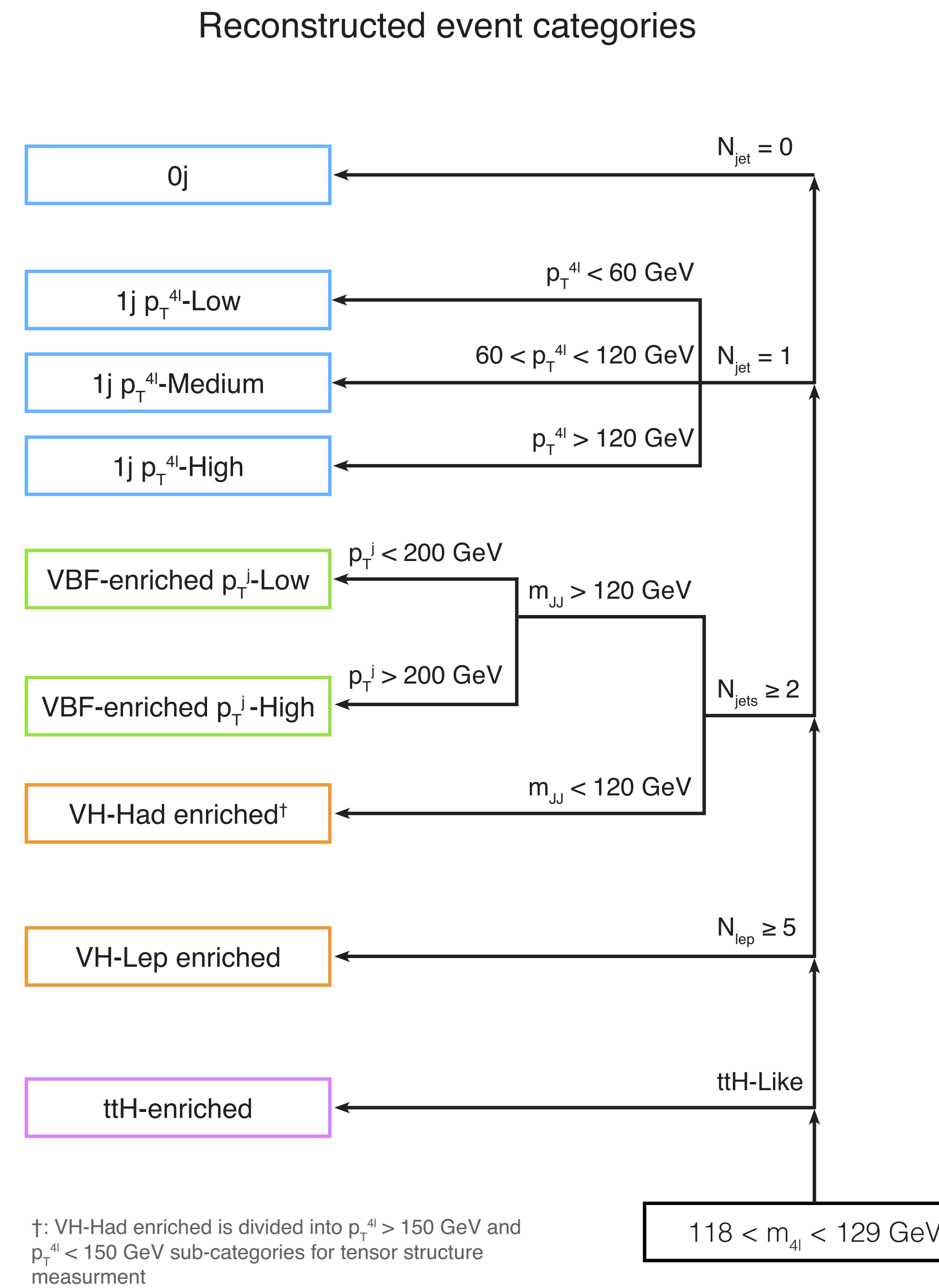

- Measurement of cross sections sensitive to:
  - (i) production modes and
  - (ii) probes of BSM contributions in tensor couplings.
- Strategy is classification into exclusive event categories (truth level)
  - Categories with high purities and small contamination from other fiducial regions.

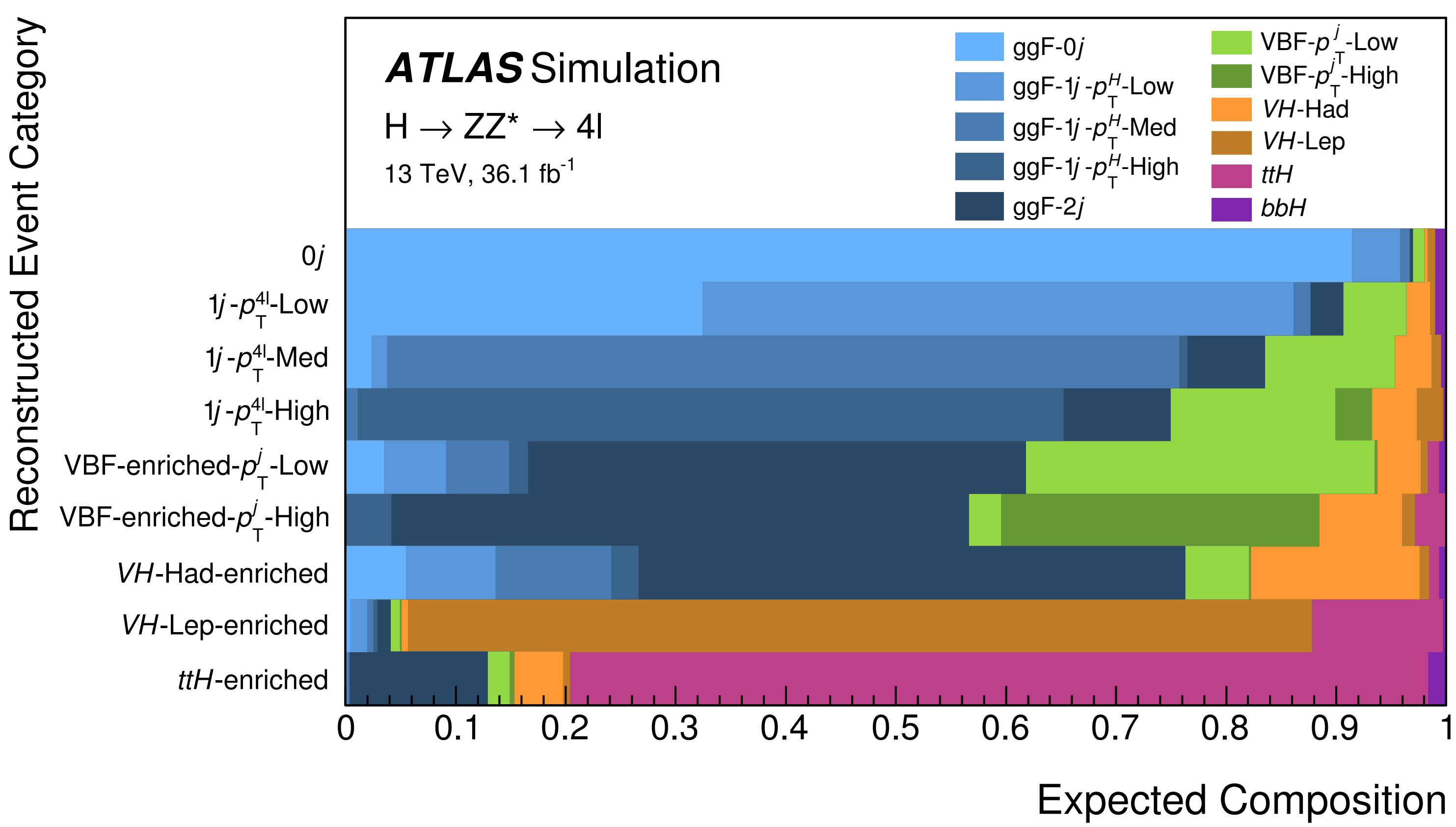

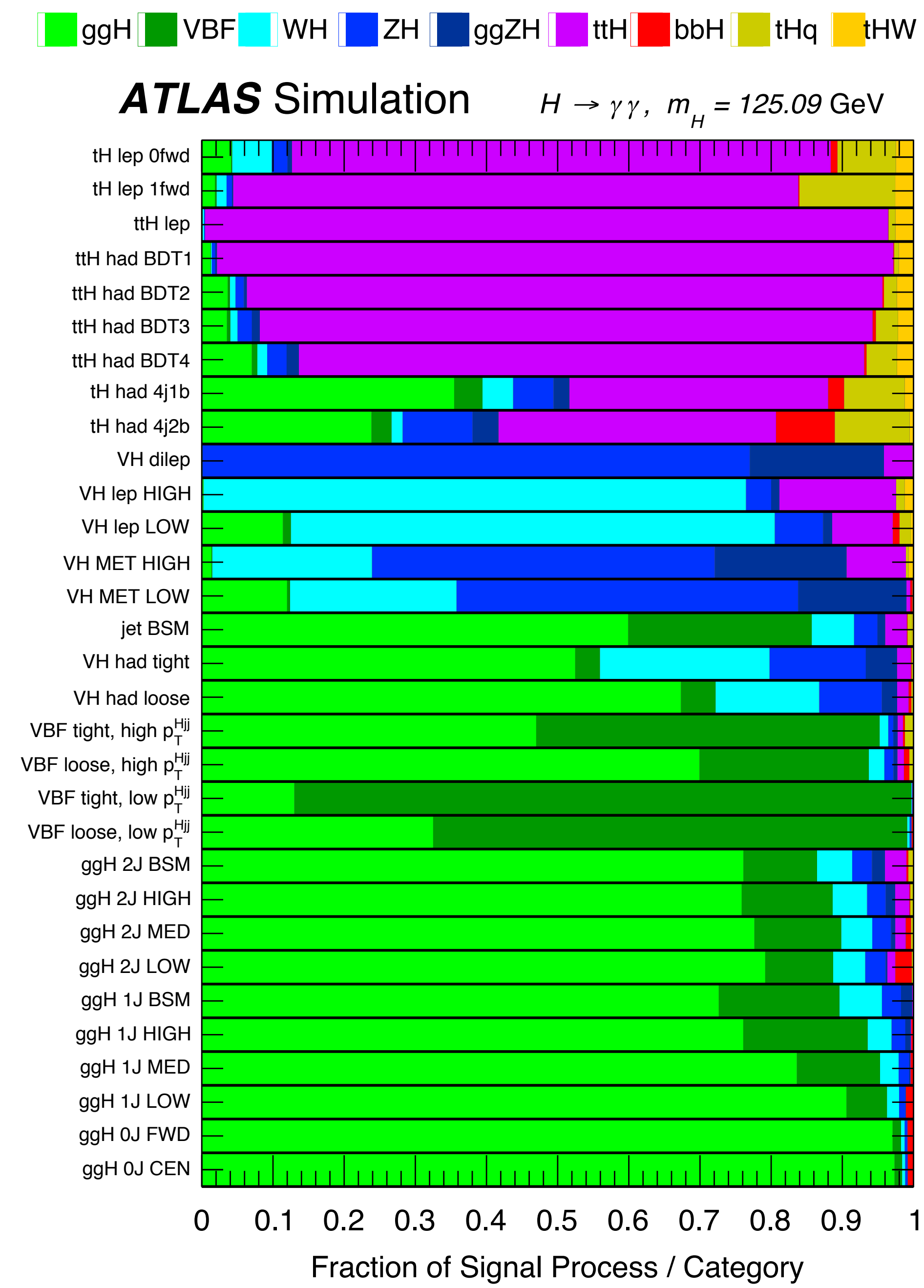

- Cut based classification of events into category.
  - Ex. Jet multiplicity (ggF), m_{jj} for (VBF) and b-tagging ($t\bar{t}\ H$)
- and multivariate analysis (BDT) to discriminate contributions.
  - ggF from ZZ^*, VBF from ggF, $\mathrm{VH(had)}$ from all.
  - Variables: $p_{\mathrm{T},4\ell}$, KD, η_{j}, $\Delta\eta_{\mathrm{jj}}$, $p_{\mathrm{T},j}$ etc.
- Detector and theoretical uncertainties

(i) Luminosity 3.2%

(ii) Lepton Identification <2%

(iii) Pileup ~2%

(iv) Jet Energy Scale (3%-7%)

(v) Jet Energy Resolution (2%-4%)

(i) μ_R and μ_F about 4% to 30%

(ii) ggF prediction in N_J categories.

(iii) (BSM only NLO/LO prediction)

$H \to ZZ \to 4\ell$ results

Production mode

- Simultaneous fit to all template cross sections
  - Extraction of global signal strength ($\mu = \sigma^{obs} / \sigma^{exp}$).

$$\mu = 1.29 \;^{+0.18}_{-0.17}\,(\text{stat.}) \;^{+0.07}_{-0.06}(\text{sys.}) \;\pm\; 0.03(\text{theo.})\;\text{fb}$$

- Extraction of individual category cross sections

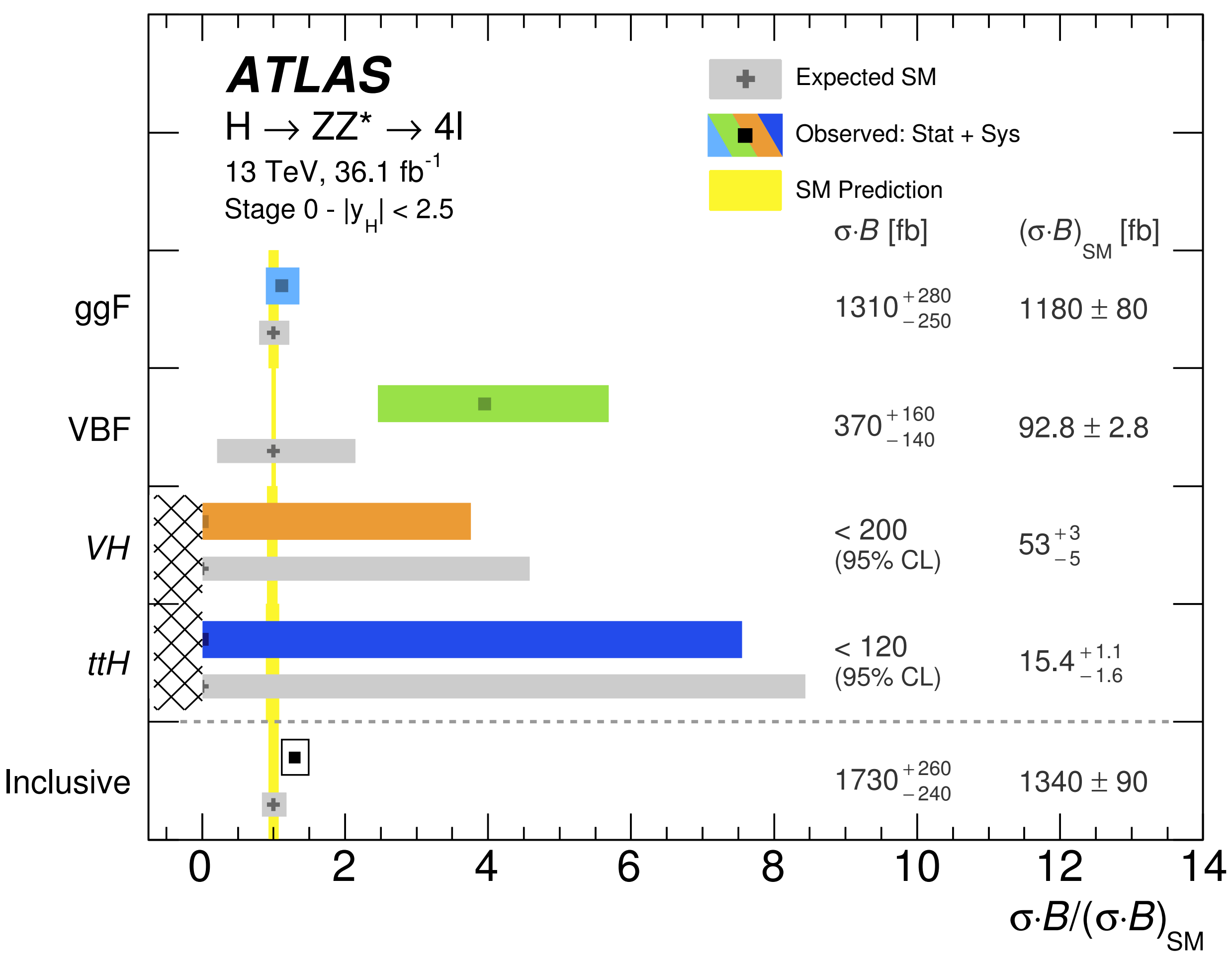

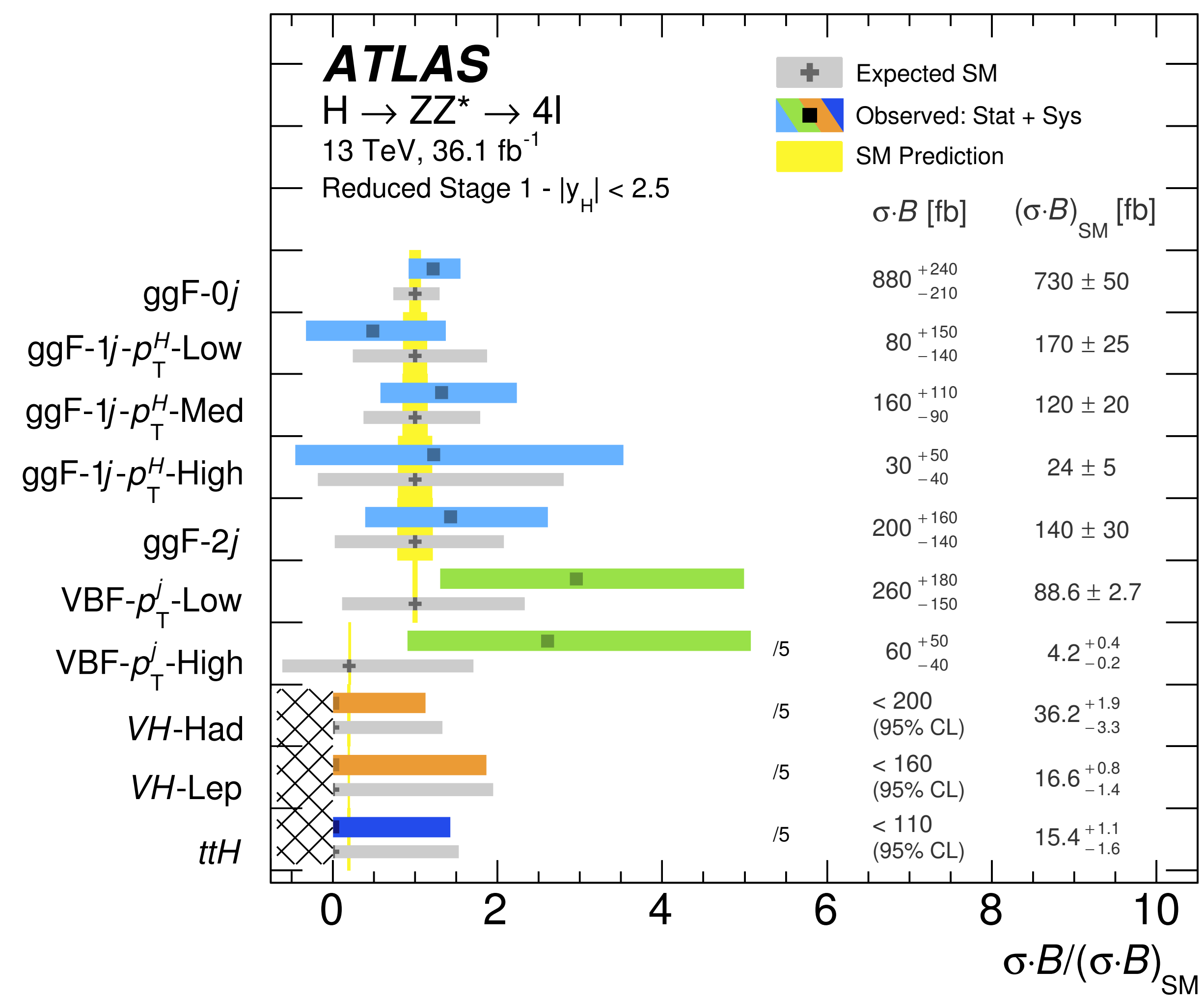

- Simultaneous fit to all template cross sections
  - Extraction of global signal strength ($\mu=\sigma^{obs}/\sigma^{exp}$).

$$\mu = 0.99 \pm 0.12\,(\text{stat.})\,^{+0.06}_{-0.05}\,(\text{exp.})\,^{+0.07}_{-0.05}\,(\text{theo.})$$

- Extraction of individual category cross sections

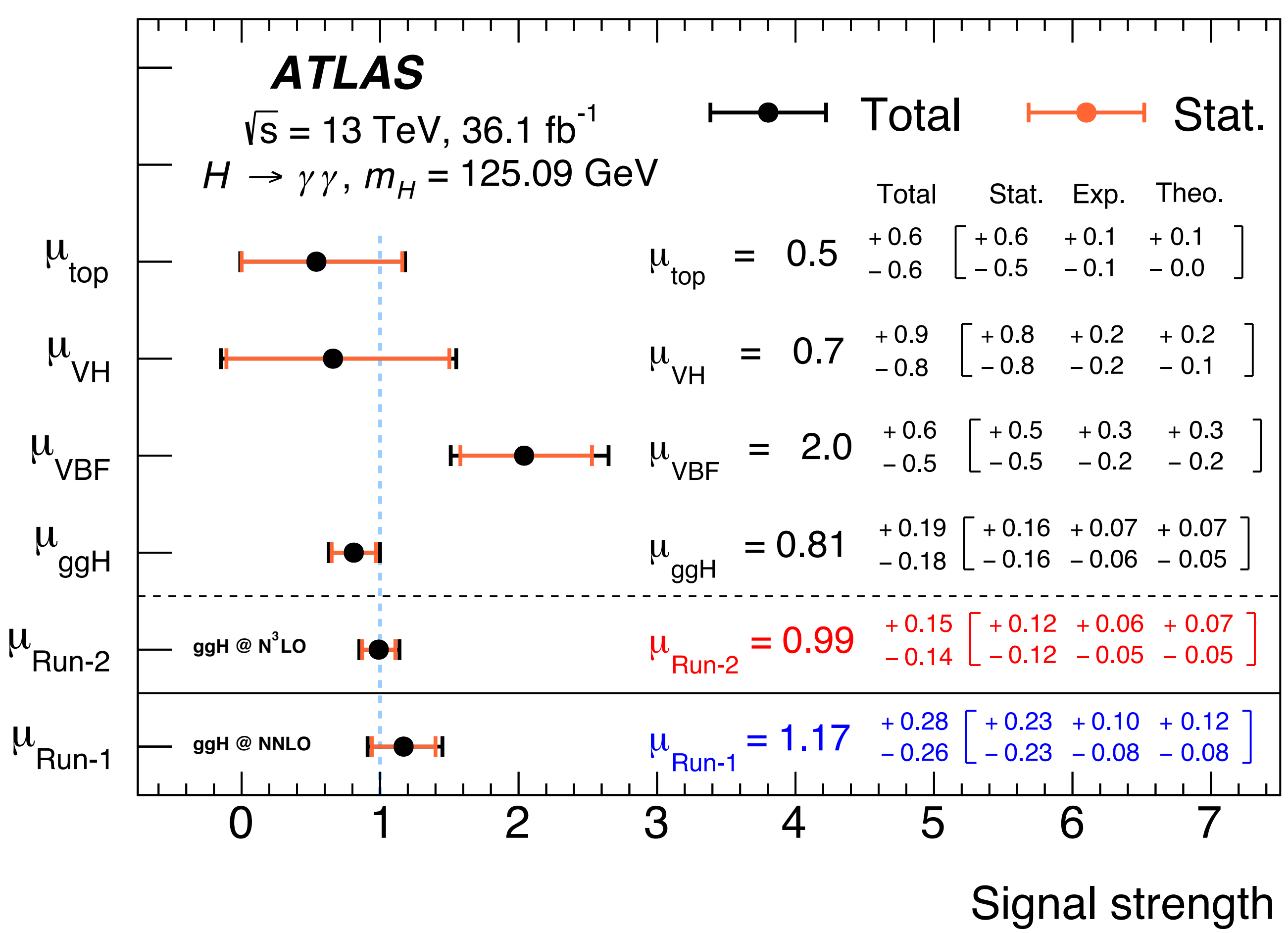

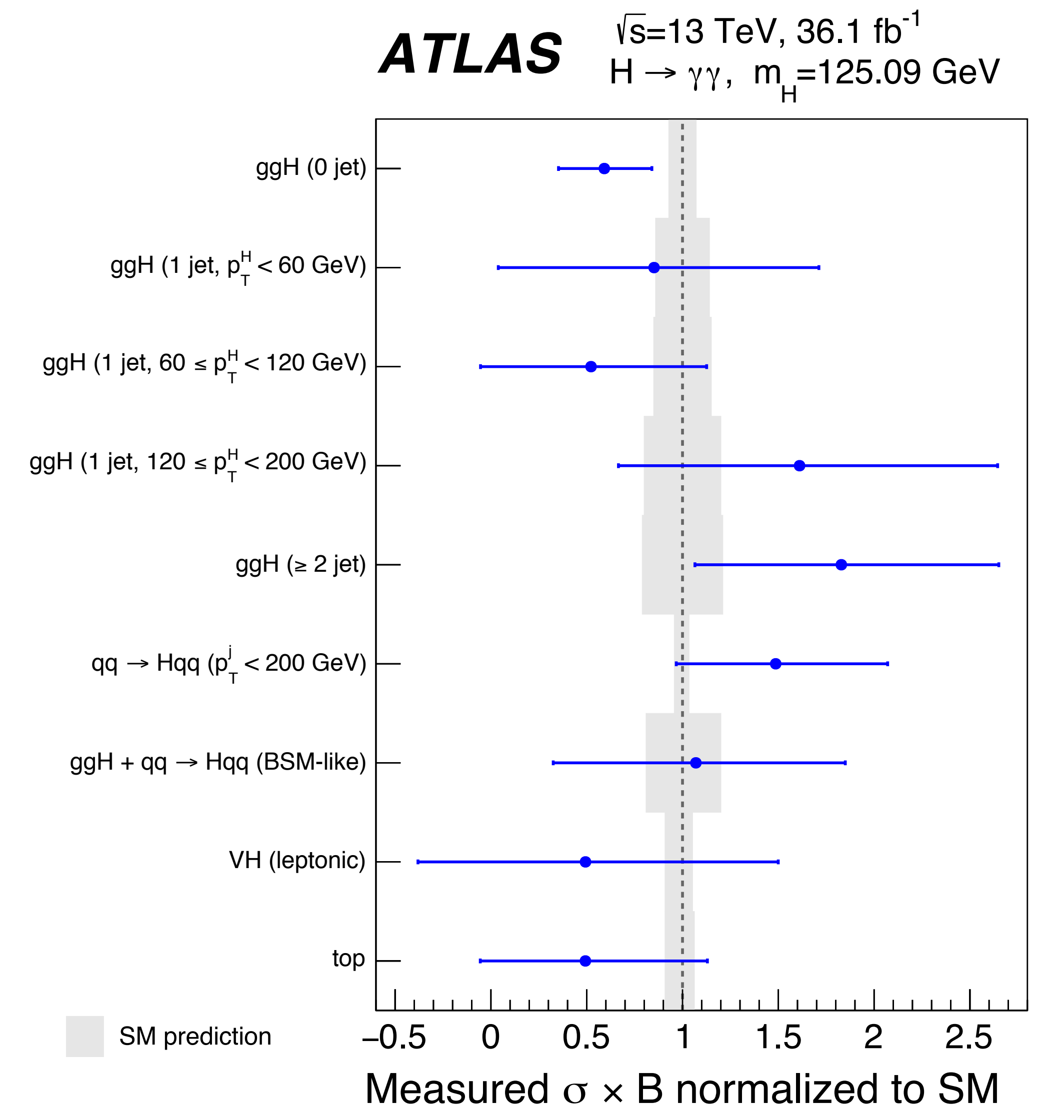

$WW^* \to \ell\bar{\nu}\ell\nu$ results

- Simultaneous fit to the ggF and VBF categories.
  - Over m_T for ggF and BDT response for ggF
  - Extraction of ggF and VBF total cross sections

$$\mu_{\mathrm{ggF}} = 1.21^{+0.12}_{-0.11}(\mathrm{stat.})^{+0.18}_{-0.17}(\mathrm{sys.})$$

$$\mu_{\mathrm{VBF}} = 0.62^{+0.30}_{-0.28}(\mathrm{stat.}) \pm 0.22(\mathrm{sys.})$$

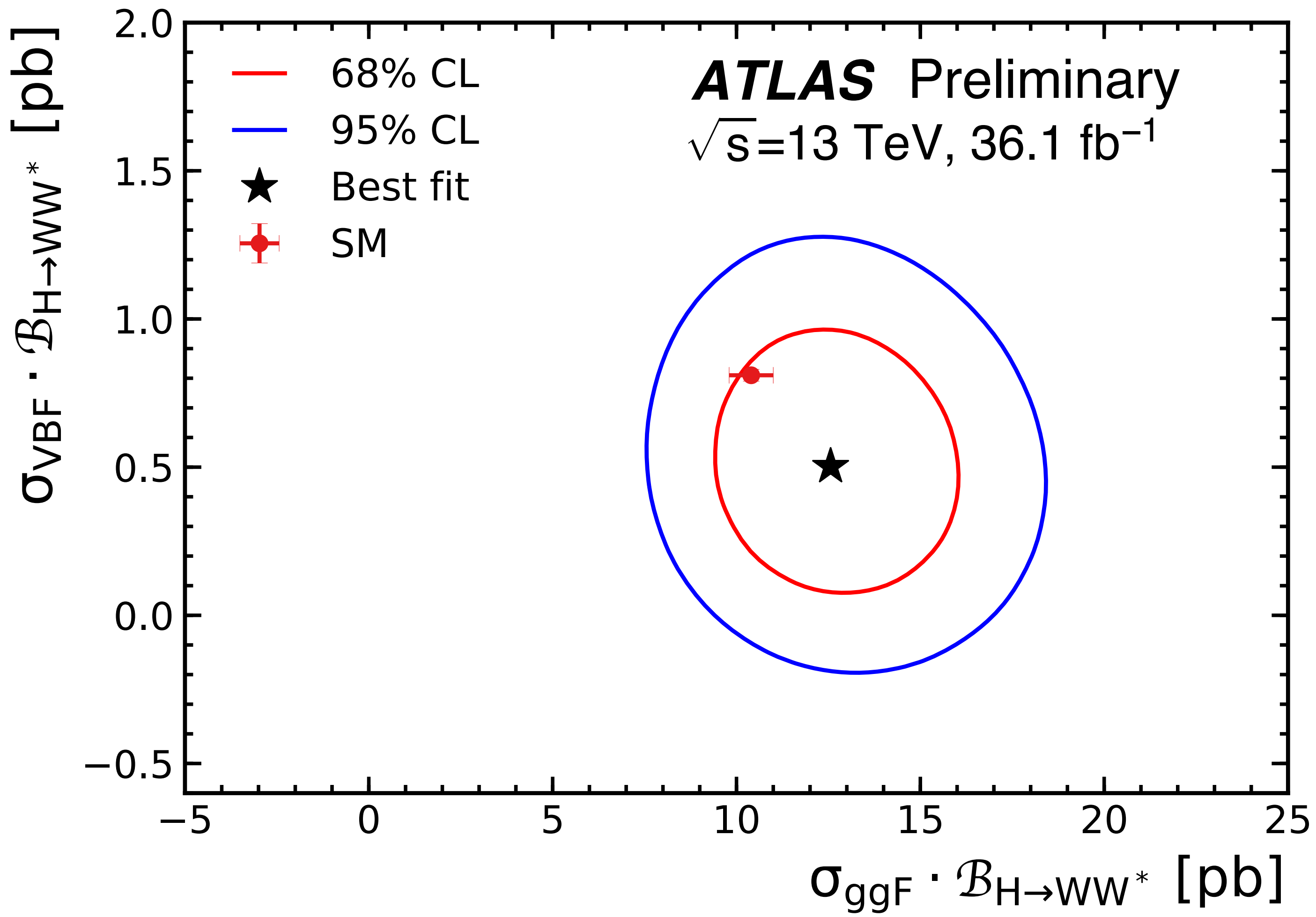

- Significances of 6.3 σ and 1.8 σ for ggF and VBF, respectively

- Combination of results from γγ and ZZ
  - still dominated by statistical component.
  - Result in agreement with expectation within stat. uncertainties.

$$\mu = 1.09\ ^{+0.09}_{-0.09}\ (\text{stat.})\ \ ^{+0.06}_{-0.05}(\text{sys.})\ \ ^{+0.06}_{-0.05}(\text{theo.})\ \text{fb}$$

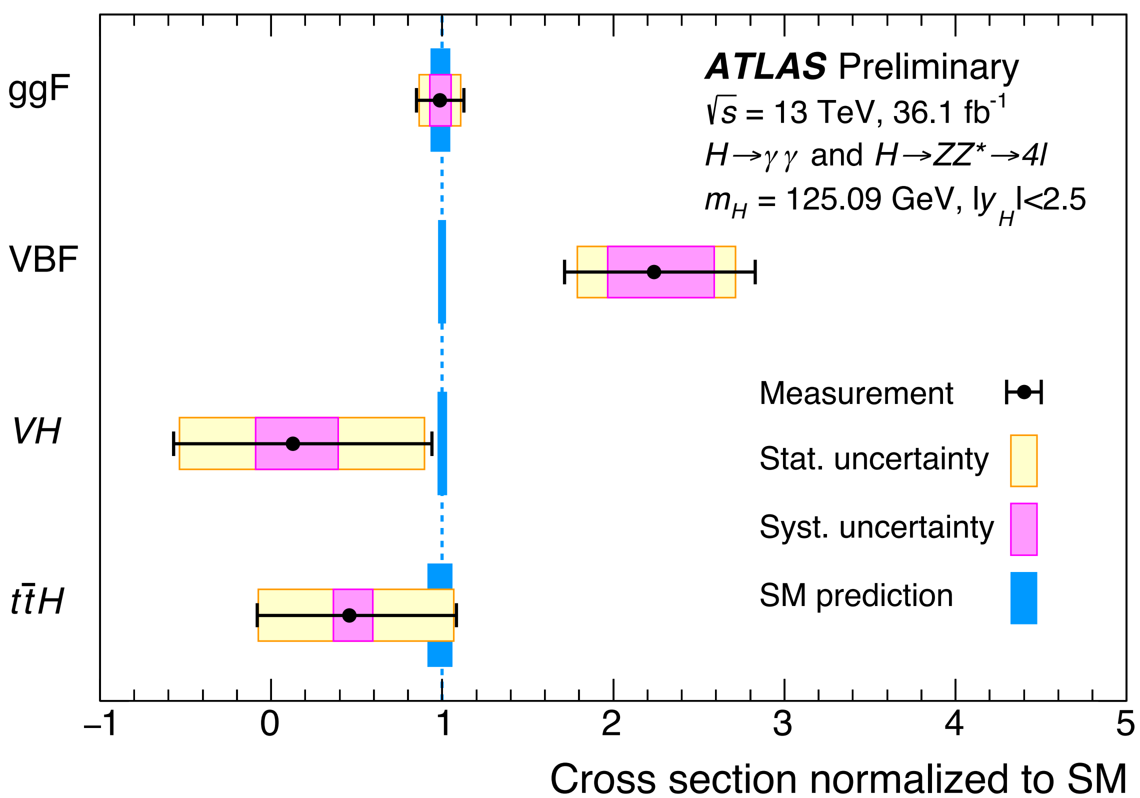

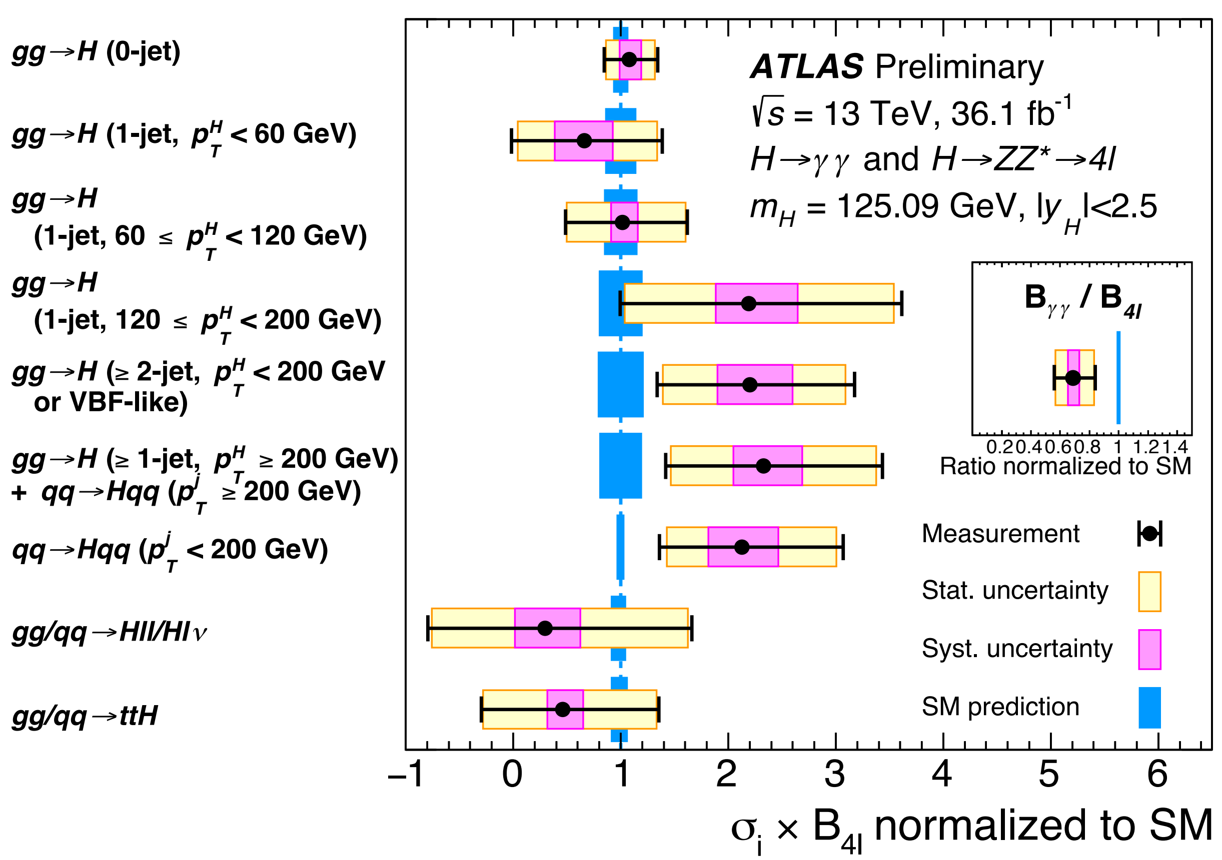

Global fit — Production mode

- Combination of results from γγ and ZZ
  - still dominated by statistical component.
    - CMS's result systematically dominated.
  - Result in agreement with expectation within stat. uncertainties.

ATLAS $$\mu = 1.09\ ^{+0.09}_{-0.09}\ (\text{stat.})\ ^{+0.06}_{-0.05}(\text{sys.})\ ^{+0.06}_{-0.05}(\text{theo.})\ \text{fb}$$

CMS $$\mu = 1.17\ ^{+0.06}_{-0.06}\ (\text{stat.})\ ^{+0.06}_{-0.06}(\text{sys.})\ ^{+0.06}_{-0.05}(\text{theo.})\ \text{fb}$$

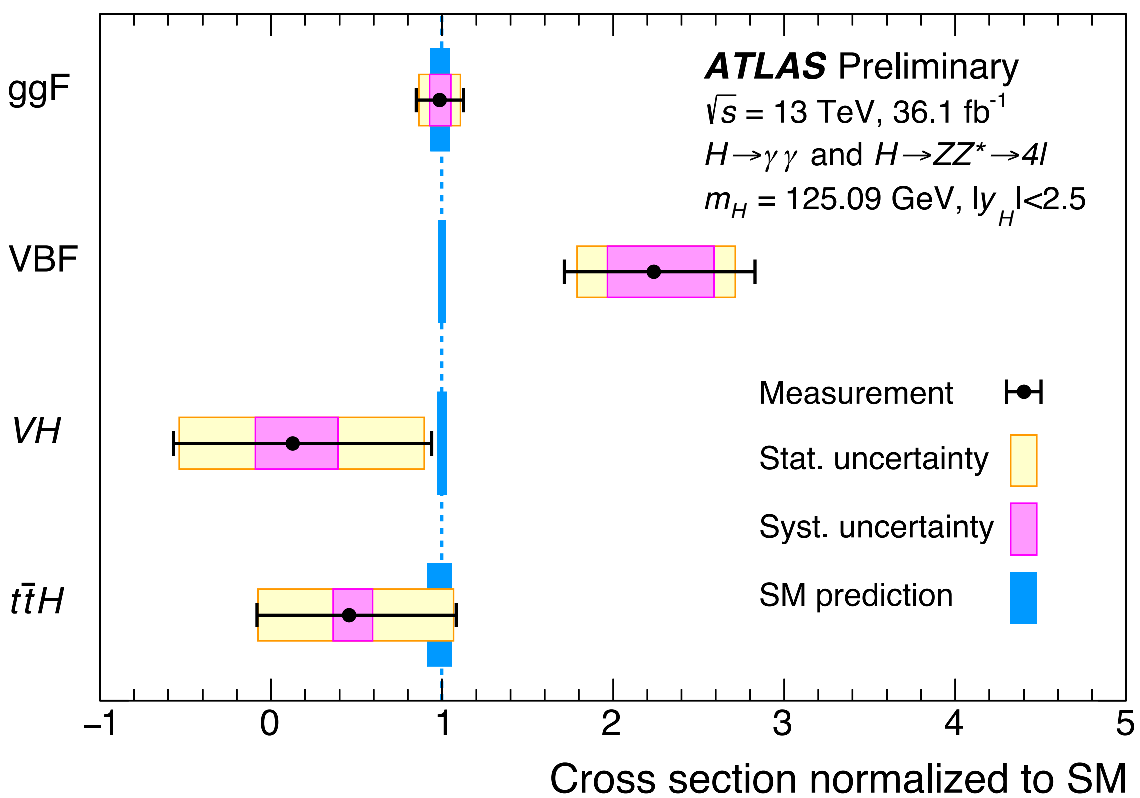

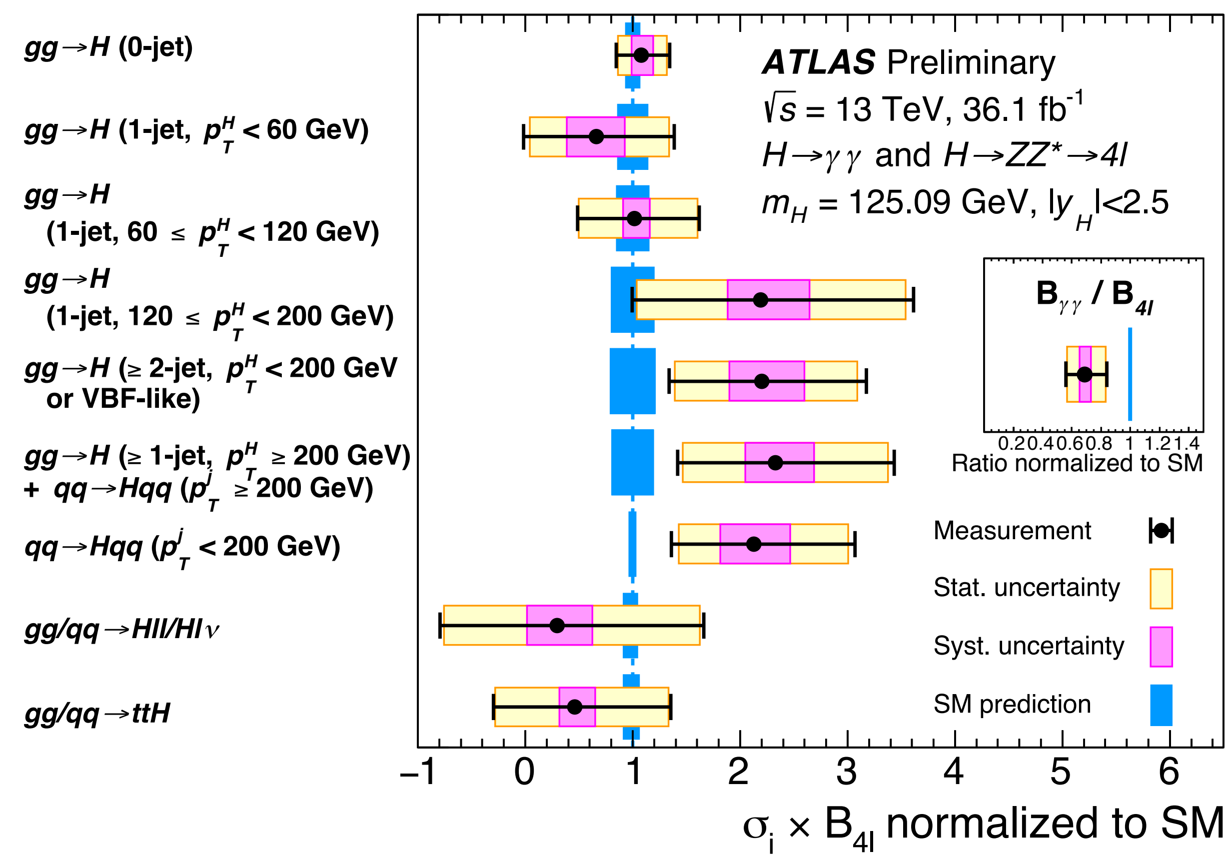

- Combination of results from γγ and ZZ
  - still dominated by statistical component.
    - CMS's result systematically dominated.
  - Result in agreement with expectation within stat. uncertainties.

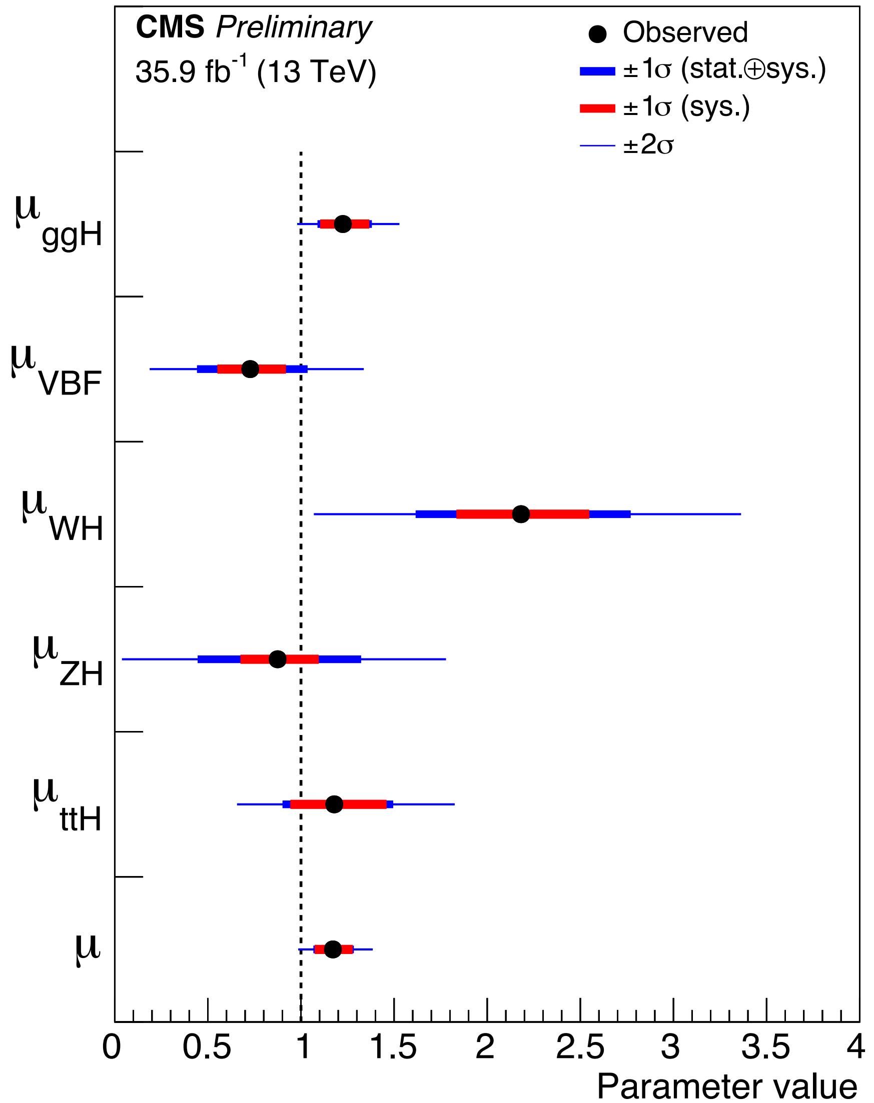

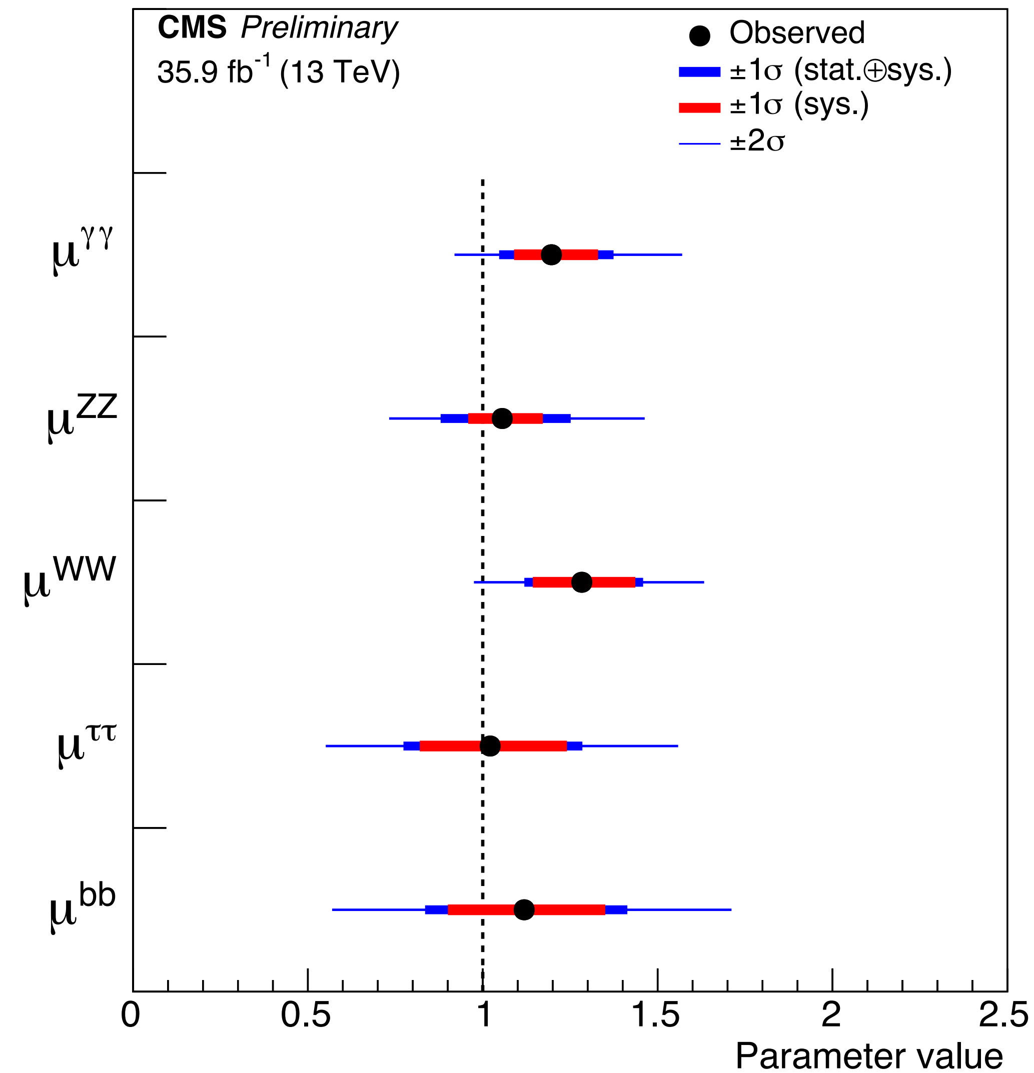

- Combination of results from γγ and ZZ
  - still dominated by statistical component.
    - CMS's result systematically dominated.
  - Result in agreement with expectation within stat. uncertainties.

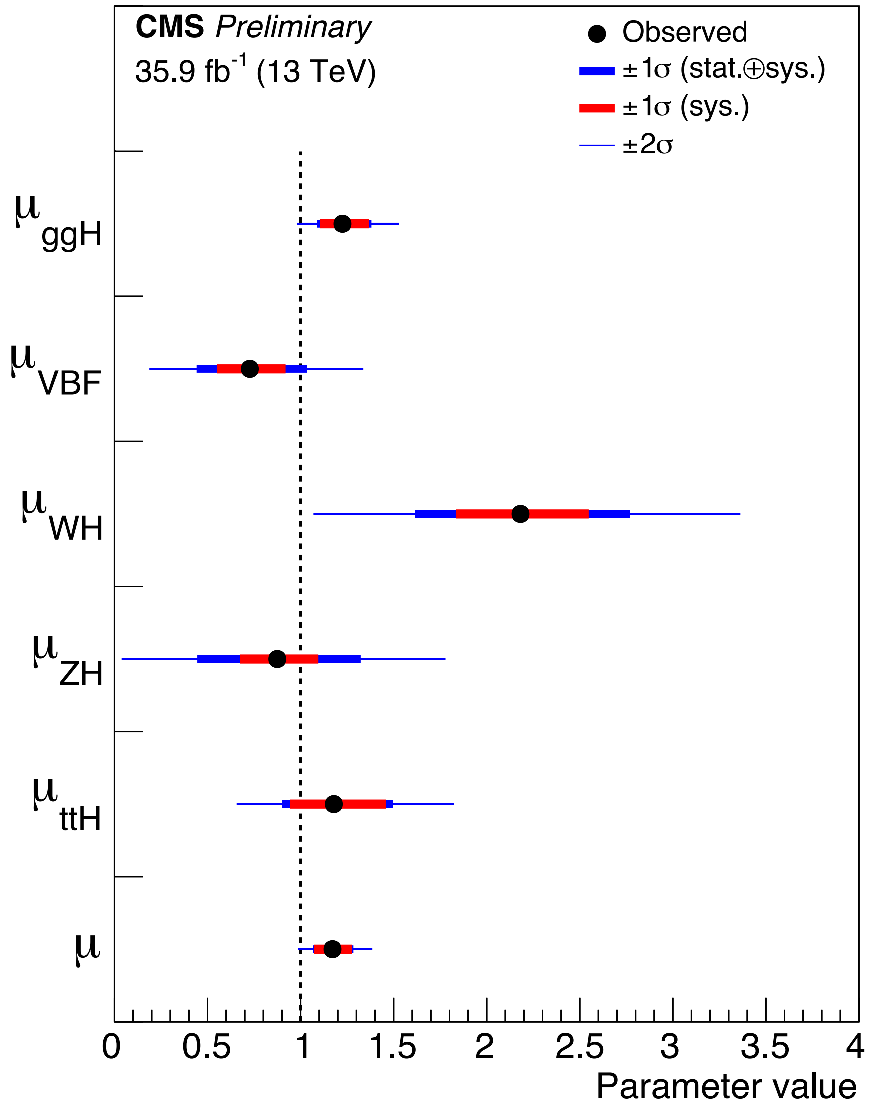

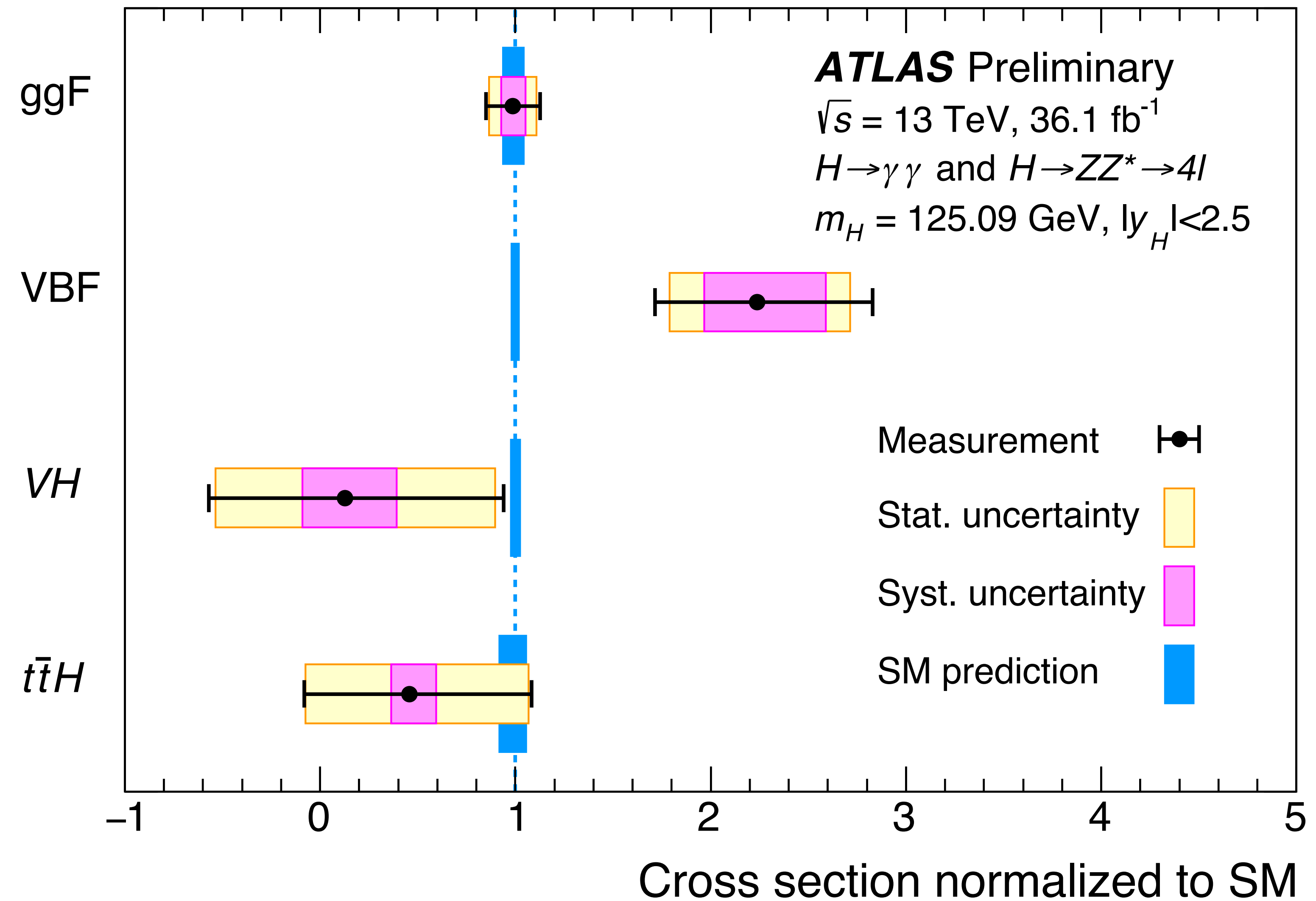

7. Conclusions

Conclusion

- Run II first results of ATLAS in the study of Higgs boson properties
    1. Measurement of m_H at 2 per mille precision level.
    2. Fiducial cross section measurements, sensitivity to several distributions
    3. Production mode analysis and template cross section measurements.

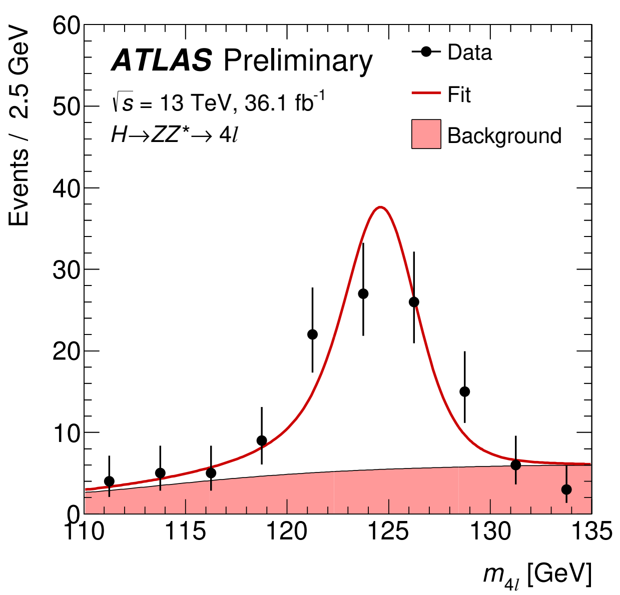

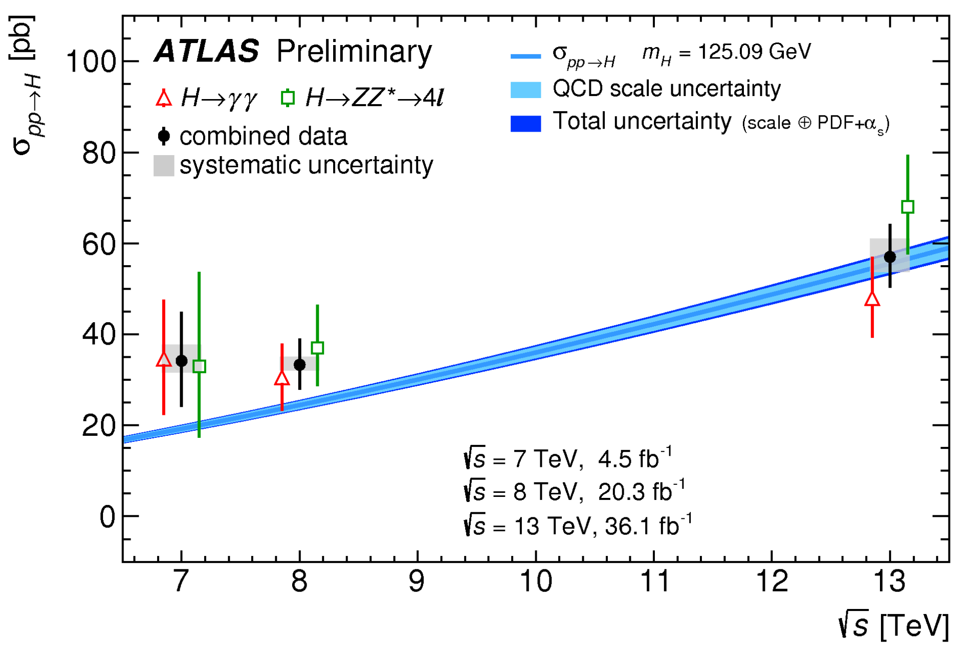

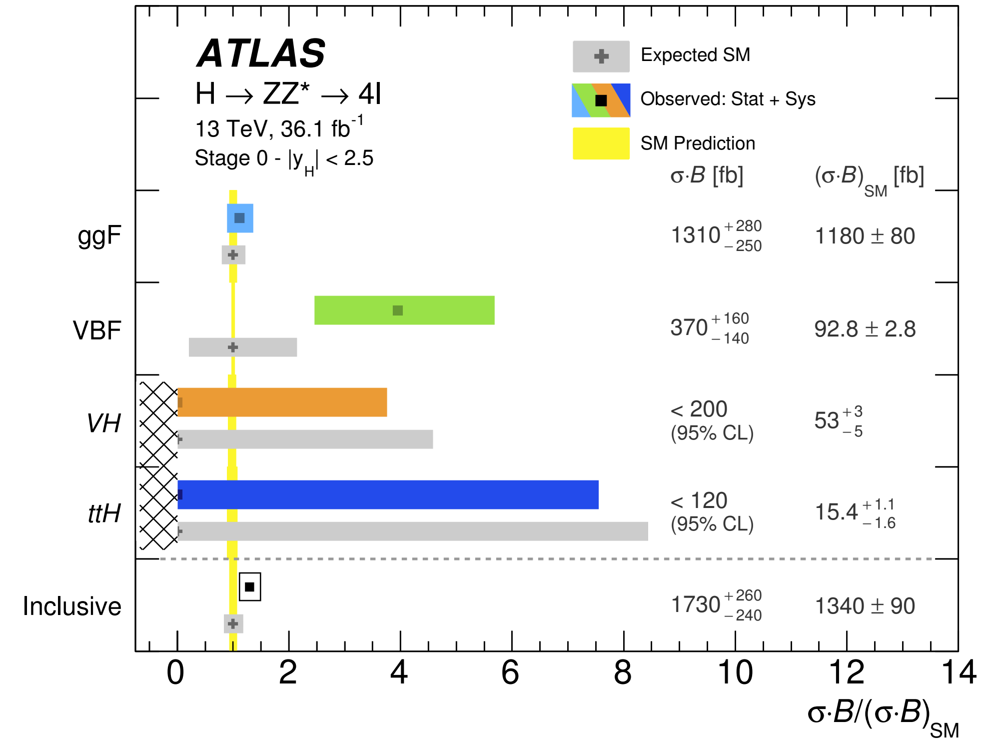

- Globally measurements dominated by statistical uncertainty
- First step in the bigger picture of the Run 2 programme

References

- Measurement of m_H
  - ATLAS-CONF-2017-046
- Measurement of the fiducial and differential distributions:
  - arXiv:1708.02810,
  - arXiv:1802.04146
  - ATLAS-CONF-2018-002
- Measurement of the couplings properties:
  - ATLAS-CONF-2017-043
  - arXiv:1712.02304
  - ATLAS-CONF-2017-047

Additional material

Higgs boson kinematics

- Higgs boson $p_{T,4\ell}$ and rapidity ($y_{4\ell}$) probe:
  - $p_{T,4\ell}$: Lagrangian structure of H interactions.

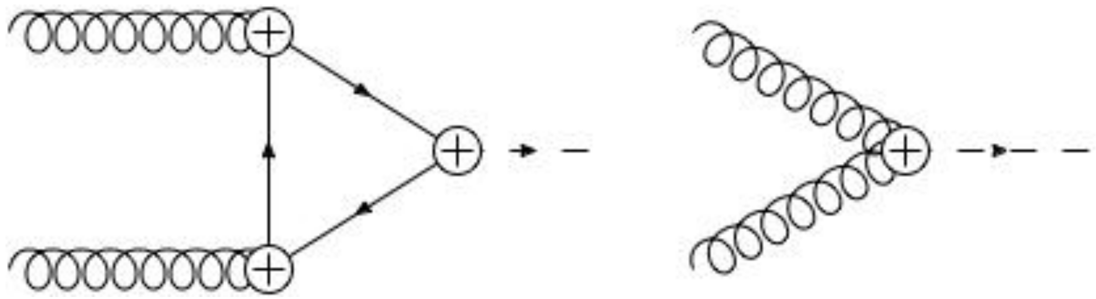

- Small perturbations to SM: dimension 6 operators most effective approach.

$$\frac{c_1}{\Lambda^2}\mathcal{O}_1 \to \frac{\alpha_S}{\pi v} c_g h G^a_{\mu\nu} G^{a,\mu\nu}\,,$$

c_g: ggH contact interaction

$$\frac{c_2}{\Lambda^2}\mathcal{O}_2 \to \frac{m_t}{v} c_t h\bar{t}t\,,$$

$$\frac{c_3}{\Lambda^2}\mathcal{O}_3 \to \frac{m_b}{v} c_b h\bar{b}b\,,$$

c_t: t and b Yukawa couplings

$$\frac{c_4}{\Lambda^2}\mathcal{O}_4 \to c_{tg}\frac{g_S m_t}{2v^3}(v+h)G^a_{\mu\nu}(\bar{t}_L\sigma^{\mu\nu}T^a t_R + h.c)$$

c_{tg}: dipole-moment, g-t interaction

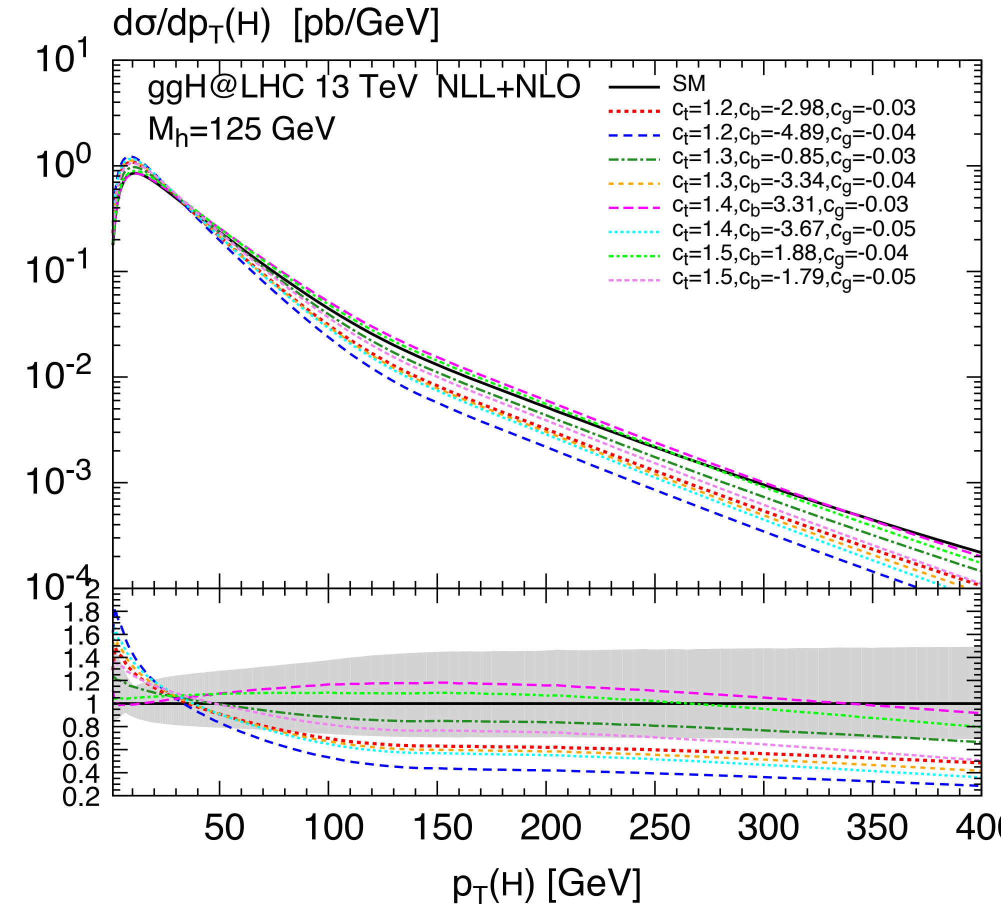

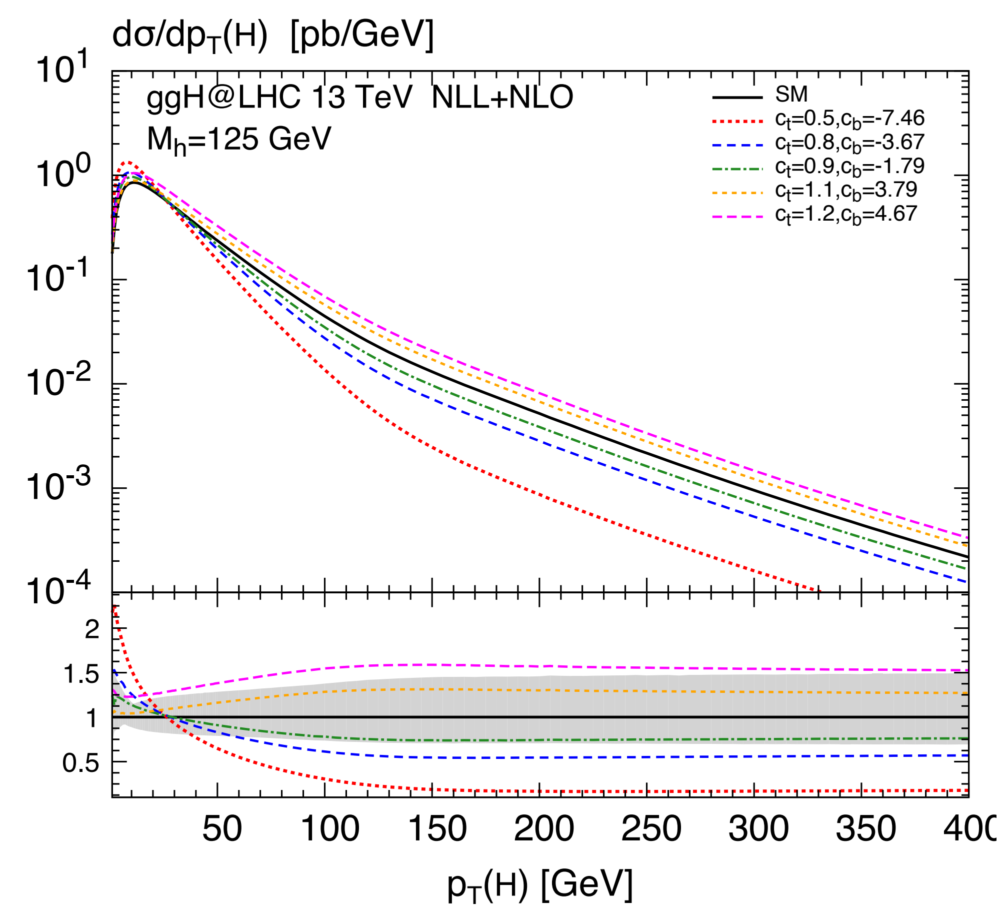

- The Large Hadron Collider
  - Two-ring superconductive proton (ion) accelerator situated at CERN.
  - Delivers collisions to four main detectors: Alice, ATLAS, CMS, and LHCb.

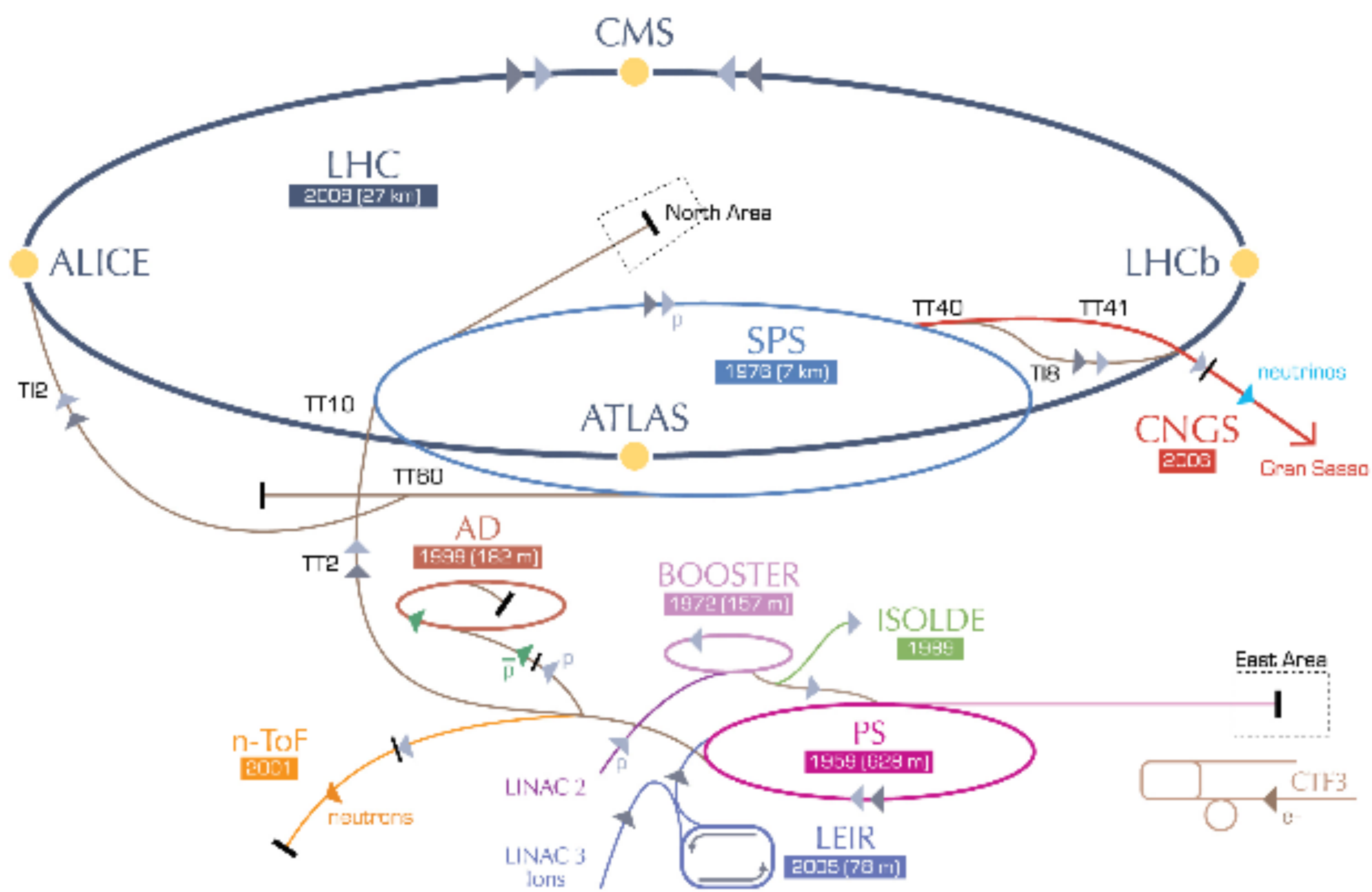

- $ZZ^* \rightarrow 4\ell$ selection:
  - For each of four final states: 4μ 2e2μ 2μ2e and 4e
- Two same-flavour opposite sign (SFOS) lepton pairs:
  - Isolated leptons with: $p_T(\ell)$ > 20 GeV , 15 GeV 10 GeV and 5 (7) GeV
  - Angular separation: $\Delta R(\ell,\ell')$ > 0.1 (0.2) for same (different) flavour
- Single candidate quadruplet identification
  - Leading pair: pair closest to m_Z,
  - Vertex refit: χ^2 cut at 99.5% signal efficiency
  - Final state photon emission recovered

Final state	Expected	Observed
4μ	38.5 ± 2.1	38
$2e2\mu$	27.5 ± 1.4	34
$2\mu 2e$	20.8 ± 1.3	26
$4e$	20.3 ± 1.3	24
Total	107 ± 6	122

$110 \text{ GeV} < m_{4\ell} < 130 \text{ GeV}$

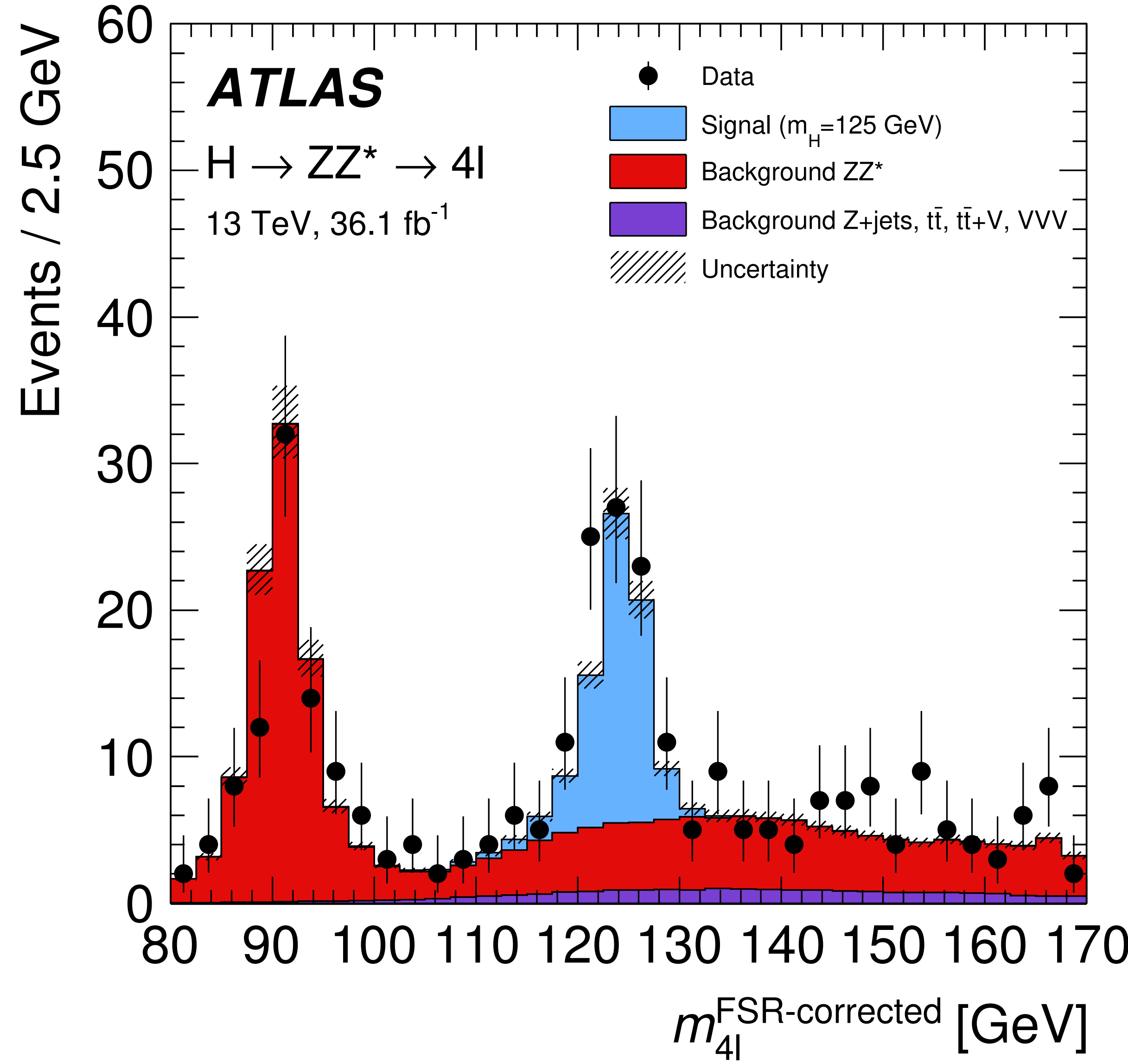

- Indistinguishable contributions from signal in final state

1. ZZ^{*} production in 4ℓ (dominant)
   - From $q\bar{q}$ annihilation and gg fusion (subdominant)
2. ZZZ, WZZ and WWZ (small).

3. Hadrons misidentified as leptons:
   - Z+jets $t\bar{t}$ and WZ production
   - Extrapolation to signal region making use of simulation

Based on simulation | **Based on data**

Final state	Signal (125 GeV)	ZZ^{*}	Z + jets, $t\bar{t}$, WZ, ttV, VVV	Expected	Observed
4μ	20.6 ± 1.7	15.9 ± 1.2	2.0 ± 0.4	38.5 ± 2.1	38
$2e2\mu$	14.6 ± 1.1	11.2 ± 0.8	1.6 ± 0.4	27.5 ± 1.4	34
$2\mu2e$	11.2 ± 1.0	7.4 ± 0.7	2.2 ± 0.4	20.8 ± 1.3	26
$4e$	11.1 ± 1.1	7.1 ± 0.7	2.1 ± 0.4	20.3 ± 1.3	24
Total	57 ± 5	41.6 ± 3.2	8.0 ± 1.0	107 ± 6	122

- Indistinguishable contributions from signal in final state

1. ZZ^* production in 4ℓ (dominant)
   - From $q\bar{q}$ annihilation and gg fusion (subdominant)
2. ZZZ, WZZ and WWZ (small).

3. Hadrons misidentified as leptons:
   - Z+jets $t\bar{t}$ and WZ production
   - Extrapolation to signal region making use of simulation

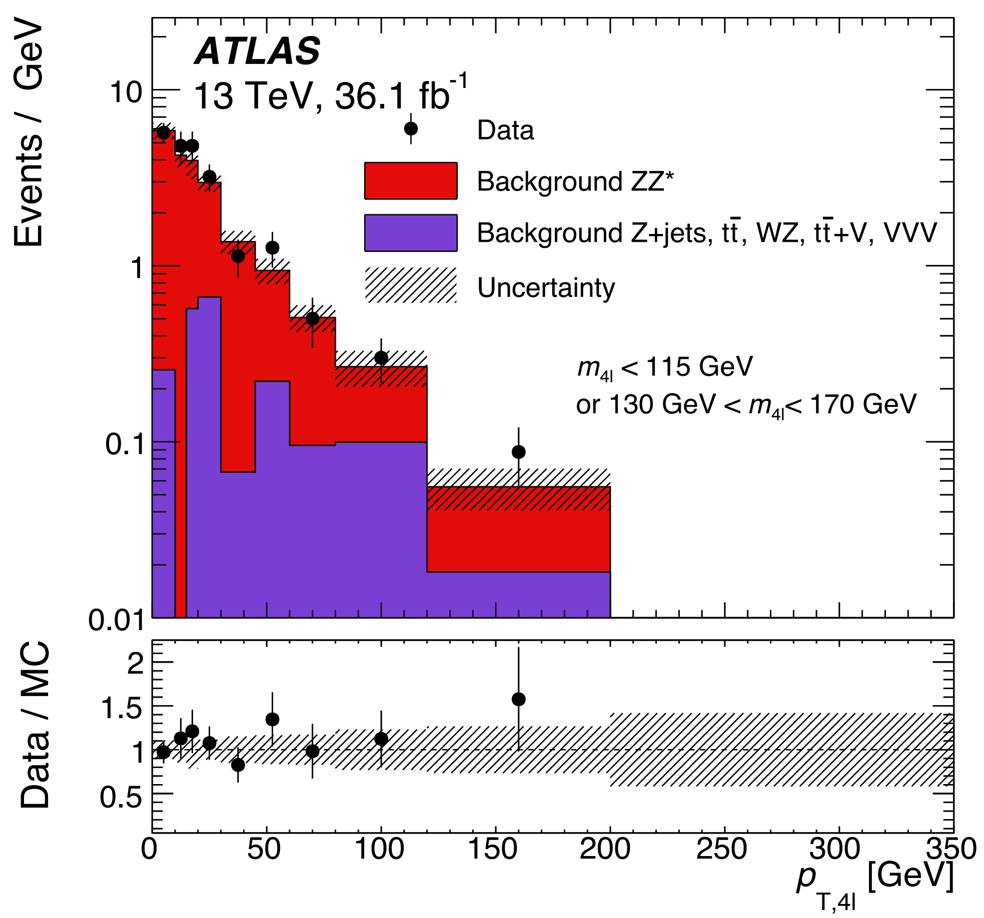

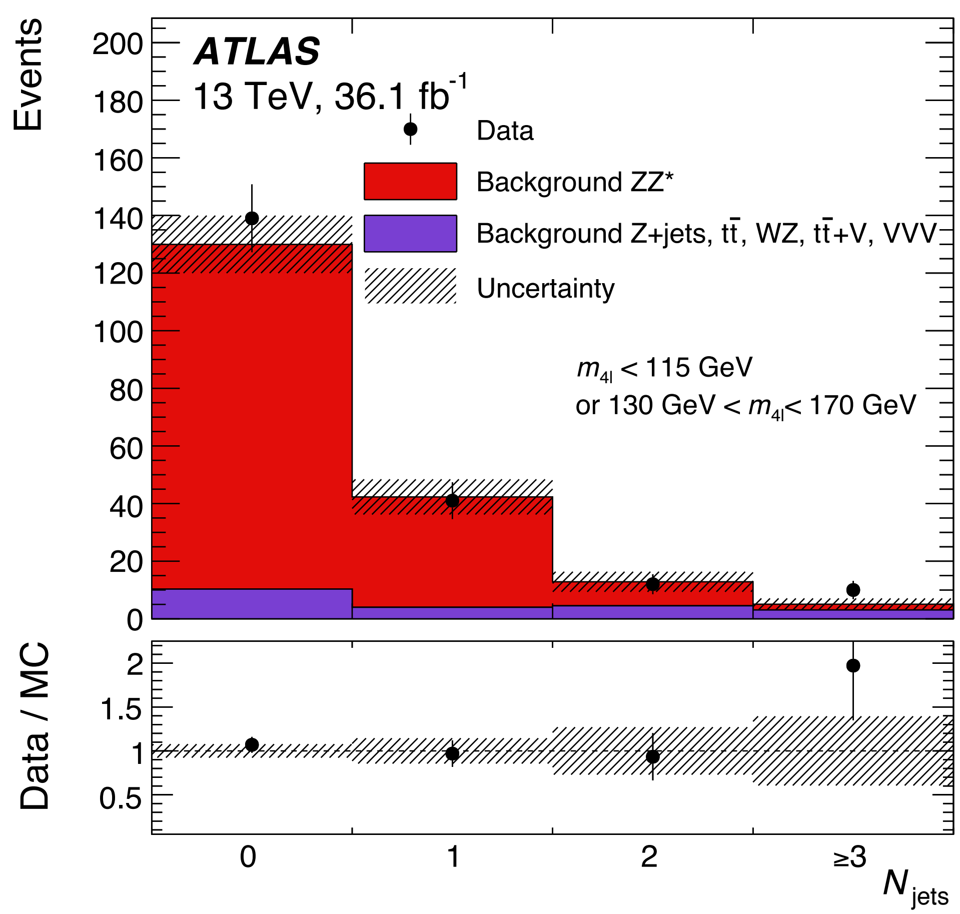

- $WW^* \to e\nu\mu\nu$ selection
  - Two isolated leptons $p_T(\ell) > 22$ GeV and $p_T(\ell) > 15$ GeV
  - $E_T^{miss} > 20$ GeV
- Background estimation

<table>
<tr><th>CR</th><th>$N_{jet} = 0$</th><th>$N_{jet} = 1$</th><th>$N_{jet} \geq 2$, VBF</th></tr>
<tr><td rowspan="3">WW</td><td>$55 < m_{\ell\ell} < 110$ GeV
$\Delta\phi_{\ell\ell} < 2.6$</td><td>$m_{\ell\ell} > 80$ GeV
$|m_{\tau\tau} - m_Z| > 25$ GeV</td><td rowspan="3"></td></tr>
<tr><td colspan="2">b-jet veto</td></tr>
<tr><td></td><td>$m_T^{\ell} > 50$ GeV</td></tr>
<tr><td rowspan="3">Top-quark</td><td rowspan="2">$N_{b\text{-jet},(20\text{ GeV}<p_T<30\text{ GeV})} > 0$
$\Delta\phi(\ell\ell, E_T^{miss}) > \pi/2$
$p_T^{\ell\ell} > 30$ GeV</td><td>$N_{b\text{-jet},(p_T>30\text{ GeV})} = 1$
$N_{b\text{-jet},(20\text{ GeV}<p_T<30\text{ GeV})} = 0$
$\max\left(m_T^{\ell}\right) > 50$ GeV</td><td>$N_{b\text{-jet},(p_T>20\text{ GeV})} = 1$
Central Jet Veto</td></tr>
<tr><td colspan="2">$m_{\tau\tau} < m_Z - 25$ GeV</td></tr>
<tr><td>$\Delta\phi_{\ell\ell} < 2.8$</td><td></td><td>Outside Lepton Veto</td></tr>
<tr><td rowspan="4">$Z \to \tau\tau$</td><td colspan="2">no $E_T^{miss,\ track}$ requirement
$m_{\ell\ell} < 80$ GeV</td><td>Outside Lepton Veto
Central Jet Veto</td></tr>
<tr><td rowspan="2">$\Delta\phi_{\ell\ell} > 2.8$</td><td colspan="2">$m_{\tau\tau} > m_Z - 25$ GeV</td></tr>
<tr><td colspan="2">$N_{b\text{-jet},(p_T>20\text{ GeV})} = 0$</td></tr>
</table>

- The Higgs boson mass (m_H) is a fundamental free parameter of the Standard Model.
  - Its precise determination allows for evermore precise higher order corrections to the cross section.
  - Sensitivity to new physics in higher order corrections.
  - Input to precision Electro Weak global fit.
  - Key measurement of the LHC program.

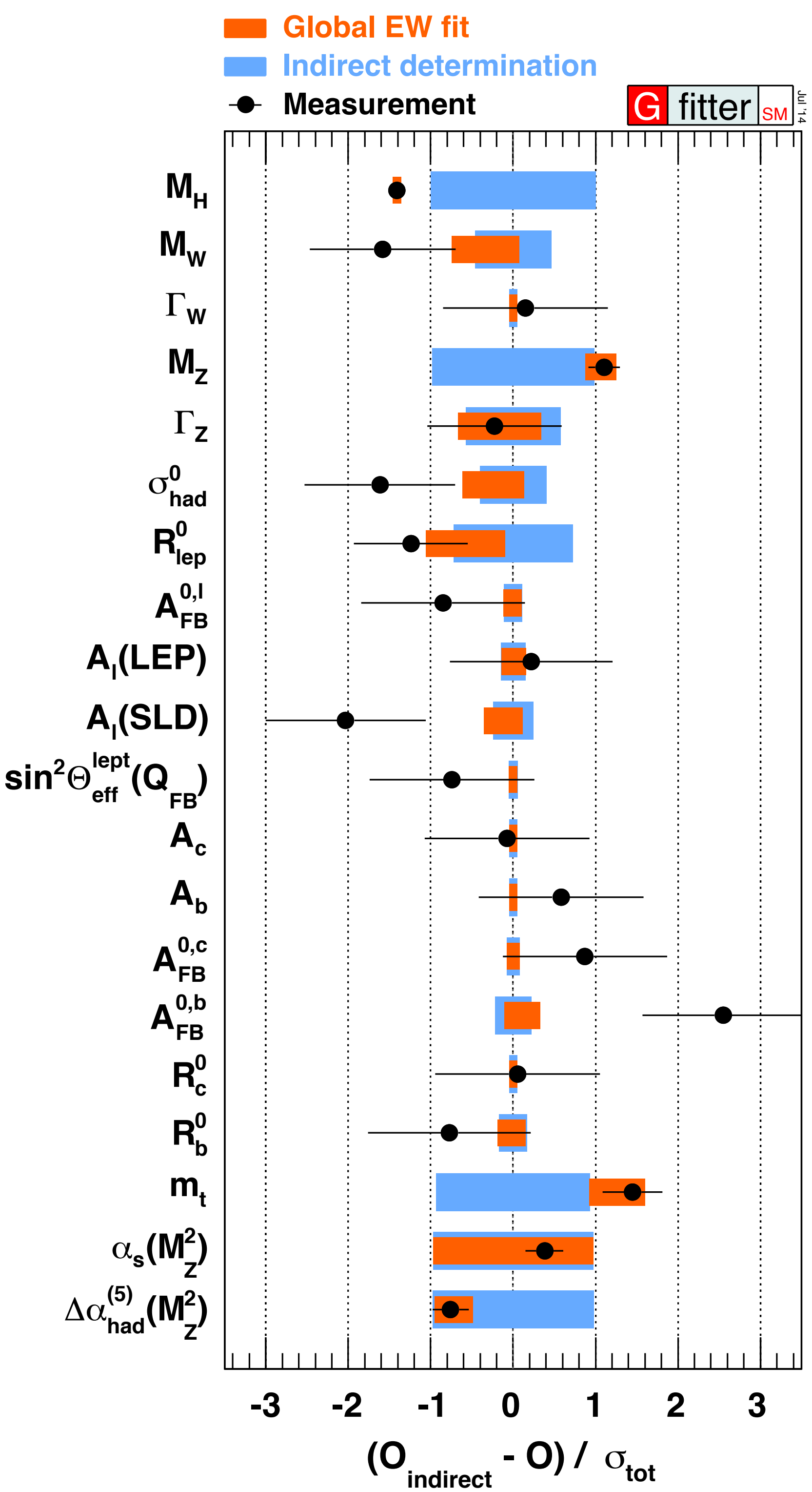

- Aim in improving significantly on δm_H
  - Expect 1.7 times more candidates, with 36 fb^{-1} at $\sqrt{s}$=13 TeV

- Narrow resonant peak above a background continuum
  - Allows for precise Higgs boson mass measurement
  - Minimise the model dependency.
- Ingredients for optimal measurement of Higgs boson mass:
  - Detector performance driven measurement

$$\delta m_H \simeq \frac{\sigma(m_{4\ell})}{\sqrt{N - N_\mathrm{b}}}$$

(I) Statistical precision precision depends upon:

- resolution of the reconstructed final state,
- number of signal events.

(II) Systematic uncertainty from understanding of detector performance:

- energy and momentum scale,
- resolution uncertainty.

- Final estimate from 4x4 simultaneous un-binned fit
  - Four kinematic categories and four final states

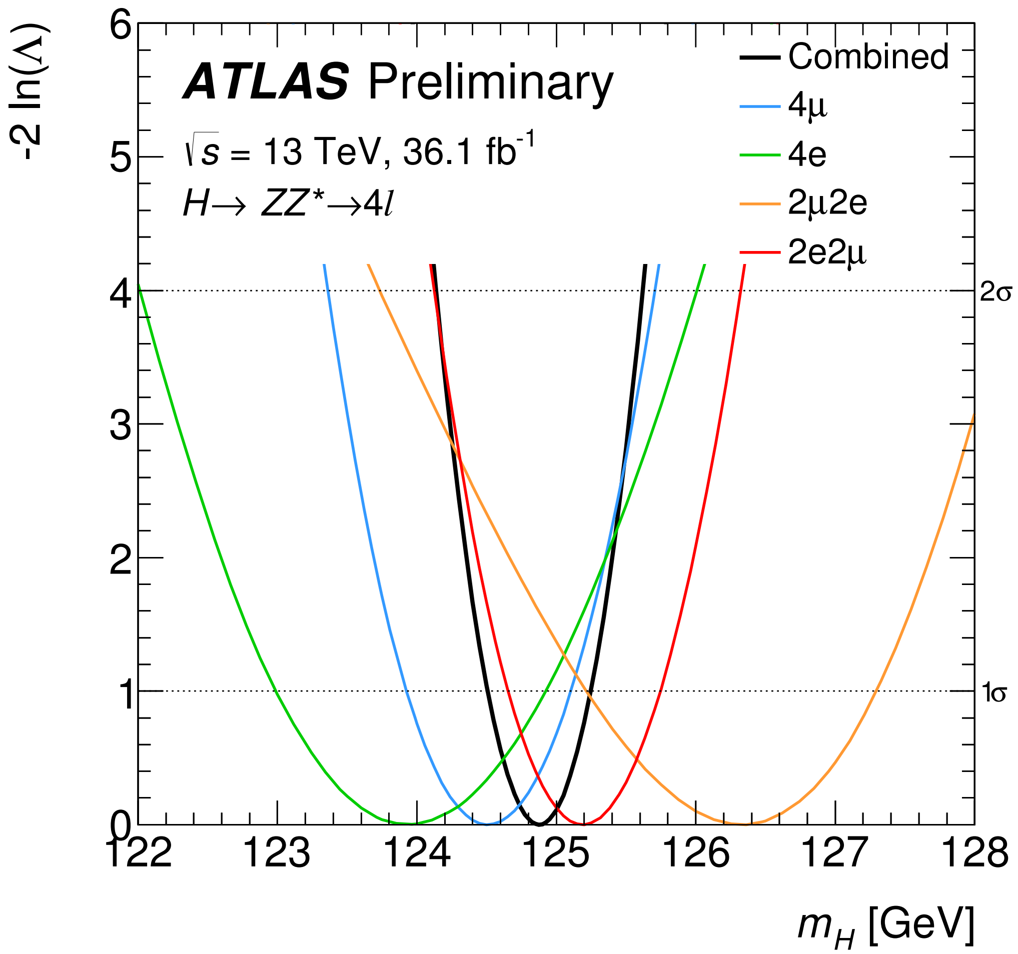

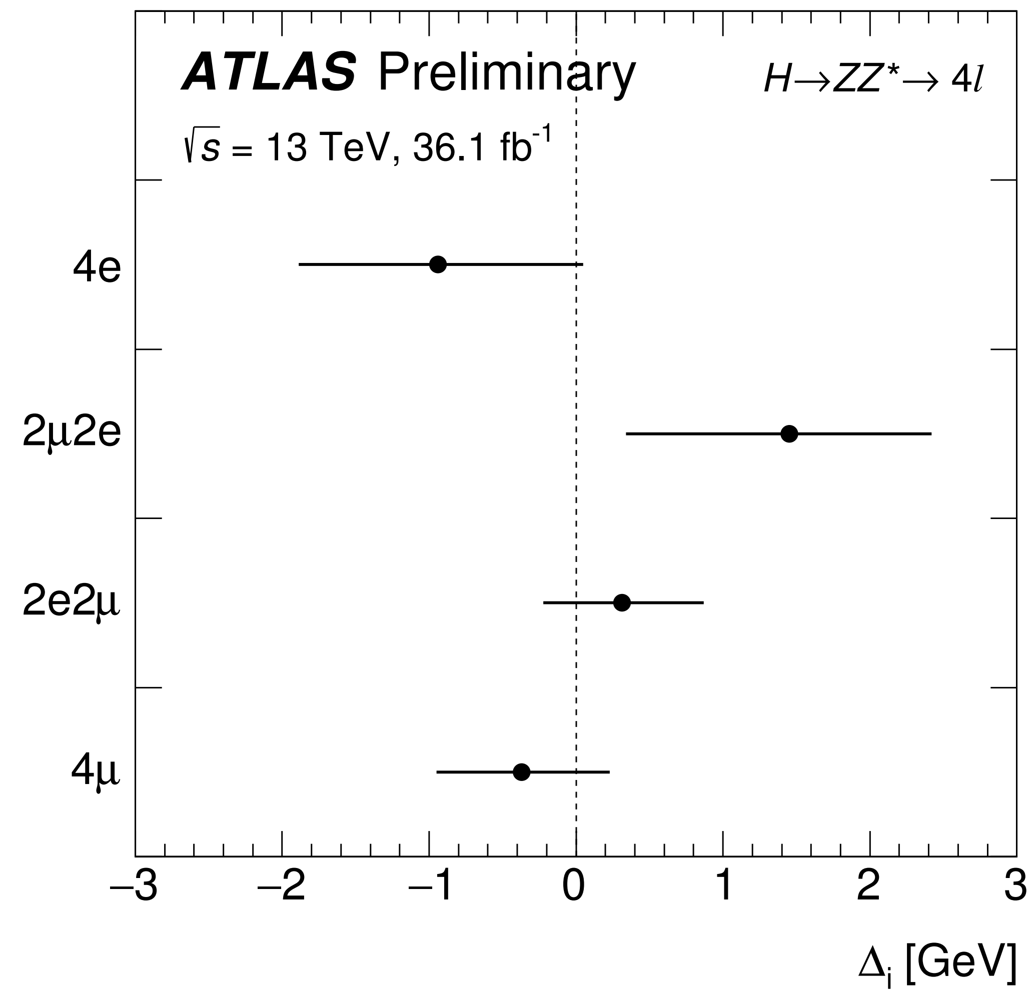

- Cross validation in channels and independent method
  - Compatibility of channels 0.6σ for 4μ and 1.3 2μ2e
  - *p*-value of 0.19 between template method and per-event.
    - ✦ 35 MeV worst resolution for template method.

- Correction for local misalignments
  - Charge dependent bias, with net effect of worsening resolution
  - In-situ correction based on $Z \rightarrow \mu\mu$ data, recovers up to 5% in resolution.
  - Iteratively removing the bias δ_s:

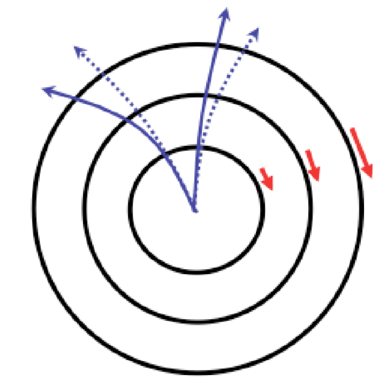

$$p_T^{corr}(\mu) = \frac{p_T^{bias}(\mu)}{1 - q(\mu)\delta_s(\eta,\phi)p_T^{bias}(\mu)}$$

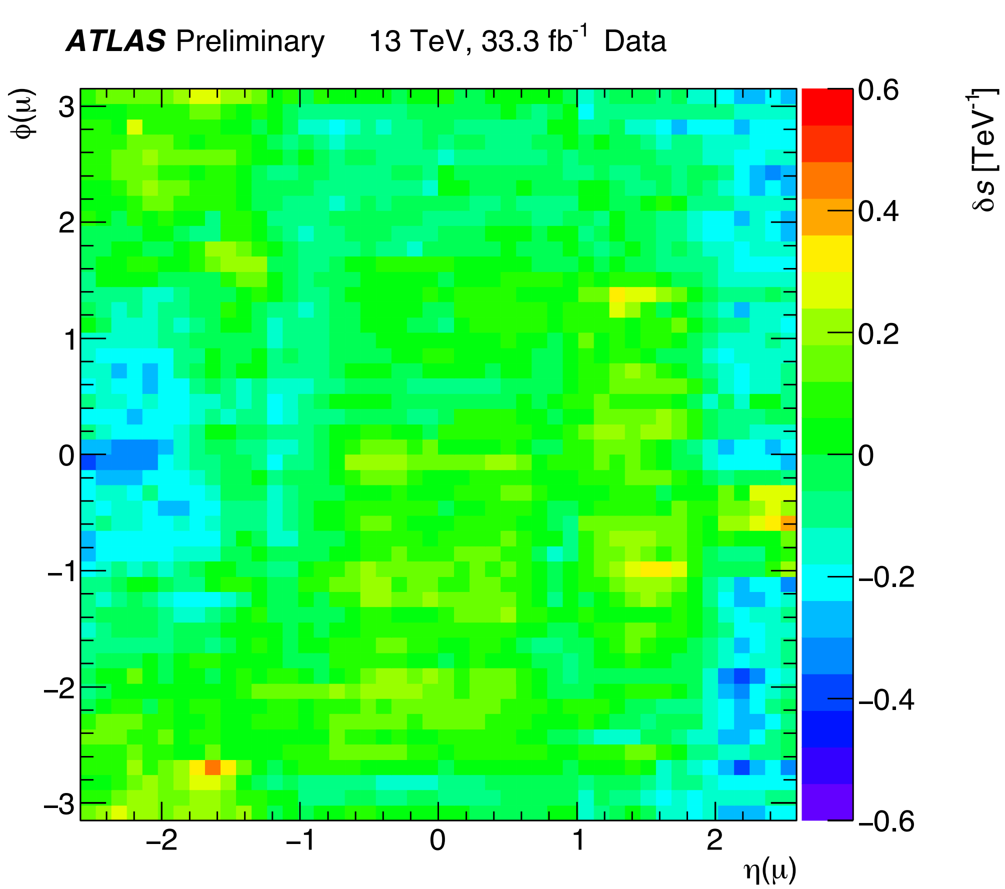

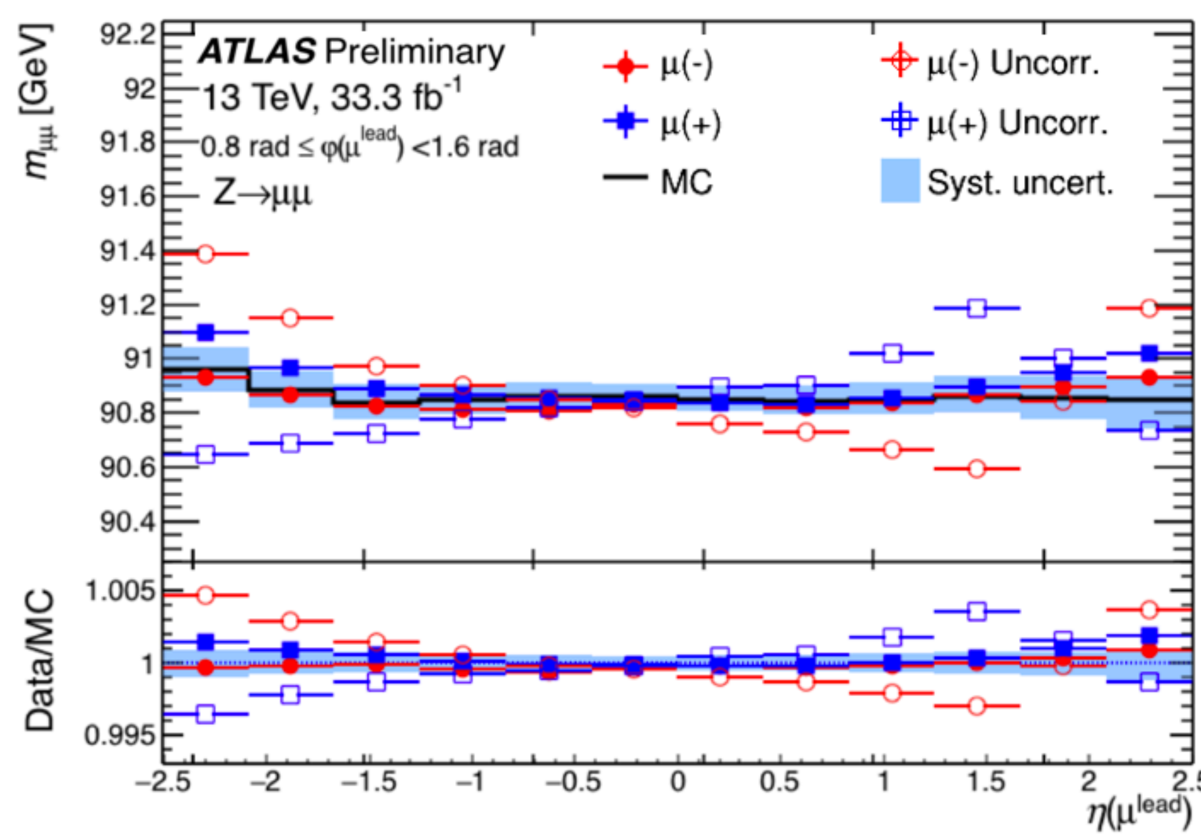

- Three-prong approach to reduce uncertainty at analysis level:
  - (i) 14% from m_{12} constraint to m_Z with kinematic fit.
  - (i) 2.4% from per-event likelihood.
    - Per lepton energy response as a function of kinematics of event
  - (ii) 6.3 % from kinematic discriminant selecting signal and background events
    - Boosted Decision Tree on $p_T(4\ell)$, $y(4\ell)$ and $\log(|\mathcal{M}_H|^2/|\mathcal{M}_{ZZ^*}|^2)$

- Expected statistical uncertainty of 340 MeV.
  - Validation on $Z \rightarrow 4\ell$ decays
  - Template fit as cross check method

Category	m_Z in simulation [GeV]	m_Z in data [GeV]
4μ	$91.19^{+0.41}_{-0.41}$	$91.46^{+0.42}_{-0.41}$
$4e$	$91.19^{+1.02}_{-1.03}$	$91.75^{+1.08}_{-1.06}$
$2\mu 2e$	$91.18^{+1.11}_{-1.11}$	$91.31^{+1.62}_{-1.33}$
$2e2\mu$	$91.19^{+0.90}_{-0.90}$	$92.49^{+0.91}_{-0.94}$
Combined	$91.19^{+0.34}_{-0.34}$	$91.62^{+0.35}_{-0.35}$

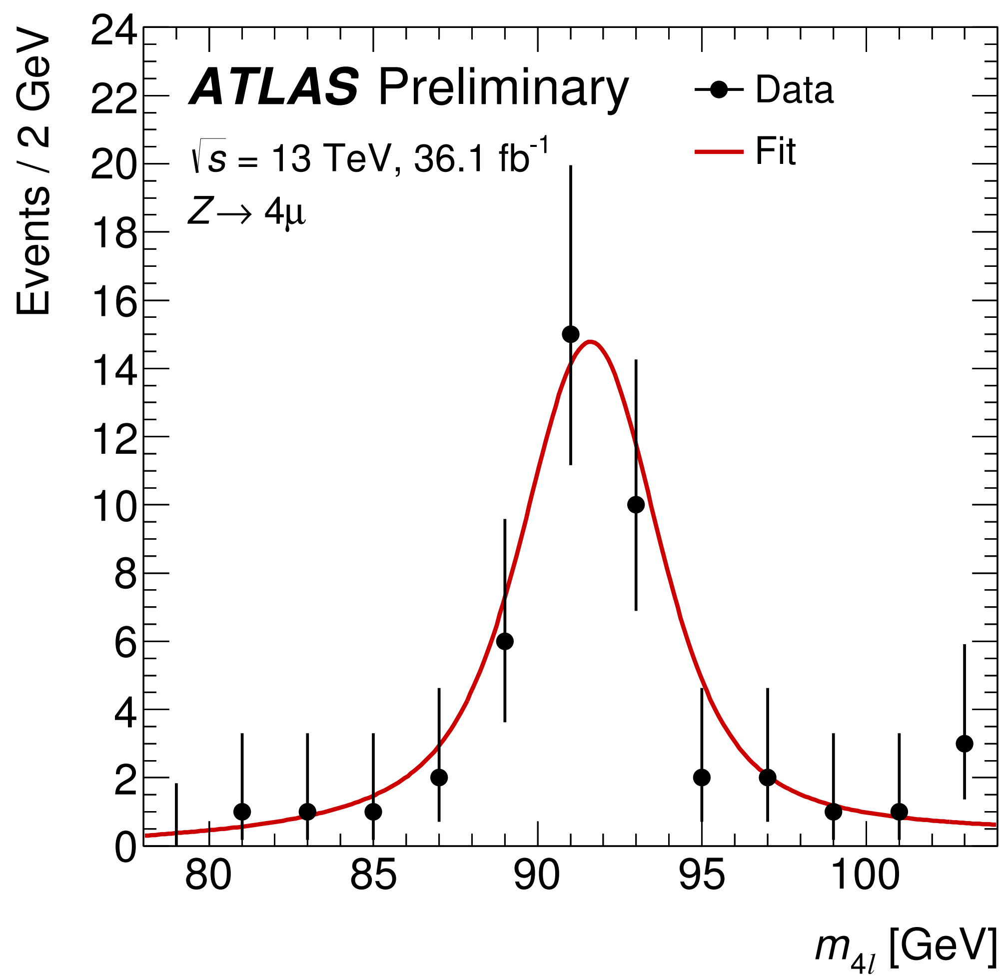

- Run I world average on m_H

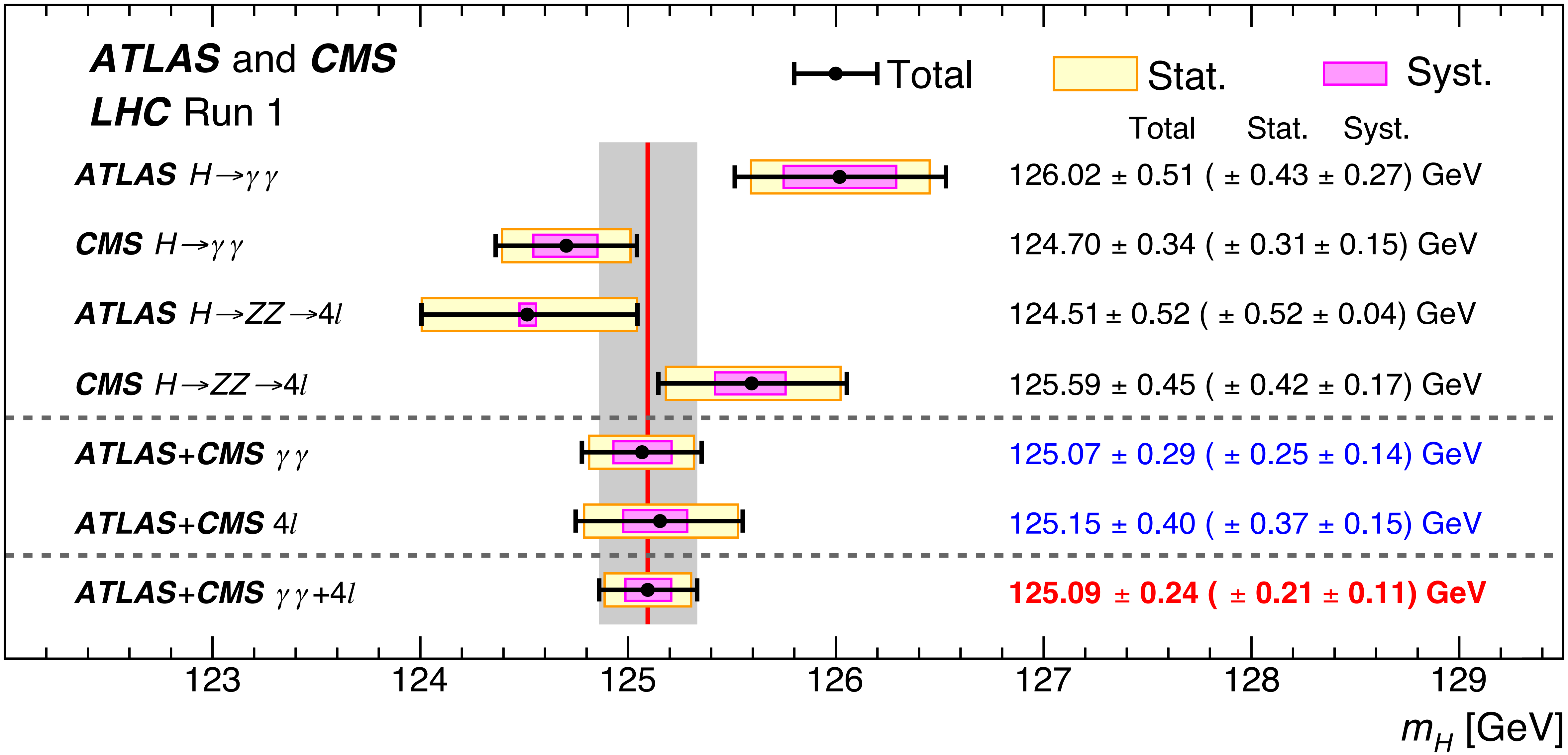

$$m_H = 125.09 \ \pm \ 0.21 \ (\text{stat.}) \ \pm \ 0.11(\text{sys.}) \ \text{GeV}$$

- $H \to \gamma\gamma$ updated result at Run II.
  - Analytical function in kinematic and detector categories.

$$m_H^{\gamma\gamma} = 125.11 \pm 0.21\ (\text{stat}) \pm 0.36\ (\text{syst})\ \text{GeV}$$

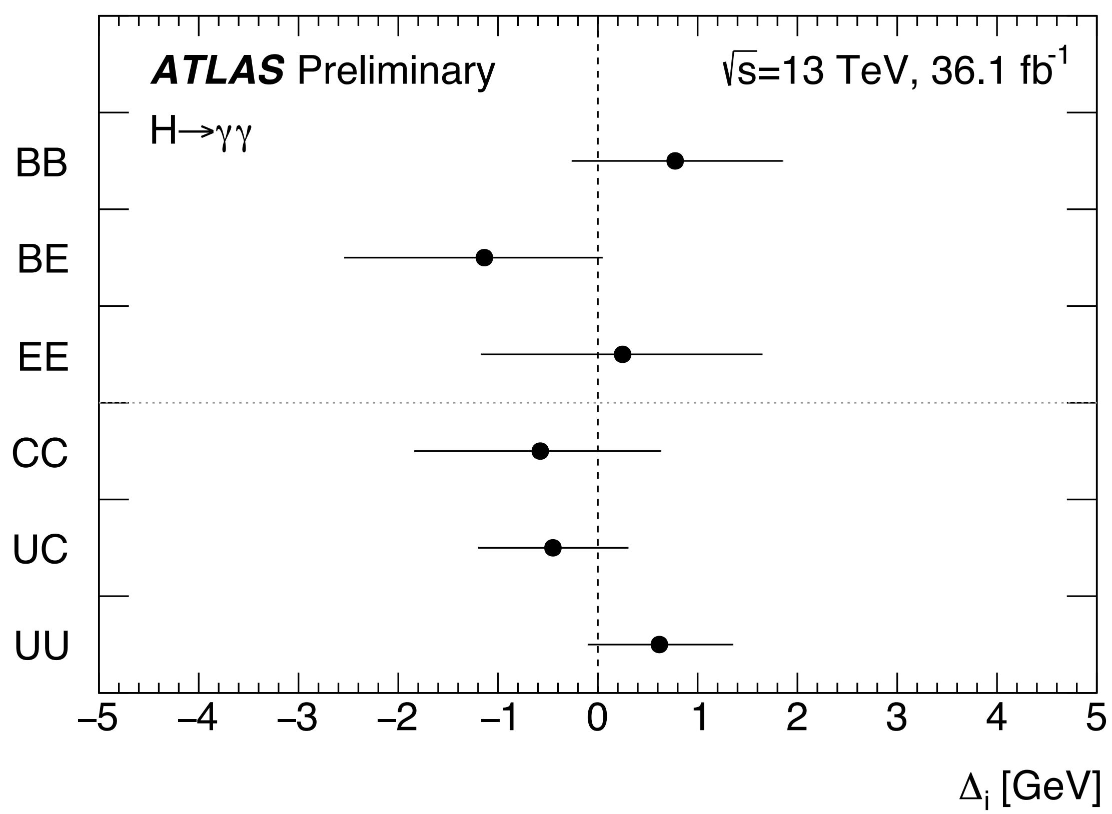

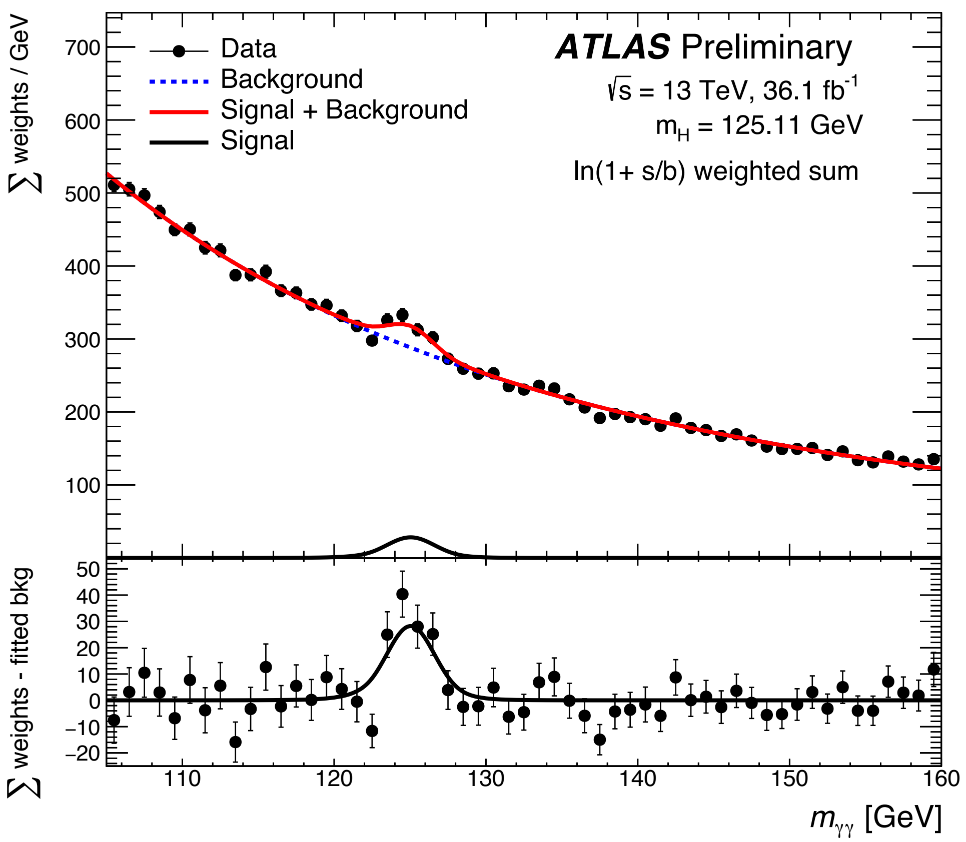

- $H \rightarrow \gamma\gamma$ updated result at Run II.
  - Analytical function in kinematic and detector categories.

$$m_H^{\gamma\gamma} = 125.11 \pm 0.21 \text{ (stat)} \pm 0.36 \text{ (syst) GeV}$$

Source	Systematic uncertainty on $m_H^{\gamma\gamma}$ [MeV]
LAr cell non-linearity	±200
LAr layer calibration	±190
Non-ID material	±120
Lateral shower shape	±110
ID material	±110
Conversion reconstruction	±50
$Z \rightarrow ee$ calibration	±50
Background model	±50
Primary vertex effect on mass scale	±40
Resolution	$^{+20}_{-30}$
Signal model	±20

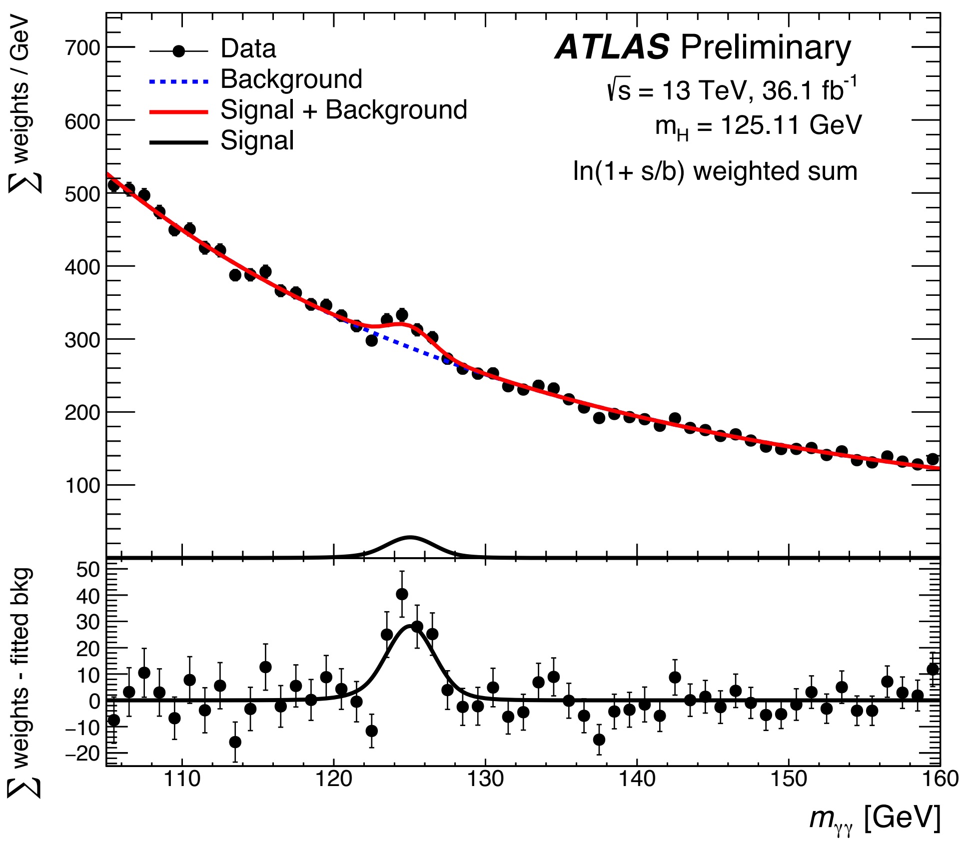

- $H \to ZZ^*$ and $H \to \gamma\gamma$ Run II combination
  - Likelihood based combination with simultaneous fit

Source	Systematic uncertainty on m_H [MeV]
LAr cell non-linearity	90
LAr layer calibration	90
Non-ID material	60
ID material	50
Lateral shower shape	50
$Z \to ee$ calibration	30
Muon momentum scale	20
Conversion reconstruction	20

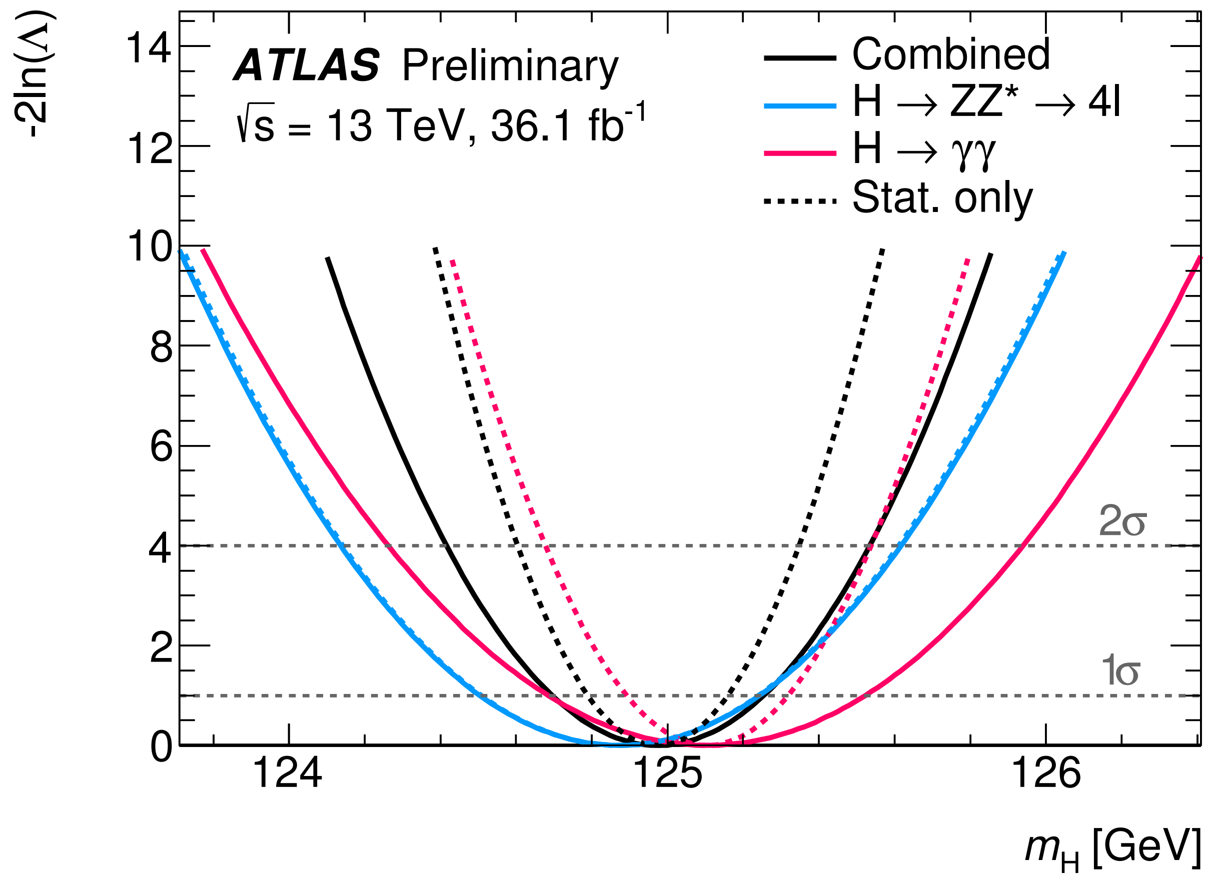

Channel	Mass measurement [GeV]
$H \to ZZ^* \to 4\ell$	124.88 ± 0.37 (stat) ± 0.05 (syst) = 124.88 ± 0.37
$H \to \gamma\gamma$	125.11 ± 0.21 (stat) ± 0.36 (syst) = 125.11 ± 0.42
Combined	124.98 ± 0.19 (stat) ± 0.21 (syst) = 124.98 ± 0.28

- Updated m_H measurement with Run-2 data.
  - With 4ℓ channel alone.
- Strategy of "3D" fit:
  - Leading lepton pair constrained to m_Z (-8%);
  - Matrix element discriminant for background rejection (-3.2%)
  - Propagation of per-lepton tracking and ECAL uncertainties to $m_{4\ell}$ (8%)

Similar to ATLAS (first two items)

Per-event resolution prediction in ATLAS (third item)

No $m(Z_1)$ constraint	3D: $\mathcal{L}(m_{4\ell}, \mathcal{D}_{\text{mass}}, \mathcal{D}^{\text{kin}}_{\text{bkg}})$	2D: $\mathcal{L}(m_{4\ell}, \mathcal{D}_{\text{mass}})$	1D: $\mathcal{L}(m_{4\ell})$
Expected m_H uncertainty change	+8.1%	+11%	+21%
Observed m_H (GeV)	125.28±0.22	125.36±0.24	125.39±0.25
With $m(Z_1)$ constraint	3D: $\mathcal{L}(m'_{4\ell}, \mathcal{D}'_{\text{mass}}, \mathcal{D}^{\text{kin}}_{\text{bkg}})$	2D: $\mathcal{L}(m'_{4\ell}, \mathcal{D}'_{\text{mass}})$	1D: $\mathcal{L}(m'_{4\ell})$
Expected m_H uncertainty change	—	+3.2%	+11%
Observed m_H (GeV)	125.26±0.21	125.30±0.21	125.34±0.23

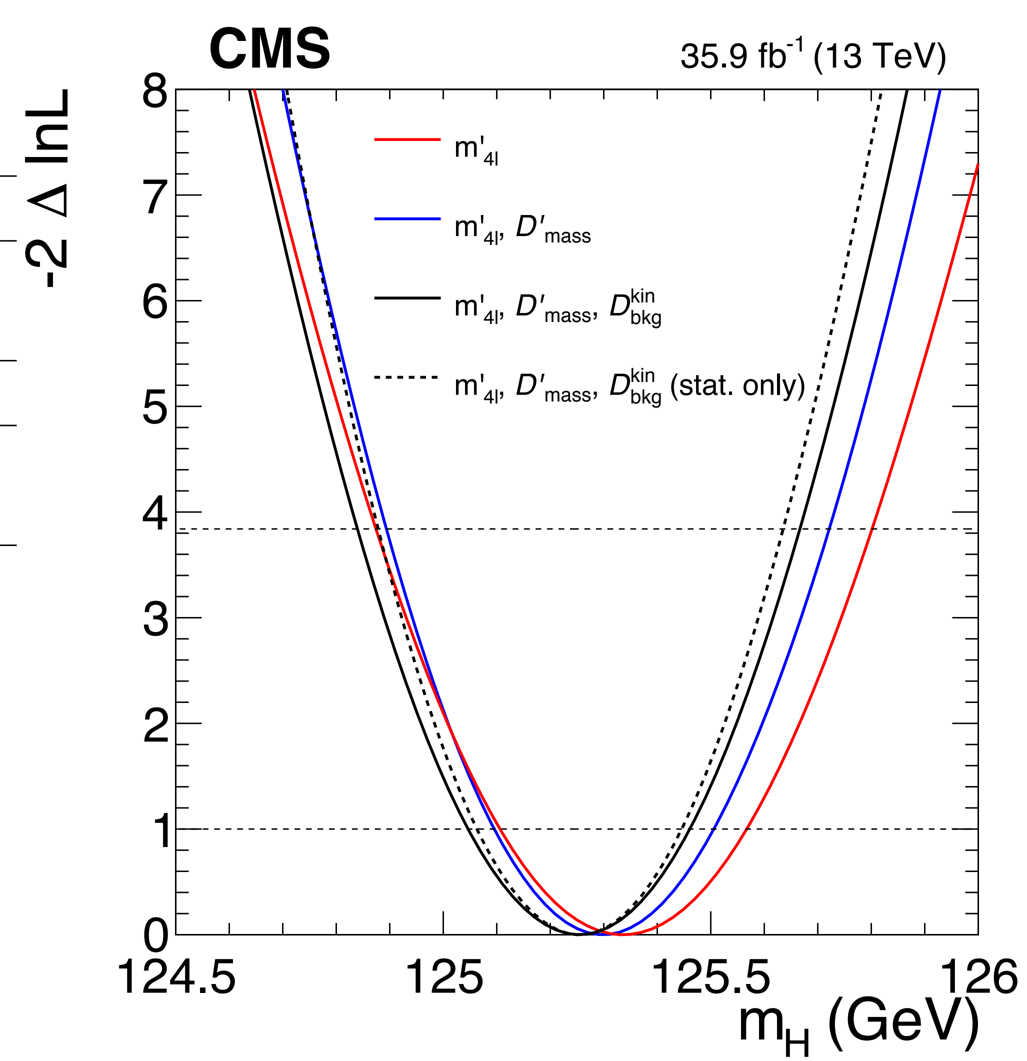

- At Run II sufficient statistics for constraining differential measurements

- Fiducial cross section definition
  - including detector efficiency (C) , detector acceptance (A) and branching $\mathscr{B}$

$$\sigma_{i,\text{fid}} = \sigma_i \times A_i \times \mathcal{B} = \frac{N_{i,\text{fit}}}{\mathcal{L} \times C_i}$$

  - Cuts mimicking reconstruction selection:
    - (i) Model independent result.
    - (ii) No extrapolation beyond observation

- Measurements dominated by statistical uncertainty

Channel	Statistical	Systematic
$H \to ZZ^*$	15%	7%
$H \to \gamma\gamma$	16%	7%
$H \to WW^*$	10%	15%

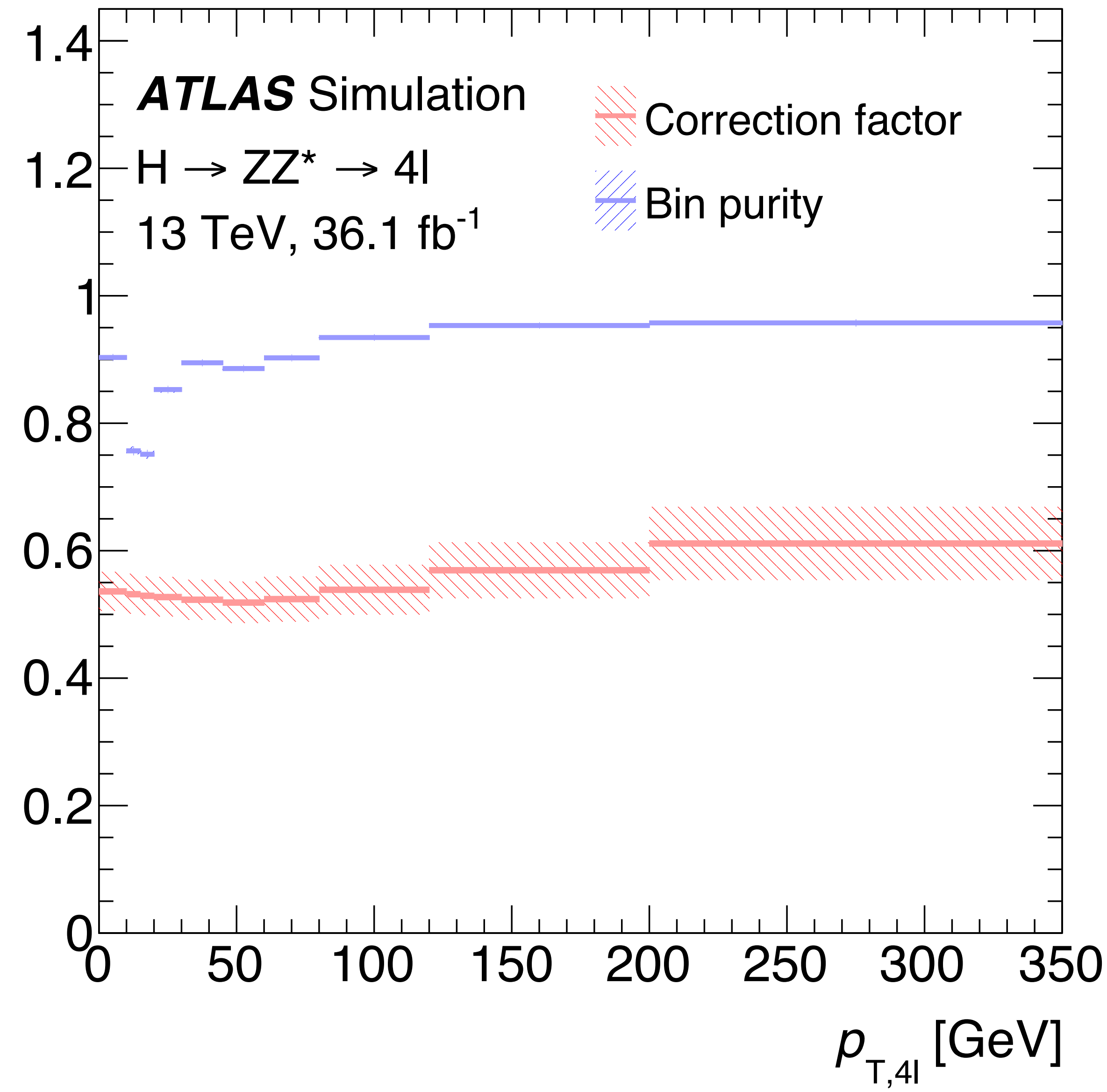

- Decay variabels: |cosϑ*|, m_{34} and $\Delta\varphi_{jj}$:
  - Probe J^{CP} of the Higgs boson and BSM sensitivity
    - ✦ Although statistical higher precision needed
  - Sensitivity to Higgs production modes

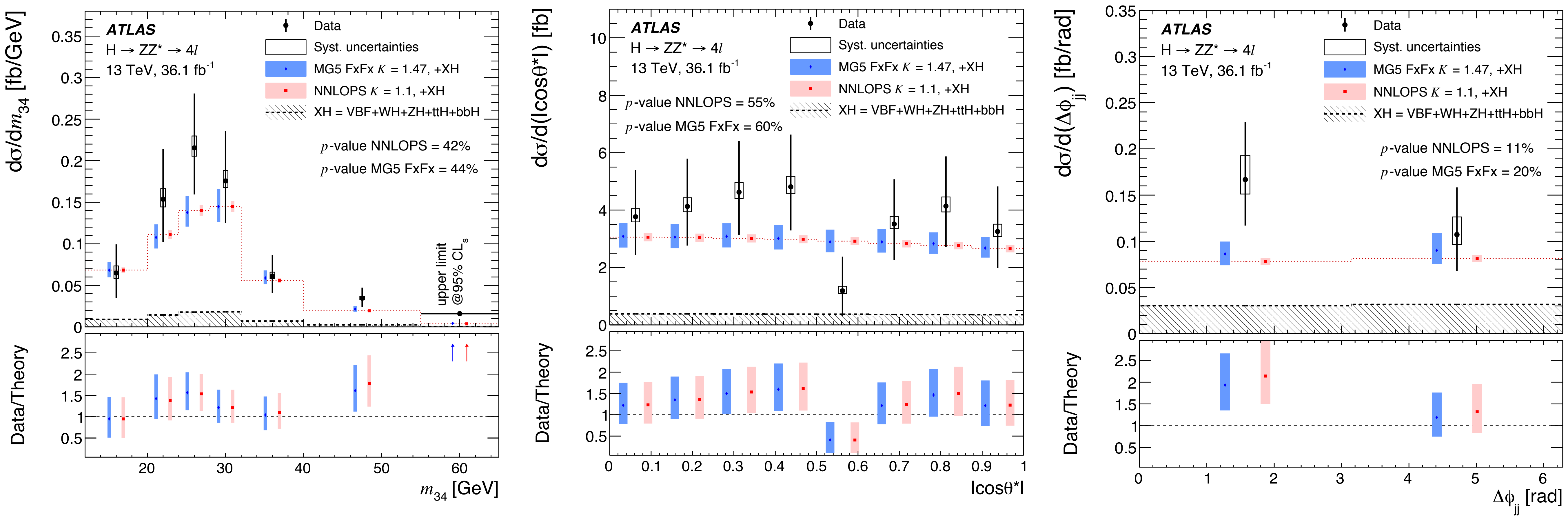

- Measured cross sections in good agreement from that measured by CMS

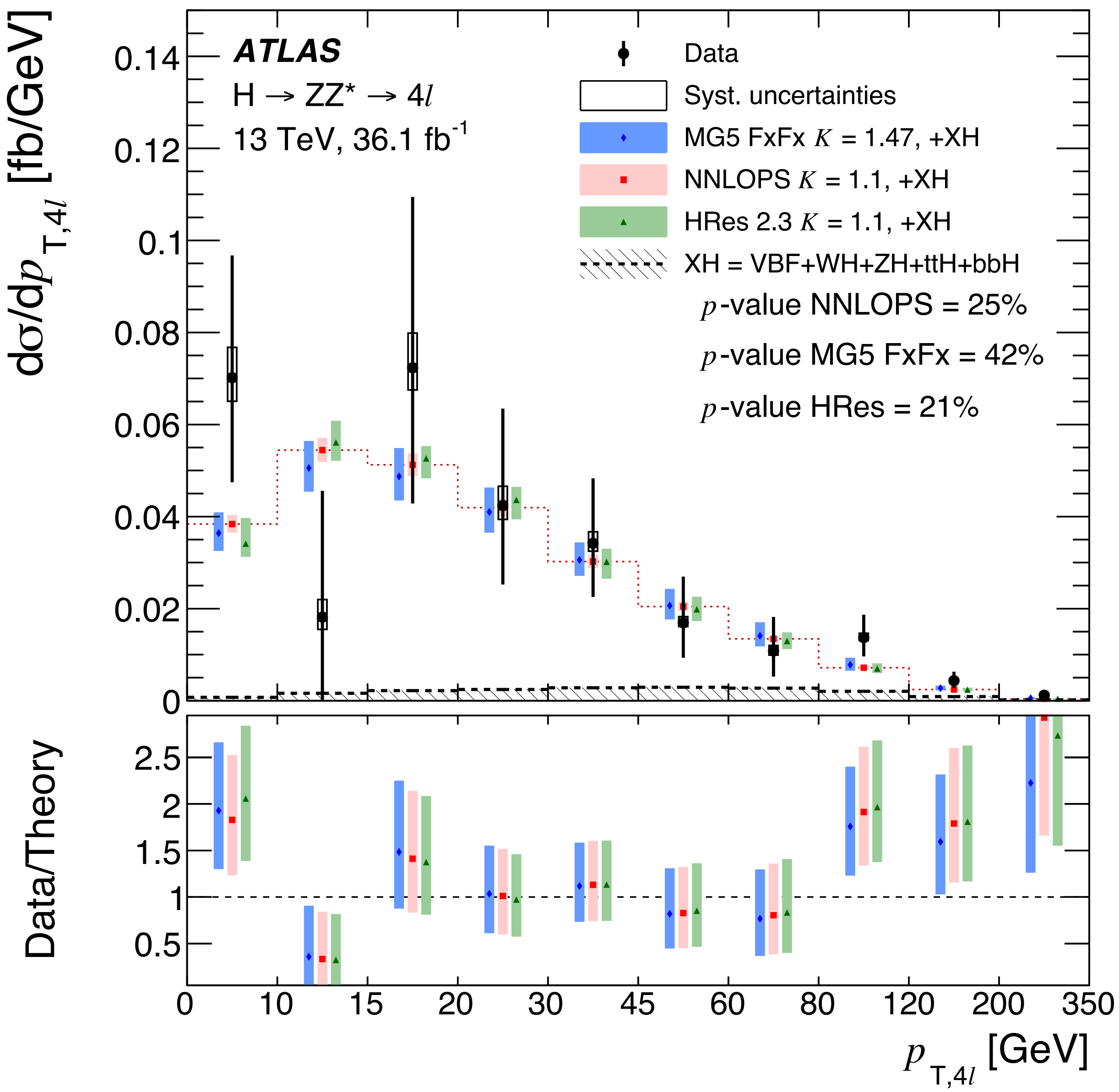

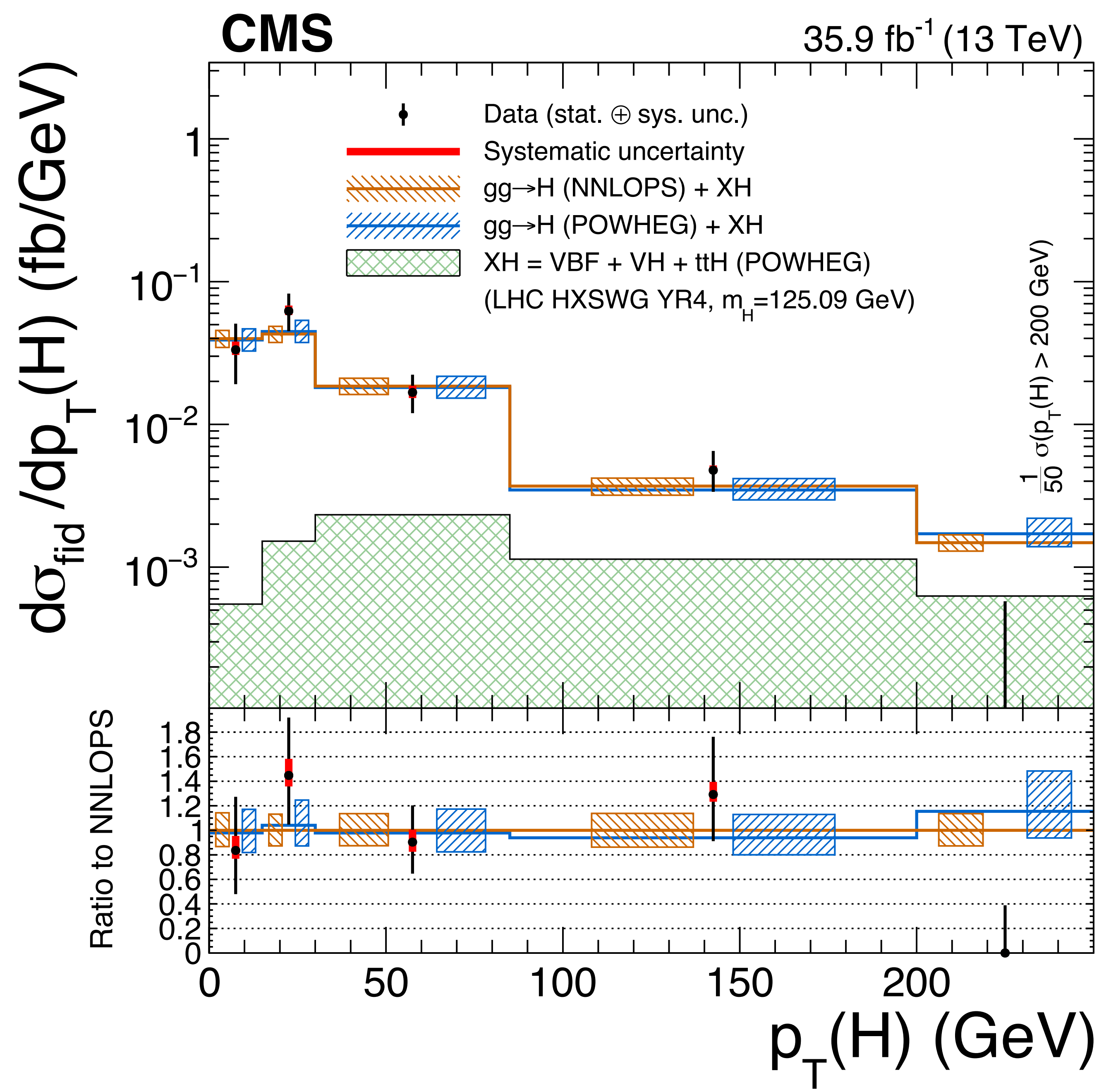

Interpretation — Differential cross section

- m_{12} vs m_{34}: sensitivity to contact interactions:
  - ε_R, ε_L and κ: flavour universal modifiers of the contact terms between H, Z and leptons (arXiv:1504.04018)
    - ✦ Angular distributions unaffected: same Lorentz structure as SM term.

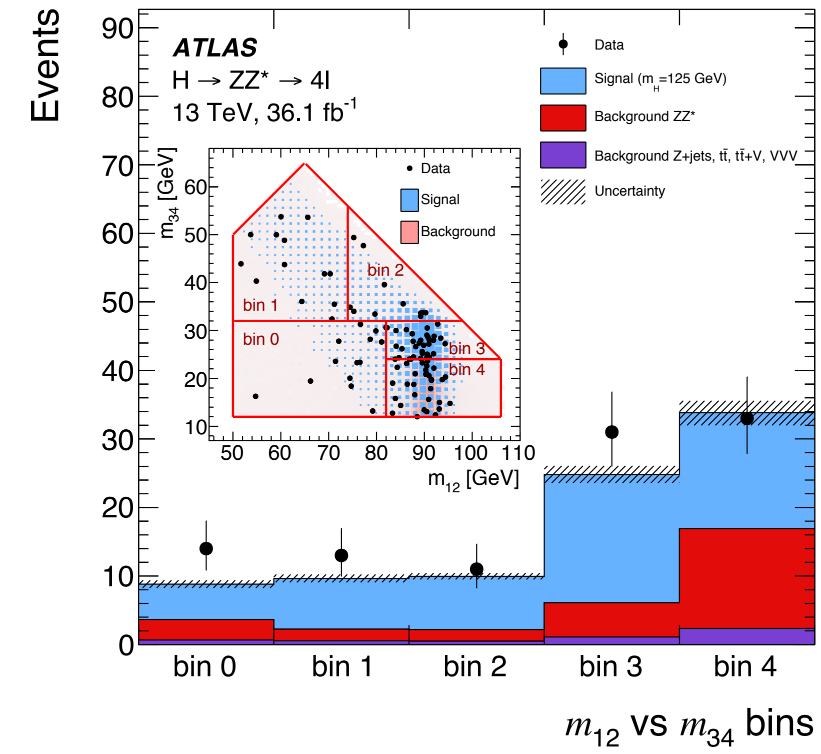

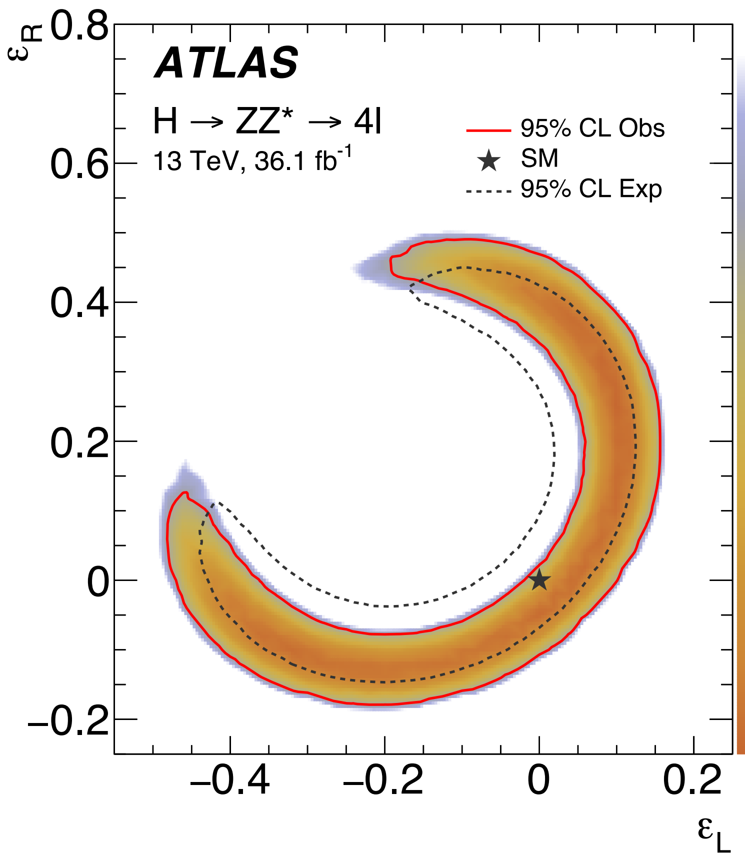

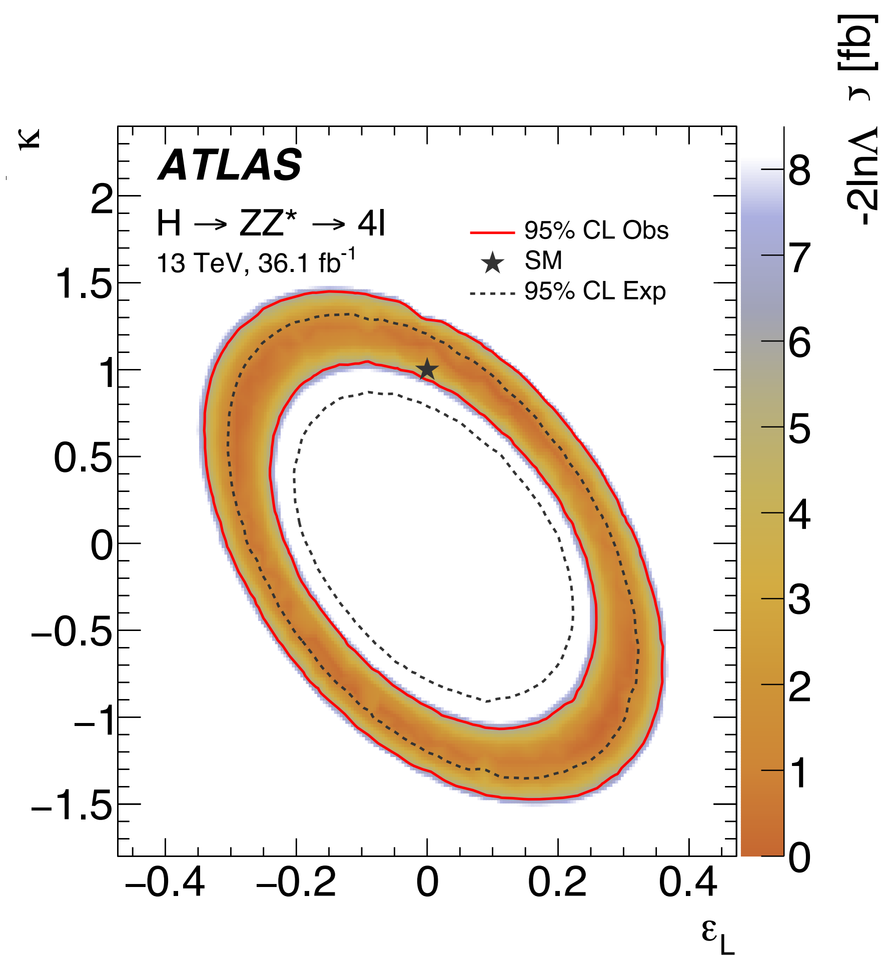

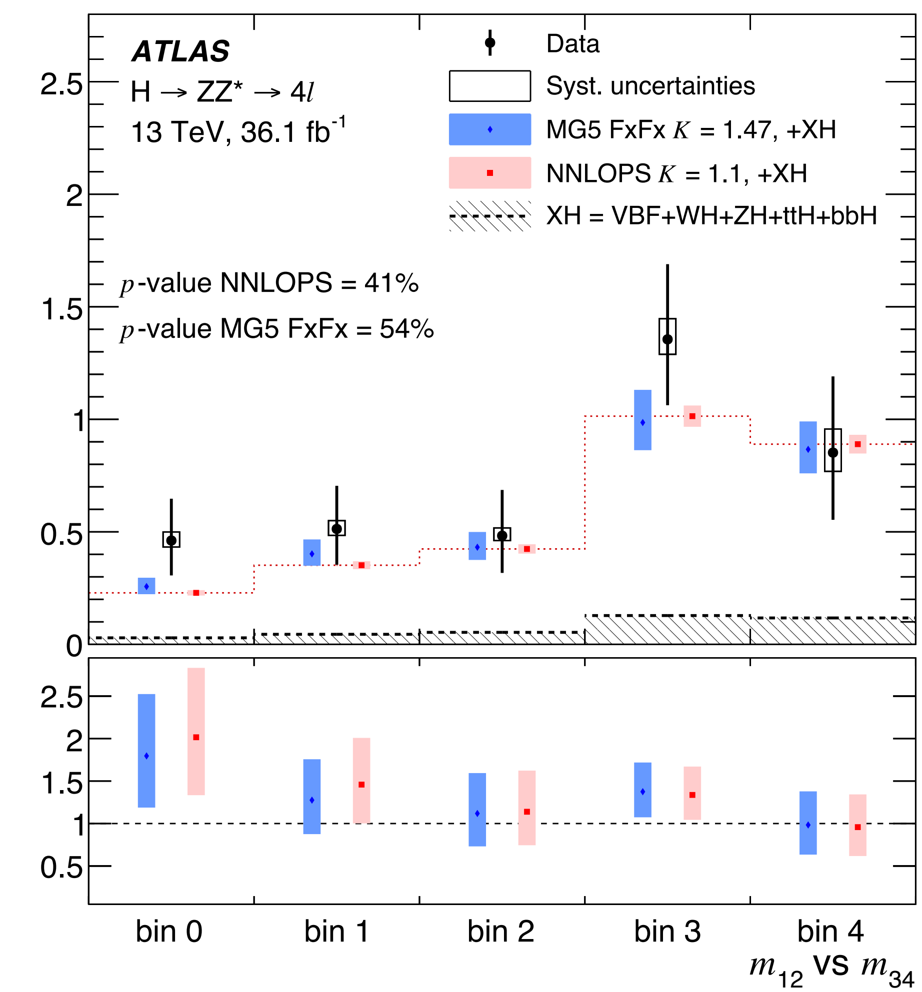

- gluon gluon fusion production modelled by
  - PowHeg Box “NNLOPS” (normalised to N3LO)
  - Madgraph5_@NLO with FxFx merging scheme (normalised to N3LO)
  - HRes 2.3 (normalised to N3LO)
- VBF, VH, $t\bar{t}\ H$ and $b\bar{b}\ H$
  - All normalised to N3LO
  - MiNLO for VH and Madgraph5_@NLO for $q\bar{q}\ H$
- $BR(H\to 4\ell)$ of 0.0124% at m_H=125 GeV
  - PROPHECY4F: including NLO QCD and EW corrections.
- Showering:
  - HERWIG++ (with UEEE5 tunes) and Pythia8 (AZNLO tunes)
- PDF:
  - PDF4LHC NLO PDF for PowHegBox (with NLO merging scheme)

- Cut based classification of events into category.
  - Ex. Jet multiplicity (ggF), m_{jj} for (VBF) and b-tagging ($t\bar{t}H$)
- Multivariate analysis (BDT) to discriminate contributions.
  - ggF from ZZ^*, VBF from ggF, VH(had) from all.
  - Variables: $p_{T,4\ell}$, KD, η_j, $\Delta\eta_{jj}$, $p_{T,j}$ etc.

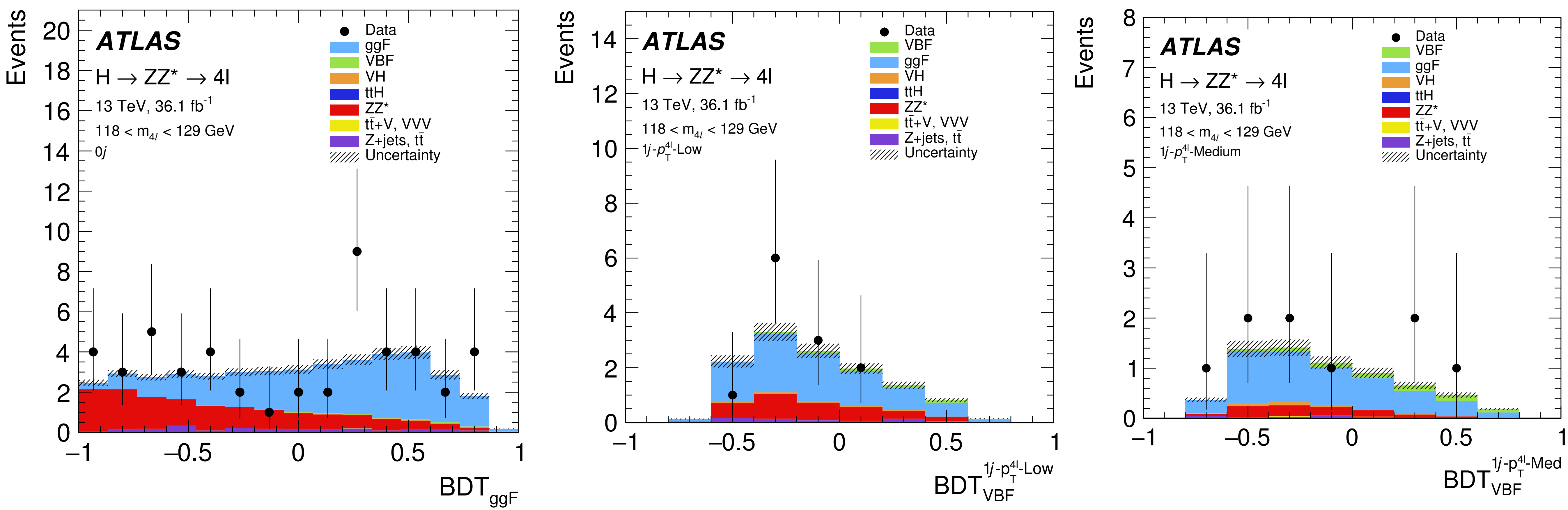

- Cut based classification of events into category.
  - Ex. Jet multiplicity (ggF), m_{jj} for (VBF) and b-tagging ($t\bar{t}\ H$)
- and multivariate analysis (BDT) to discriminate contributions.
  - ggF from ZZ^*, VBF from ggF, VH(had) from all.
  - Variables: $p_{\mathrm{T},4\ell}$, KD, η_{j}, $\Delta\eta_{\mathrm{jj}}$, $p_{\mathrm{T},j}$ etc.

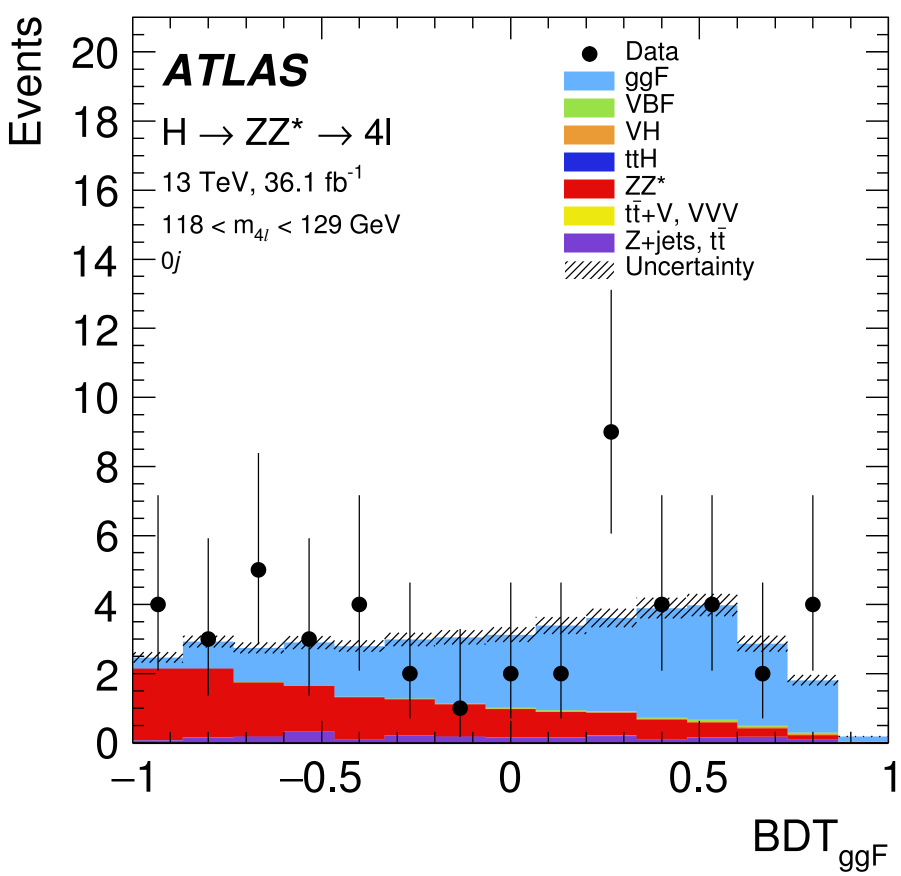

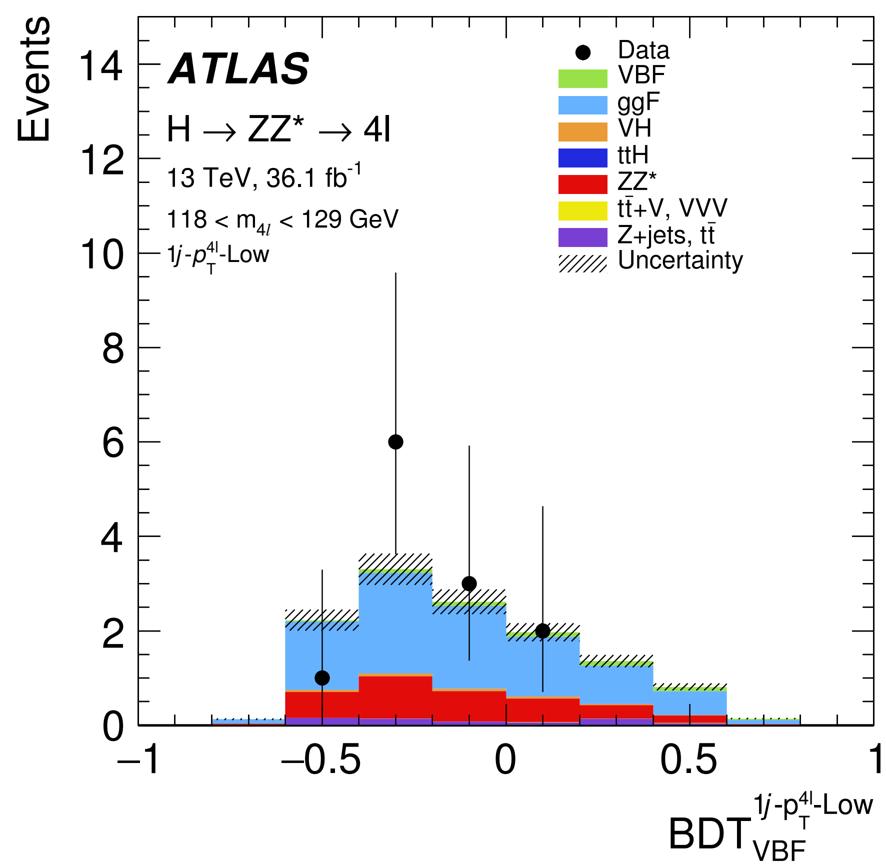

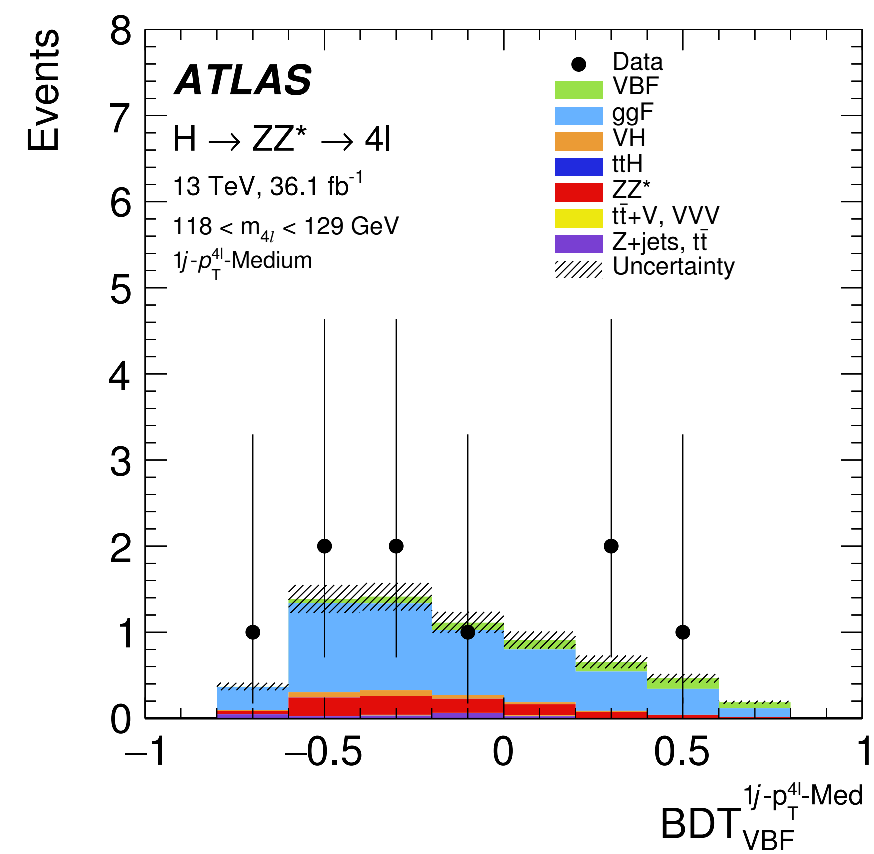

- Cut based classification of events into category.
  - Ex. Jet multiplicity (ggF), m_{jj} for (VBF) and b-tagging ($t\bar{t}$ H)
- Multivariate analysis (BDT) to discriminate contributions.
  - ggF from ZZ^{*}, VBF from ggF, $\mathrm{VH(had)}$ from all.
  - Variables: $p_{\mathrm{T},4\ell}$, KD, η_{j}, $\Delta\eta_{\mathrm{jj}}$, $p_{\mathrm{T},j}$ etc.
- Detector and theoretical uncertainties

(i) Luminosity 3.2%

(ii) Lepton Identification <2%

(iii)Pileup ~2%

(iv)Jet Energy Scale (3%-7%)

(v) Jet Energy Resolution (2%-4%)

(i) μ_R and μ_F about 4% to 30%

(ii) ggF prediction in N_J categories.

(iii)(BSM only NLO/LO prediction)

- Simultaneous fit to all BDT distributions

Production bin	Cross section (pb) Observed	SM expected	$(\sigma\cdot BR)/(\sigma\cdot BR)_{SM}$ Observed	μ Observed
Stage-0 production bins, $\|y_H\| < 2.5$				
ggF	$1.31^{+0.26+0.09}_{-0.24-0.07}\pm0.05$	1.18 ± 0.08	$1.11^{+0.22+0.09}_{-0.20-0.07}$	$1.11^{+0.22+0.11}_{-0.20-0.08}$
VBF	$0.37^{+0.15}_{-0.13}\pm0.03\pm0.03$	0.0928 ± 0.0028	$4.0^{+1.7}_{-1.4}\pm0.4$	$4.0^{+1.7+0.5}_{-1.4-0.4}$
VH	< 0.20	$0.053^{+0.005}_{-0.003}$	< 3.7	< 3.8
ttH	< 0.12	$0.0154^{+0.0015}_{-0.0011}$	< 7.5	< 7.7
Reduced Stage-1 production bins, $\|y_H\| < 2.5$				
ggF-0j	$0.88^{+0.22+0.09}_{-0.20-0.07}$	0.73 ± 0.05	$1.22^{+0.30+0.13}_{-0.27-0.09}$	$1.22^{+0.30+0.16}_{-0.27-0.11}$
ggF-1j-p_T^H Low	$0.08^{+0.15+0.04}_{-0.12-0.06}$	0.174 ± 0.025	$0.5^{+0.8+0.3}_{-0.7-0.4}$	$0.5^{+0.8}_{-0.7}\pm0.3$
ggF-1j-p_T^H Med	$0.16^{+0.11+0.03}_{-0.09-0.01}$	0.120 ± 0.018	$1.3^{+0.9}_{-0.7}\pm0.2$	$1.3^{+0.9+0.4}_{-0.7-0.2}$
ggF-1j-p_T^H High	$0.03^{+0.05}_{-0.04}\pm0.01$	0.024 ± 0.005	$1.2^{+2.3}_{-1.7}\pm0.3$	$1.3^{+2.3+0.8}_{-1.7-0.3}$
ggF-2j	$0.20^{+0.16}_{-0.14}\pm0.03$	0.137 ± 0.029	$1.4^{+1.2}_{-1.0}\pm0.2$	$1.5^{+1.2+0.7}_{-1.0-0.2}$
VBF-p_T^j Low	$0.26^{+0.18+0.03}_{-0.14-0.02}$	0.0886 ± 0.0027	$3.0^{+2.0+0.4}_{-1.6-0.2}$	$2.9^{+2.0+0.4}_{-1.6-0.3}$
VBF-p_T^j High	$0.06^{+0.05}_{-0.04}\pm0.01$	$0.0042^{+0.0002}_{-0.0004}$	$13^{+12}_{-8}\pm1$	$13^{+12}_{-8}\pm1$
VH-Had	< 0.20	$0.0362^{+0.0033}_{-0.0019}$	< 5.6	< 5.6
VH-Lep	< 0.15	$0.0166^{+0.0015}_{-0.0008}$	< 9.3	< 9.5
ttH	< 0.11	$0.0154^{+0.0015}_{-0.0011}$	< 7.1	< 6.9

- Simultaneous fit to all BDT distributions

Production bin	Cross section (pb)		$(\sigma \cdot BR)/(\sigma \cdot BR)_{SM}$	μ
	Observed	SM expected	Observed	
Stage-0 production bins, $\lvert y_H \rvert < 2.5$				
ggF	$1.31^{+0.26}_{-0.24}{}^{+0.09}_{-0.07}\pm 0.05$	1.18 ± 0.08	$1.11^{+0.22}_{-0.20}{}^{+0.09}_{-0.07}$	$1.11^{+0.22}_{-0.20}{}^{+0.11}_{-0.08}$
VBF	$0.37^{+0.15}_{-0.13}\pm 0.03\pm 0.03$	0.0928 ± 0.0028	$4.0^{+1.7}_{-1.4}\pm 0.4$	$4.0^{+1.7}_{-1.4}{}^{+0.5}_{-0.4}$
VH	< 0.20	$0.053^{+0.005}_{-0.003}$	< 3.7	< 3.8
ttH	< 0.12	$0.0154^{+0.0015}_{-0.0011}$	< 7.5	< 7.7

- Simultaneous fit to all BDT distributions
  - Extraction of global signal strength ($\mu=\sigma^{obs}/\sigma^{exp}$).

$$\mu = 1.28^{+0.18}_{-0.17}(\text{stat.})^{+0.08}_{-0.06}(\text{exp.})^{+0.08}_{-0.06}(\text{th.})$$

- Extraction of individual category cross sections

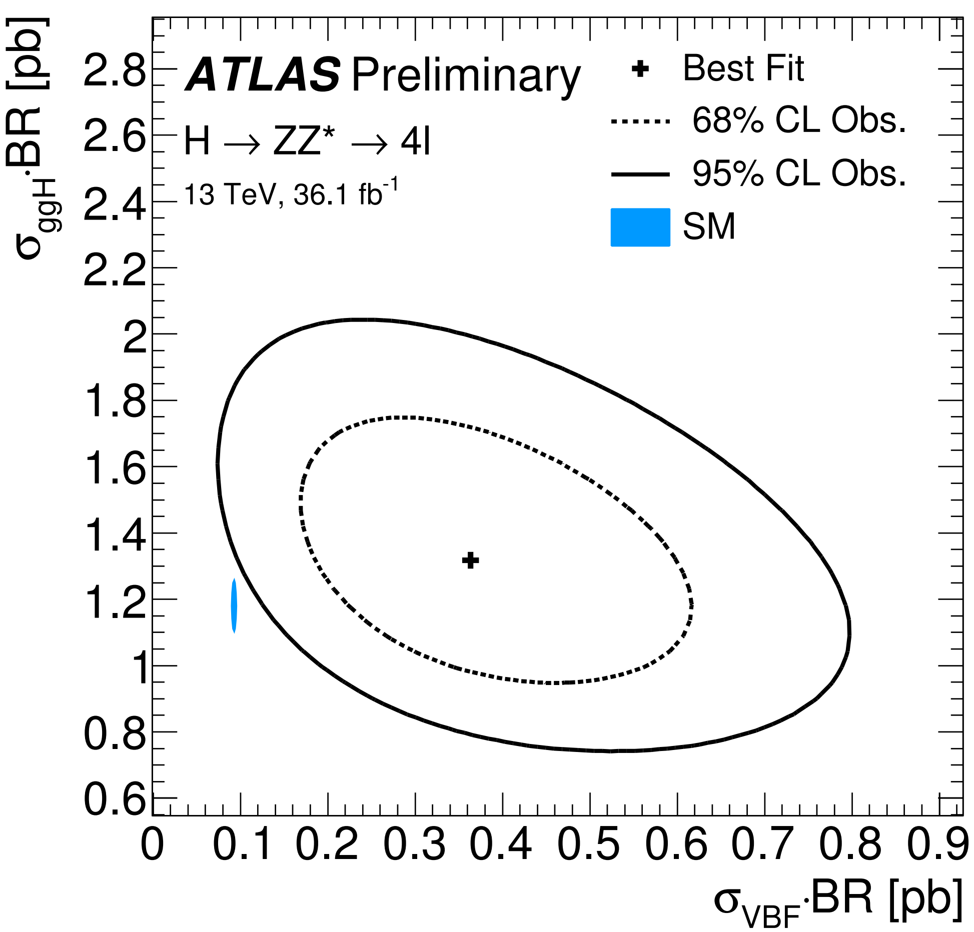

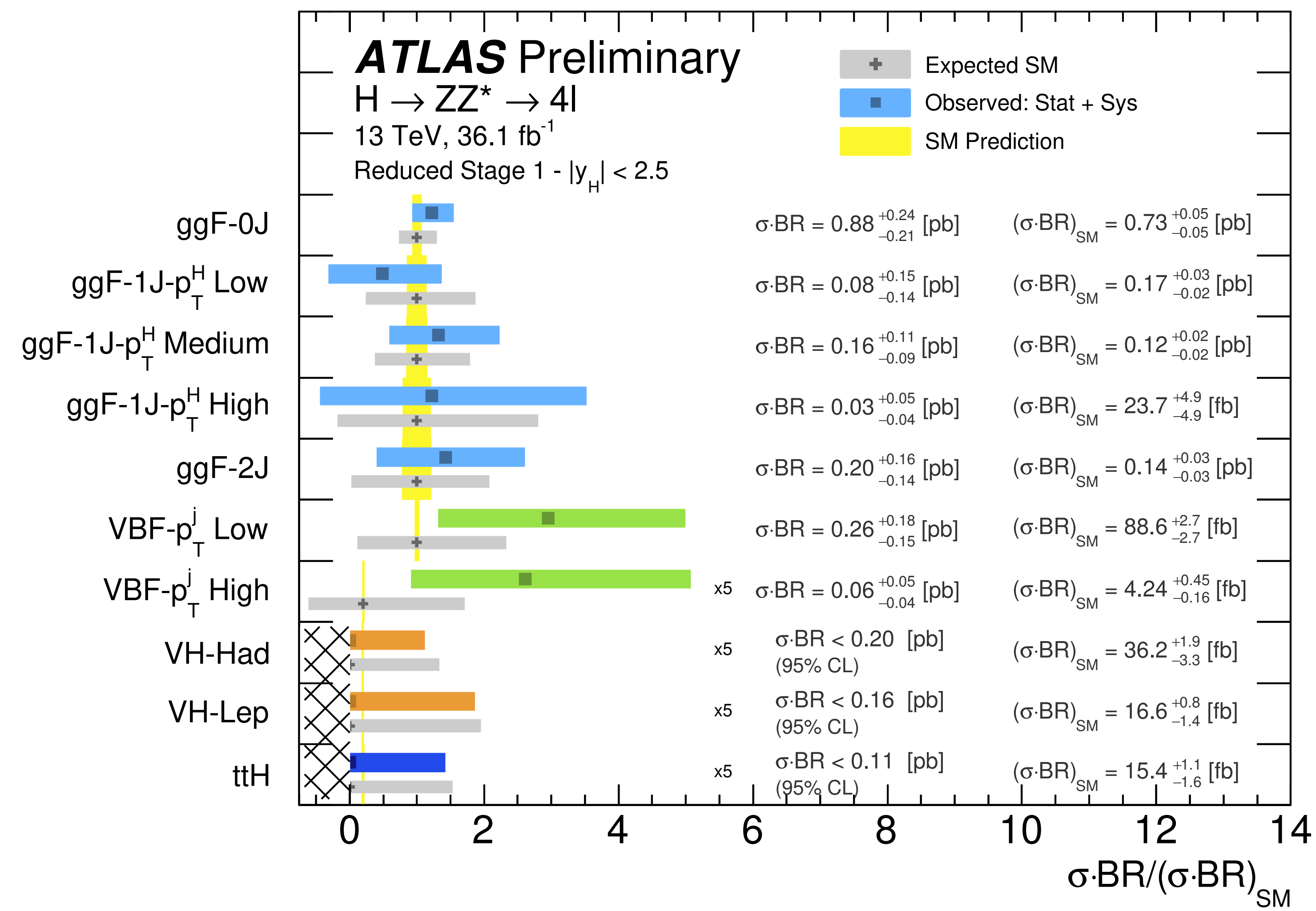

- Simultaneous fit to all BDT distributions
  - Extraction of global signal strength ($\mu=\sigma^{obs}/\sigma^{exp}$).

$$\mu = 1.28^{+0.18}_{-0.17}(\text{stat.})^{+0.08}_{-0.06}(\text{exp.})^{+0.08}_{-0.06}(\text{th.})$$

- Interpretation with coupling modifiers

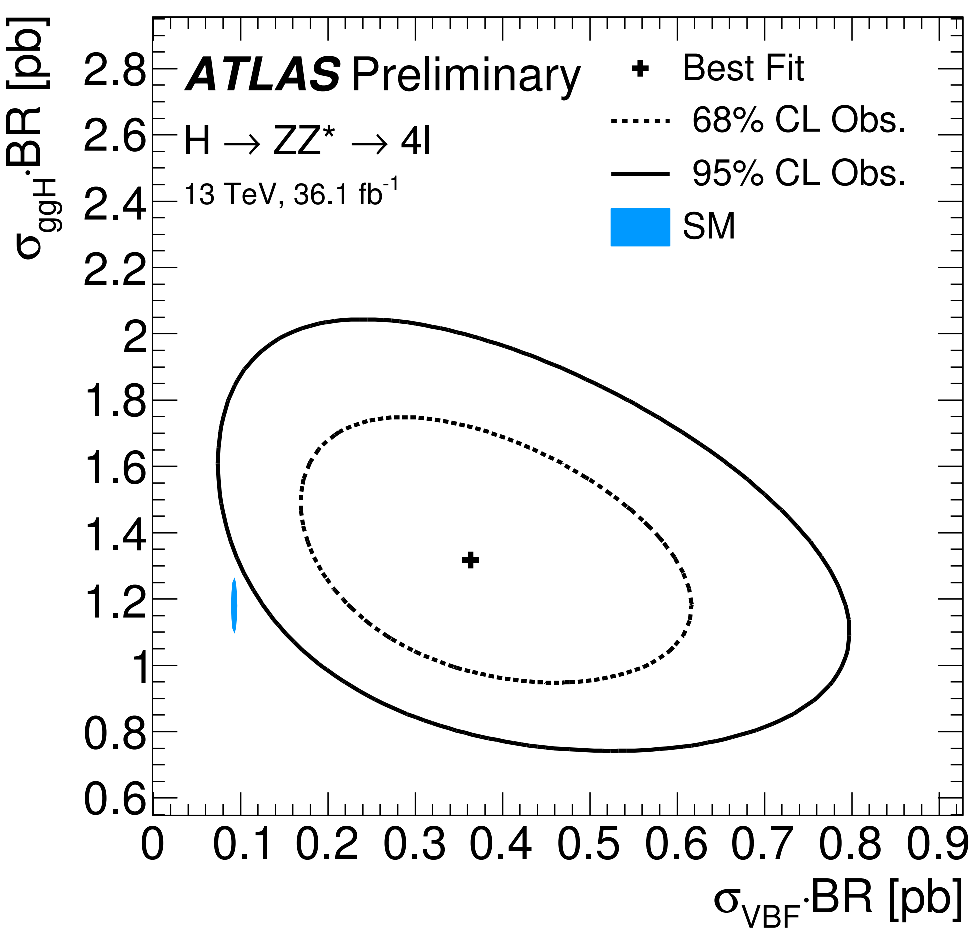

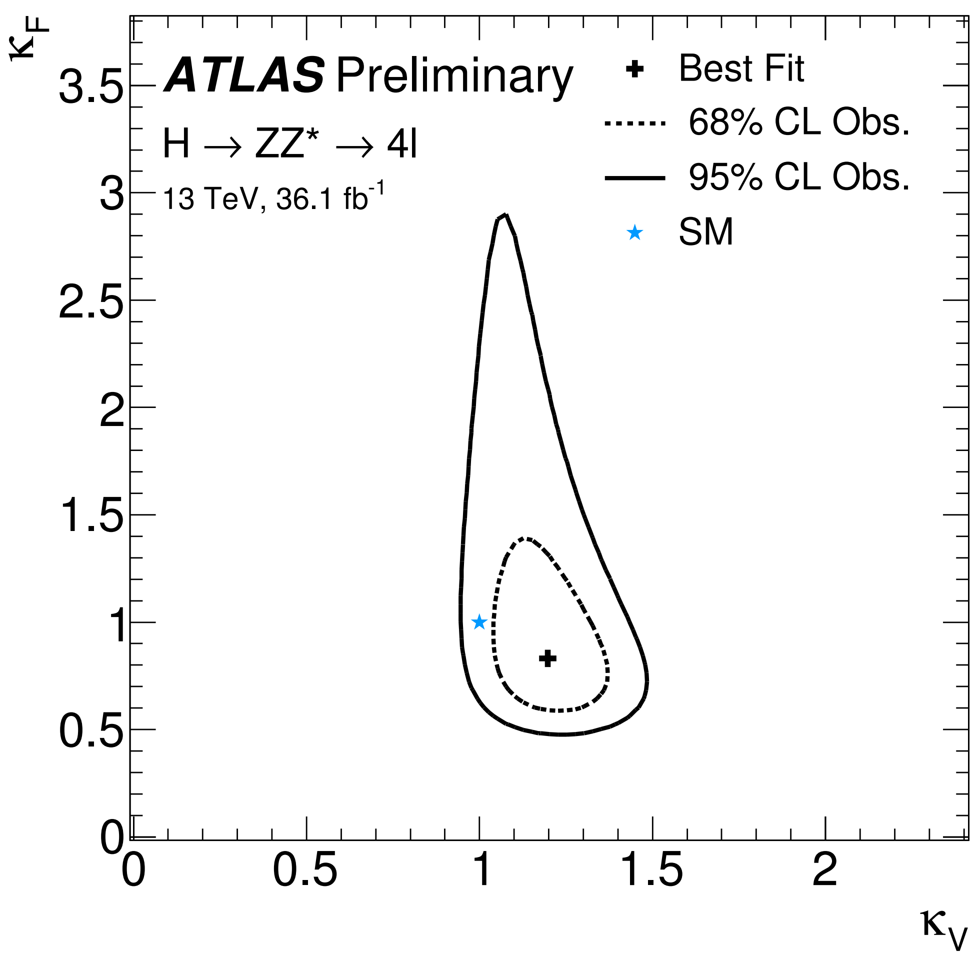

- Using the Higgs characterisation model Lagrangian
  - Effective field theory which assumes no new physics below Λ = 1 TeV

$$\mathcal{L}_0^V = \Big\{ \kappa_{\rm SM} \Big[\tfrac{1}{2} g_{HZZ} Z_\mu Z^\mu + g_{HWW} W_\mu^+ W^{-\mu} \Big] - \tfrac{1}{4} \Big[\kappa_{Hgg} g_{Hgg} G_{\mu\nu}^a G^{a,\mu\nu} + \tan\alpha\, \kappa_{Agg} g_{Agg} G_{\mu\nu}^a \tilde{G}^{a,\mu\nu} \Big] - \tfrac{1}{4} \tfrac{1}{\Lambda} \Big[\kappa_{HZZ} Z_{\mu\nu} Z^{\mu\nu} + \tan\alpha\, \kappa_{AZZ} Z_{\mu\nu} \tilde{Z}^{\mu\nu} \Big] - \tfrac{1}{2} \tfrac{1}{\Lambda} \Big[\kappa_{HWW} W_{\mu\nu}^+ W^{-\mu\nu} + \tan\alpha\, \kappa_{AWW} W_{\mu\nu}^+ \tilde{W}^{-\mu\nu} \Big] \Big\} \mathcal{X}_0 .$$

Standard Model modifiers ($\kappa_{SM} = \kappa_{Hgg} = 1$)

CP odd (κ_{AZZ}) and CP even (κ_{HZZ}) components of vector boson interaction

BSM gluon gluon fusion modifiers (κ_{Agg})

- Extraction from events counts
  - With additional split of VH hadronic at $p_{T,4\ell}$ = 150 GeV.
  - Allow only of κ_{AZZ}, κ_{HZZ} and κ_{Agg} to vary.

- Likelihood models from interpolation between SM and BSM components

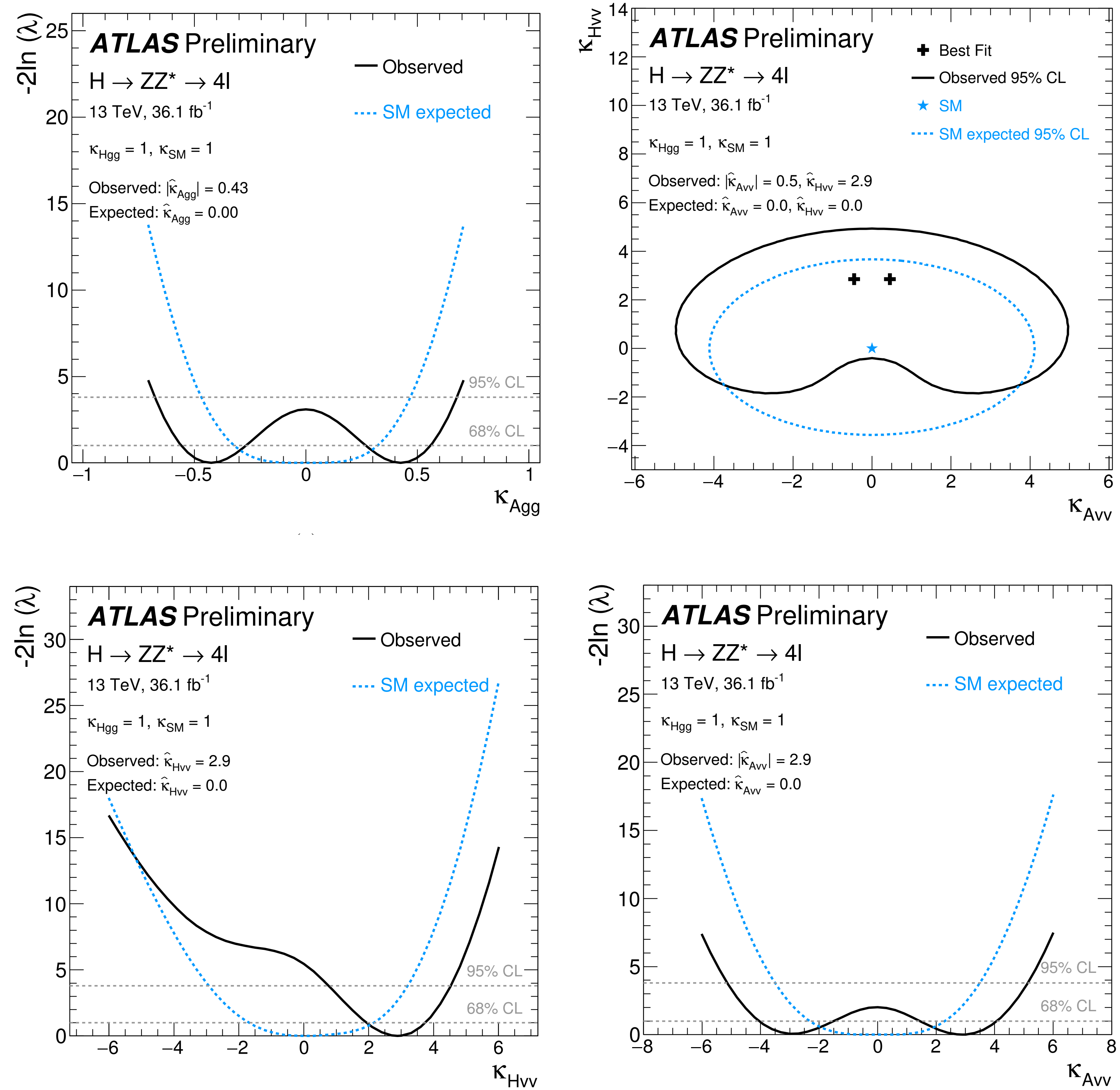

- No indications of new physics:
  - Excess in VBF production explains the non zero values for the κ values.
    - ✦ Interferes with SM assumption